Thesis for the Master's degree in chemistry

Lene Grutle

Monolithic precolumns and porous layer open tubular columns for separation of peptides and digested proteins

60 study points

DEPARTMENT OF CHEMISTRY

Faculty of mathematics and natural sciences

UNIVERSITY OF OSLO 6/2013

Acknowledgements

I would like to thank my supervisors Professor Elsa Lundanes, Professor Tyge Greibrokk, and Ph.D. student Magnus Røgeberg for their kind assistance and support during my participation in the master program in analytical chemistry at the University of Oslo from August 2011 to June 2013. Thanks to their patient and generous supervision, I have been able to make steady progress in the work with my master thesis. It has truly been an interesting and challenging experience.

Oslo, June 14, 2013
Lene Grutle

Abbreviations

1D	One-dimensional
2D	Two-dimensional
A/D	Analog-to-digital
ACN	Acetonitrile
AIBN	2,2'-azobis(2-methylpropionitrile)
BMA	Butyl methacrylate
DDT	DL-dithiothreithol
DMF	N,N-dimethylformamide
DPPH	2,2-diphenyl-1-picrylhydrazyl hydrate
EDMA	Ethylene dimethacrylate
EIC	Extracted ion chromatogram
ESI	Electrospray ionization
FA	Formic acid
γ-MAPS	3-(trimethoxysilyl)propyl methacrylate
HPLC	High-performance liquid chromatography
IAM	Iodoacetamide
I.D.	Inner diameter
IUPAC	International Union of Pure and Applied Chemistry
LFD	Large field detector
LHRH	Luteinizing hormone releasing hormone
LC-MS	Liquid chromatography-mass spectrometry
m/z	Mass-to-charge ratio
OT	Open tubular
PFS	PEEK coated fused silica
PLOT	Porous layer open tubular
PS-DVB	Polystyrene-divinylbenzene
RP	Reversed phase
RSD	Relative standard deviation
SEM	Scanning electron microscope
S/N	Signal-to-noise
SSD	Solid state detector
TFA	Trifluoroacetic acid
THF	Tetrahydrofuran
UHPLC	Ultrahigh performance liquid chromatography
UV	Ultraviolet
WT %	Weight %

Abstract

A simple, half-automated liquid chromatography-mass spectrometry (LC-MS) column switching system, with a 50 µm i.d. × 4.5 cm butyl methacrylate-ethylene dimethacrylate (BMA-EDMA) precolumn and a 10 µm i.d. polystyrene-divinylbenzene (PS-DVB) porous layer open tubular (PLOT) analytical column with 0.75 µm layer thickness, has been successfully used for separation of protein digests. Good repeatability with a ≤0.2% relative standard deviation (RSD) of retention time was found by injections of trypsinated transferrin. The loading capacity was found to be ~120 fmol for a tryptic digest of cytochrome C. The effect of flow rate (20-80 nL/min) and gradient time on peak capacity was investigated on a 2.4 m long column by using tryptic digest of cytochrome C. Highest peak capacity was obtained with a flow rate of 40 nL/min followed by 20 nL/min at all gradient times. Furthermore, the effect of PLOT column length (2.4, 5.4 and 8.0 m) on peak capacity was investigated, and highest peak capacity was obtained using the longest PLOT column. Polystyrene-divinylbenzene (PS-DVB) precolumns, using a binary porogenic mixture of toluene (13 wt%) and 1-dodecanol (47 wt%), were prepared in length of ~10 cm as alternative precolumns to 50 µm i.d. BMA-EDMA precolumns used in the LC-MS column switching system. LC-ultraviolet (UV) testing of a BMA-EDMA precolumn and three batches of PS-DVB precolumns showed that two out of three batches of PS-DVB precolumns had satisfactory efficiency while the batch 3 precolumn did not perform as well, indicating that reproducible precolumn preparation is difficult. In the LC-MS column switching system a 50 µm i.d. × 4 cm PS-DVB precolumn performed as well as the BMA-EDMA precolumn. The often higher signal intensities obtained with the PS-DVB precolumn indicated good trapping of peptides. The findings from the LC-MS experiments are very promising, and it seems worth while to further study the composition of PS-DVB polymerization mixture and polymerization time and temperature to find reproducible polymerization conditions.

Table of contents

3. Results and discussion

1. Introduction

1.1 Proteomics and high-performance liquid chromatography (HPLC)

The term "proteome" originates from the words protein and genome. It represents the entire collection of proteins encoded by the genome in an organism [1]. Proteomics, defined as the study of proteomes, aims to characterize the full protein complement of a cell, a tissue or an organism at a certain time under given conditions [2, 3]. Proteomics play a central role in the discovery of disease biomarkers and drug targets [1, 4].

One of the main methodologies for proteomics is mass spectrometry (MS) used in combination with a wide variety of separation methods [4]. In high-performance liquid chromatography (HPLC)-based proteomics, a protein sample of interest is usually first enzymatically digested by trypsin and the peptides generated are then analysed by MS and MS/MS [3-6]. This is because peptides in general are easier to separate, ionize and fragment than proteins [3, 4].

The HPLC-separations of peptides and intact proteins are typically carried out using silica-particulate based reversed phase (RP) columns [7-9]. This is because porous silica packings can withstand high pressures, are compatible with most organic and aqueous mobile-phase solvents, and offer high mass loadability [9]. Separation of peptides in proteomic studies are mostly carried out using C18-silica columns. Chemical and physical properties of a peptide such as length, sequence, net charge, degree of hydrophobicity, solubility, and polypeptide structure, determine its retention [7, 10].

1.2 Miniaturization

Downsizing of analytical columns has been a part of the mainstream in HPLC for many years. Miniaturization is essentially to reduce the internal diameter (i.d.) of a column [11, 12]. Capillary columns range in size from 0.1 to 0.5 mm i.d., while nano-columns range in size from 0.01 to 0.1 mm i.d. [13].

With concentration sensitive detectors, reducing the column i.d. from d_1 to d_2 theoretically results in an increased sensitivity *f*, given by [14, 15]:

$$f \approx \frac{d_1^2}{d_2^2} \qquad (1)$$

But this is only true if the other column parameters remain constant, and if equal absolute amounts of analytes are injected into both systems. According to Chervet et al., all system components, including flow rate, connecting tubing, detection, and injection volumes, should be downscaled to miniaturize the HPLC system [14]. The operation of nano-columns therefore requires volumetric flow rates in the nL/min range [14-16].

Miniaturized HPLC has several advantages over conventional HPLC. In situations of limited amounts of sample, which is often the case in proteomics, the signal-to-noise ratio (S/N) will strongly improve with concentration sensitive detectors, such as electrospray ionization (ESI)-MS. The flow rates used for nano-HPLC couple well with ESI-MS with no need for post-column splits. A further advantage is the decrease in consumption of solvent. Low solvent consumption not only reduces cost, but also waste and pollution [11-13, 17].

To improve the concentration detection limits in miniaturized HPLC, column-switching systems with large volume injection of low elution strength sample solvents, are used. Using enrichment columns, the full sample can be trapped on the column and then eluted in the smallest possible volume to reach maximum concentration levels [18-20].

1.3 Column performance in HPLC

Separation performance of particulate columns can be increased by decreasing the size of the stationary phase particles. But the smaller the particle, the higher is the pressure needed to drive the mobile phase through the packed bed [16, 21, 22]. The column pressure drop, Δp, is inversely proportional to the average particle diameter, d_p, given by equation (2):

$$\Delta p = \frac{\Phi \eta L u}{d_p^2} \qquad (2)$$

where Φ is the flow resistance parameter, η is the viscosity of the solvent, L is the column length and u is the linear velocity of the solvent (L/t_M) [16, 22]. Furthermore, packing difficulty increases dramatically with decreasing particle and column diameters [16, 23].

Performance beyond the limit of common HPLC has been achieved by ultrahigh performance liquid chromatography (UHPLC) using higher operational pressure for sub-2 µm particles [22, 24, 25]. But ultrahigh pressures require special pumps, injectors and connectors [11].

To overcome some practical constraints, such as high back pressure associated with small particles, monoliths have been proposed as alternative stationary phases [25].

1.4 Monoliths

Monoliths were first developed and successfully used for HPLC in the early 1990s, and have been regarded as an alternative to particulate columns [25, 26]. Monoliths can be considered as a single porous particle that entirely fills the column volume without any interparticular voids typically found in particulate columns. Most of the pores inside the monolith are open, forming a highly interconnected network of channels [26-28].

According to their diameter, pores have been classified into three different types by the International Union of Pure and Applied Chemistry (IUPAC). Macropores have a pore diameter greater than 49 nm, mesopores have a pore diameter between 2 nm and 49 nm, while micropores have diameters smaller than 2 nm [29]. Macropores, which play a similar role as that of the interparticle volume in packed columns, provide the channels for convective flow through the material. The mesopores, which correspond to the inner pores of particles in packed columns, contribute to the overall surface area, providing the surface for interaction with the active sites of the material. A balance must be found between the requirements of low resistance to flow and high surface area. An ideal monolith should contain both large pores for convective flow and a connected network of shorter and smaller pores for high loading capacity [27, 28, 30, 31].

Major advantages of monolithic columns are high permeability and low mass transfer resistance. The mass transfer within the pores is greatly enhanced by convective flow. Separations can therefore be performed at much higher flow rates than in particulate columns [32-35]. In contrast to particulate columns where the interparticle volume strongly

depends on the particle diameter, permeability and performance can be controlled independently with monolithic columns [25, 34, 36].

Other main advantages of monolithic columns are easy fabrication in narrow formats and fritless design [25, 32, 35]. Although monolithic columns have several advantages in terms of structure, production time and equipment requirements, they are still in their infancy, and much more research is required to optimize their design and preparation for improved performance [25].

Monolithic separation media can be divided into two general categories based on their manufacturing material. One is silica-based monoliths and the other is organic polymer-based monoliths [28, 37, 38].

Silica-based monolithic columns have some advantages over organic polymer-based ones. These include a well-controlled pore structure, good mechanical strength, and high column efficiency, especially for small molecules. On the other hand, organic polymer-based monolithic columns have unique characteristics, such as applicability over a wide pH range and simple preparation [38]. In this thesis, organic polymers have been used, and they are described in more detail in 1.5.

1.5 Organic polymer-based monoliths

Organic polymer-based monoliths, or so-called polymer monoliths, have generally been used in microscale separation systems because of the simplicity of preparation in wide range of narrow dimensions by *in situ* polymerization, and good chromatographic performance [39, 40]. The term *in situ* refers to the polymerization within the confines of a capillary as a mold [29].

Polymer monoliths have been playing an important role especially for separation of large molecules such as peptides, proteins and polynucleotides, primarily because of rapid mass transfer within the column. Polymer monoliths contain large through-pores, but few, if any, mesopores [41-43].

Monolithic columns based on organic polymers are so far mostly prepared in research laboratories [32, 41]. The bed structure of the polymer monoliths resembles a loose packing of nearly spherical particles (microglobules) with a broad size distribution [37, 44], see Figure 1.

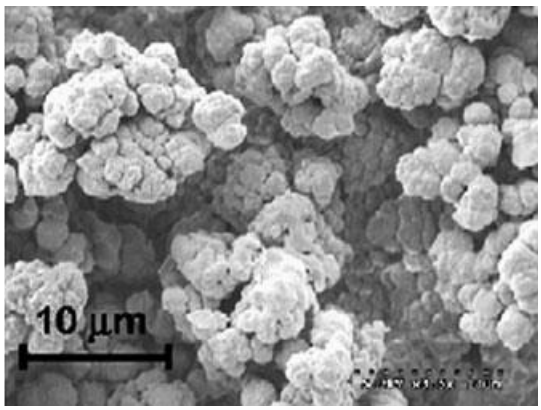

Figure 1. Scanning electron micrograph of a poly(butyl methacrylate-co-ethylene dimethacrylate) monolithic column. Reprinted from [44].

Polymer monoliths are in general prepared by polymerization of monomers (in the presence of an initiator) in a so-called porogenic solvent in which the monomers and not the polymers are soluble [32]. Free-radical copolymerization is the most common polymerization technique used for the preparation of polymer monoliths, see Figure 2. Free radicals are most often generated by using increased temperature (thermal initiation) or ultraviolet (UV) radiation (photochemical initiation) [29, 40, 41]. Monolithic columns prepared by thermal initiation may exhibit somewhat poorer homogeneity compared to monoliths obtained with UV initiation, due to radial pore size distribution caused by a radial gradient of the degree of polymerization [41]. However, UV initiation has some important limitations. UV transparent liquids must be used and the brown polyimide-coated capillaries, impenetrable for UV rays, are excluded. Thermal initiation, being applicable to polyimide-coated capillaries, is most commonly used among the two initiation methods [41].

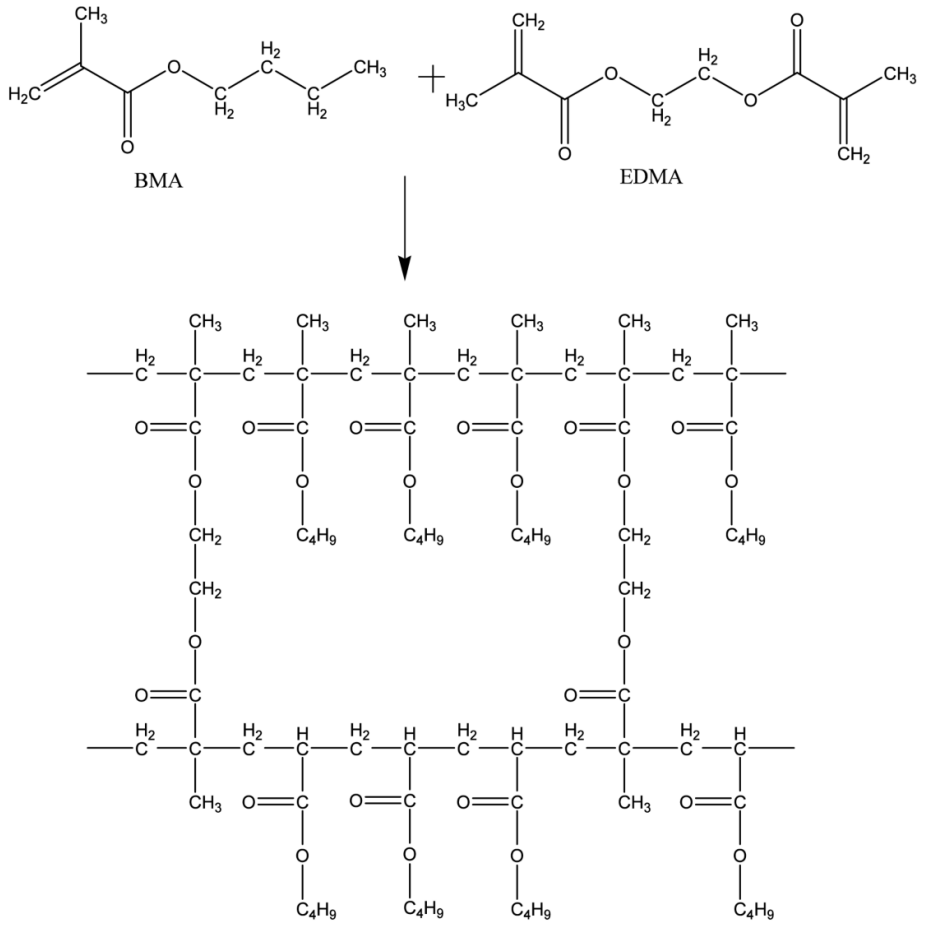

Figure 2. A schematic figure of copolymerization of butyl methacrylate (BMA) and ethylene dimethacrylate (EDMA) monomers. Reprinted from [45].

The preparation of organic polymer monoliths in a fused silica capillary usually consists of three processes – pretreatment, silanization and polymerization [29, 46]. A key element for polymeric monolithic structures is the proper attachment of the monolith to the capillary wall. Proper preparation of the capillary surface by pretreatment and silanization is therefore very important [37, 46]. Chemical attachment of the monolith to the capillary surface prevents the monolith from being pushed out of the column when pressure is applied. It also ensures that void channels are not formed between the monolith and the capillary wall due to shrinkage of the monolith during polymerization [46].

1.5.1 Pretreatment

Pretreatment of the inner wall of a fused-silica capillary involves surface etching under alkaline conditions. Alkaline solutions are applied to increase the density of silanol groups at

the inner surface by hydrolyzing siloxane groups. The silanol groups serve as anchors for the subsequent silanization [29, 46, 47].

There are different procedures for capillary pretreatment. Courtois et al. [46] have described what they regard as three of the most representative pretreatment procedures. It was shown that alkaline etching provided the best surface roughness promoting polymer adhesion. A higher surface concentration of silanols was observed using high-temperature etching compared to room temperature-etching [46].

1.5.2 Silanization

In the silanization process the internal surface of the capillary is silanized using reagents that contain double bonds which will participate in the subsequent radical polymerization. The silanizing reagents react with the silanol groups on the inner surface and create a monomolecular layer of reactive chains covalently attached to the capillary wall by siloxane linkages. This provides anchoring sites for the grafting of the monolith to the capillary surface. A common silanizing reagent is 3-(trimethoxysilyl)propyl methacrylate (γ-MAPS), see Figure 3 [46-48].

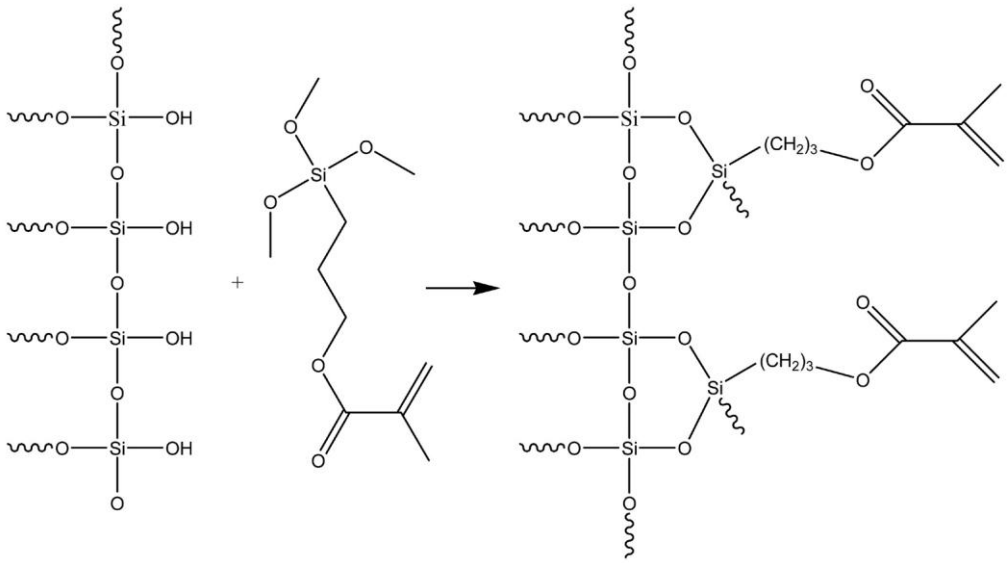

Figure 3. Silanization with γ-MAPS. Reprinted from [46].

Courtois et al. [46] have also described what they have found to be the most representative silanization procedures. In some of the procedures the inhibitor 2,2-diphenyl-1-picrylhydrazyl hydrate (DPPH) was added to slow down the polymerization of the silanizing reagent (γ-MAPS) via the vinyl groups at high temperatures [46, 47]. The commonly used silanization procedures involving water in the silanization or washing steps were shown to give inadequate surface treatment [46].

1.5.3 Polymerization

In the polymerization process the pretreated and silanized capillary is filled with a polymerization mixture. A polymerization mixture consists of a functional monomer, a cross-linker (a monomer with two or more double bonds), an initiator and porogenic solvents. The most common initiator is 2,2'-azobis(2-methylpropionitrile) (AIBN), which produces two radicals at temperatures that exceed 50^{o}C, see Figure 4. The in situ polymerization starts by thermal initiation or UV light initiation [27, 29, 39, 40, 41, 48, 49].

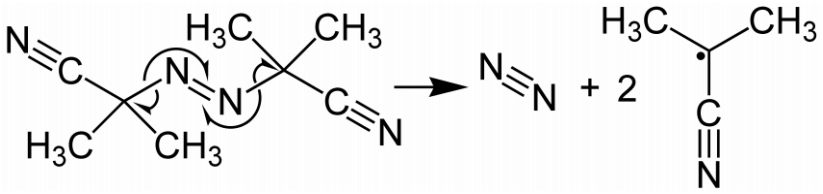

Figure 4. The most common initiator in the preparation of monolithic stationary phases is AIBN, which produces two radicals at temperatures that exceed 50^{o}C.

When the in situ polymerization is completed, the capillary column is attached to a pump and flushed with a suitable solvent to remove porogens and unreacted residues that remain in the pores after the polymerization has finished [29].

1.5.4 Porous properties

The porous properties of organic polymer-based materials are usually controlled by the initiation rate of polymerization and composition of the polymerization mixture [44, 48]. A variety of preparation factors, including polymerization temperature, initiator concentration,

monomer composition (functional monomer and cross-linker), ratio of monomer-to-porogen, type of porogens, and ratio of porogenic solvent mixtures, determine both the morphology and pore size distribution [43, 50].

An increase in concentration of the initiator or an increase in the temperature leads to a larger number of polymerization centres and smaller microglobules. This results in a decrease of the mean pore size accompanied by an increase in the total surface area [27, 39, 48].

The functional monomer in the polymerization mixture determines the polarity of the final monolithic material [27, 41]. Increasing the amount of cross-linker at the expense of monomer leads to a decrease in the average pore size because of the early formation of highly cross-linked microglobules. As a result, the total surface area increases [29, 48, 51].

The porogenic solvents in the polymerization mixture control the porous properties without affecting the chemical composition of the final polymer. The polymer phase that is formed during radical polymerization, separates from the solution as a result of its limited solubility in the polymerization mixture as well as the intrinsic insolubility that results from crosslinking. Larger amount of poor solvent (macroporogen) in the polymerization mixture results in an increase in pore size and a decrease in the total surface area of the polymer [27, 29, 32, 51]. The choice of porogens for the preparation of porous polymer monoliths still remains an art rather than science. This is because few porogens have been utilized and most often already proven porogen mixtures are applied [51].

It is well accepted that free-radical copolymerizations inherently lead to heterogeneous polymers [49]. Materials formed by simple free-radical cross-linking copolymerization are always inhomogeneous because the cross-linker has at least two vinyl groups. If equal vinyl group reactivity is assumed, the rate of consumption of the cross-linker is twice that of the monovinyl monomer. As a result, the cross-linker molecules are incorporated into the growing copolymer chains much more rapidly than the monomer molecules. The final network therefore exhibits a cross-link density distribution [49]. The different reactivites of all species present in the polymerization mixture with different vinyl group reactivity urther complicate the reaction kinetics and lead to polymers with spatial inhomogeneities [49].

The pore sizes in organic polymer monoliths vary continuously within a certain range. It is therefore at present not possible to formulate a general model analogous to that for silica monoliths, in which the pore sizes are more rigorously defined [41]. The description of the properties of polymer monoliths and their prediction are much more empirical and subject to greater uncertainty. Individual parameters of such monoliths must be studied individually for the various polymer types [41].

1.5.5 Methacrylate-based and polystyrene-based monoliths

Methacrylate-based monoliths and polystyrene-divinylbenzene (PS-DVB) monoliths are the most popular organic polymer monoliths for proteomics, see Figure 5. Methacrylate and PS-DVB columns are used for the separation of peptides and proteins in a wide pH range [32].

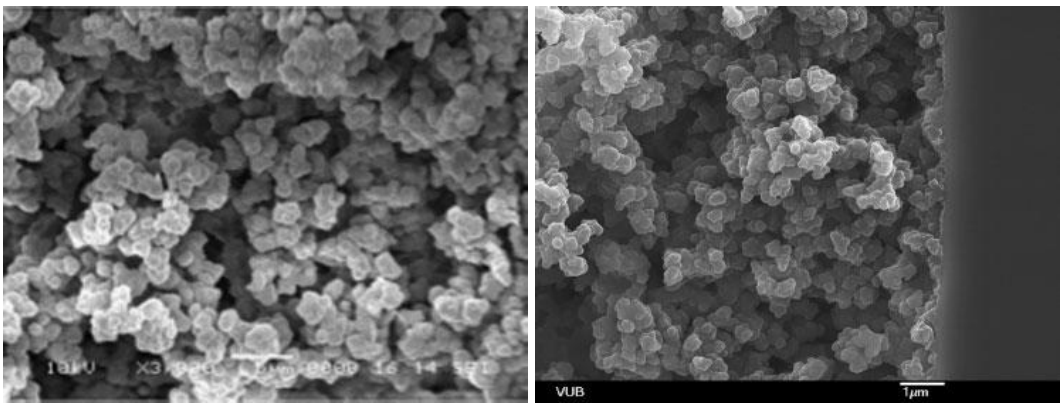

Figure 5. Scanning electron micrographs of a methacrylate column (left) and a PS-DVB column (right). Reprinted from [32].

Methacrylate-based monoliths, which are moderately polar, can be prepared by polymerization of butyl methacrylate (BMA) or other methacrylic acid esters with e.g. ethylene dimethacrylate (EDMA) as the cross-linker [27, 41].

PS-DVB monoliths are prepared by polymerization of styrene and its derivatives with DVB as the cross-linker [27, 41]. Because of its highly hydrophobic nature, a PS-DVB phase can be used directly as a RP stationary phase and is comparable with a C4 or C8 RP column [52].

Peroni et al. prepared PS-DVB and BMA-EDMA monoliths using binary mixture of aqueous and organic solvents. Toluene and dodecanol were used as porogens for PS-DVB monoliths. 1-propanol and 1,4-butanediol were used as porogens for BMA-EDMA. Contact angle measurements showed that the hydrophobicity was higher for the PS-DVB monoliths [53].

1.6 Porous layer open tubular (PLOT) columns

From the late 1970s there have been attempts to apply open tubular (OT) format columns to HPLC separations. But in most early cases there was limited success because of practical and instrumental restrictions [40, 54, 55].

The introduction of MS instrumentation for nanoflow HPLC has opened new possibilities. Porous layer open tubular (PLOT) columns, coupled with nano ESI-MS, have recently been used successfully for proteomic applications [40, 54-58]. Karger's group has pioneered the 10 µm i.d. PLOT format for one-dimensional (1D) and two-dimensional (2D) separations in proteomics, and that of hydrophilic interaction chromatography for glycan analysis [44, 56, 57]. Røgeberg et al. used 10 µm i.d. PLOT PS-DVB columns for separation of intact standard proteins and skimmed milk proteins [58].

PLOT columns possess a porous layer of stationary phase (typically 1 µm) covering the inner surface of a capillary, preserving an open-tubular structure after the completion of all column preparation steps [54], see Figure 6. To date, the majority of PLOT columns produced, based on immobilization of a polymeric phase as a single porous layer (monolithic structure) onto the inner surface of the capillary, have been obtained through the application of thermally initiated polymerization [54]. One advantage of this column format is the ability to use extremely small amounts of sample. Another advantage is the increased column permeability, allowing very long column lengths (e.g. 1–5 m) [40]. Theoretical calculations suggest that the potential benefits of PLOT columns are worthy of further experimental work [40].

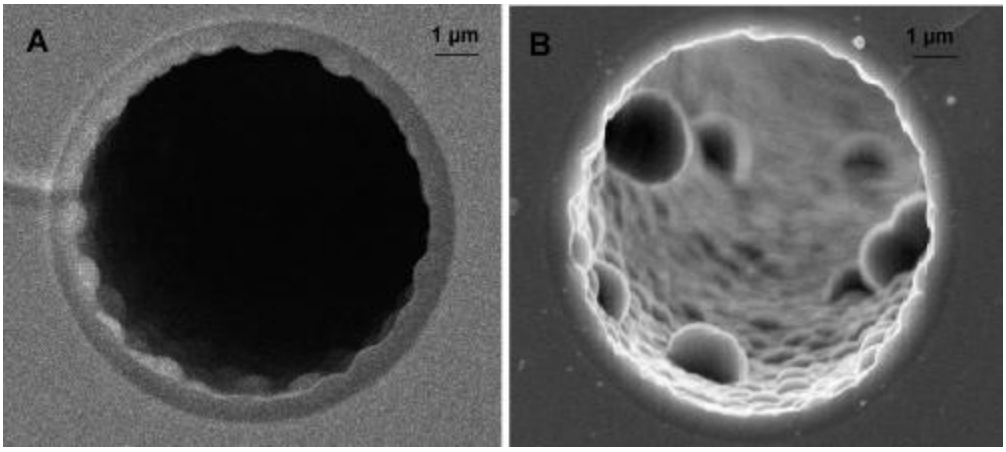

Figure 6. Scanning electron micrographs of the cross-section of a 10 µm i.d. PS-DVB PLOT column. (A) middle section and (B) end section. The layer thickness is approximately 1 µm. Reprinted from [56].

1.7 Aim of Study

The main goal of this study was to prepare, characterize and use 49 µm i.d. PS-DVB monolithic precolumns which could be used as an alternative to 49 µm i.d. BMA-EDMA precolumns in a monolith-PLOT LC-MS column switching system for separation of digested proteins. Another aim was to prepare and use 10 µm i.d. PS-DVB PLOT columns with thinner layer than 1 µm for lower back pressure to allow the use of longer columns. Peak capacity measurements were utilized to study the performance of the columns in a switching system. A further aim was to study high temperature effects in monolith-PLOT LC-MS column switching system with the goal of increasing chromatographic performance.

2. Experimental

2.1 Chemicals

Type 1 water was obtained from a Milli-Q ultrapure water purification system from Millipore (Bedford, MA, USA). Nitrogen gas (99.99%) was obtained from AGA (Oslo, Norway). HPLC grade acetonitrile (ACN) was purchased from VWR (Radnor, PA, USA). Ethanol was purchased from Arcus (Oslo, Norway). Toluene was purchased from Rathburn Chemicals (Walkerburn, UK). Sodium hydroxide pellets (99%), tetrahydrofuran (THF) (≥99.9%) and 1-propanol were purchased from Merck (Darmstadt, Germany). Formic acid (FA) (50%), anhydrous N,N-dimethylformamide (DMF) (99.8%), 2,2-diphenyl-1-picrylhydrazyl (DPPH), 3-(trimethoxysilyl)propyl methacrylate (γ-MAPS) (98%), 2,2'-azobis(2-methylpropionitrile) (AIBN), styrene (99%), divinylbenzene (DVB) (80% mixture of isomers), butyl methacrylate (BMA) (98%), ethylene dimethacrylate (EDMA) (98%), 1,4-butanediol (99%), 1-dodecanol (98%), 1-decanol (99%), Tris, DL-dithiothreithol (DDT), iodoacetamide (IAM), 1M triethylammonium bicarbonate buffer, cytochrome C from bovine heart (≥95%), human holo transferrin (≥98%), trypsin from bovine pancreas, [D-Trp^6]-LHRH Fragment 1-6 (>96%), angiotensin II (human), glycyl-L-tryptophan, L-alanyl-L-tryptophan, L-leucyl-L-tryptophan and ammonium bicarbonate were purchased from Sigma Aldrich (St. Louis, MO, USA). Uracil (Calbiochem) was purchased from EMD Millipore (Billerica, MA, USA). Complete ultra protease inhibitor tablets and phosphatase inhibitor cocktail tablets were purchased from Roche Diagnostics GmbH (Mannheim, Germany).

2.2 Equipment and materials

A 10-100 µL Finnpipette and a 100-1000 µL Finnpipette F2 from Thermo Scientific (Waltham, MA, USA) and a Mettler AE 166 delta range analytical balance from Mettler (Columbus, OH, USA) were used for solution and sample preparations. A 10 µL syringe from SGE (Ringwood, VIC, Australia) was used for manual injections of samples in both the LC-MS column switching system and the UV-system. All polyimide-coated fused silica capillaries were purchased from Polymicro Technologies (Phoenix, AZ, USA). A GC 8000 series oven from SpectraLab Scientific (Markham, ON, Canada) and a Polaratherm Series

9000 oven from Selerity Technologies (Salt Lake City, UT, USA) were used for heating the capillaries during silanization and polymerization. Ultrasonication of polymerization mixtures was done using a model USC100T ultrasonic cleaning bath from VWR International (Leicestershire, England, UK).

A 500 µL syringe from Hamilton (Reno, NV, USA), a 2.5 mL syringe from Agilent (Melbourne, VIC, Australia) and a Mettler AE 166 analytical balance were used in the weighing processes for the preparation of PLOT columns. A 0.2-2 µL Finnpipette F1 from Thermo Scientific, a 10-100 µL pipette from Eppendorf Research (Hamburg, Germany) and a Sartorius BL210S analytical balance from Sartorius (Goettingen, Germany) were used in the weighing processes for the preparation of monolithic columns.

After completed polymerization, a microscope with W10X/20 mm eyepiece magnification from Motic was used to check the presence/absence of polymers along the monolithic capillaries. To check the presence/absence of a polymer layer at the end parts of the prepared PLOT columns, the cross section of each end was inspected using an Olympus PME microscope with 20X eyepiece magnification and 100X objective magnification from Olympus Optical (Tokyo, Japan). A Samsung Galaxy S II smartphone from Samsung Electronics was used to take pictures of the end part of a freshly prepared 10 µm i.d. PLOT column during inspection with the Olympus PME microscope. Scanning electron microscope (SEM) images of the columns were taken using a FEI Quanta 200 FEG-ESEM (FEI, Hillsboro, OR, USA). The columns were cut to pieces of about 1 cm and placed on a holder with carbon tape inside the sample chamber. The images were taken using low vacuum mode with large field detector (LFD) and solid state detector (SSD). Other parameters are given under each SEM image.

2.3 Sample preparation

Angiotensin II was dissolved in water (with 0.1% TFA) to a concentration of 50 pg/µL. Reduction and alkylation of transferrin were carried out as described by Røgeberg et al. [59]. Transferrin was dissolved in water to a concentration of 1 mg/mL. 1 µg of DDT was added per 50 µg of protein. Incubation was done at 95^{o}C for 15 minutes, followed by cooling to room temperature. 5 µg of IAM was added per 50 µg of protein. The sample was then

incubated in the dark at room temperature for 15 minutes. Thereafter, 5 µL of 1M triethylammonium bicarbonate buffer (pH 8.5) and 5 µL of 1 mg/mL trypsin solution were added to the 100 µL protein solution. Digestion was performed over night at 37^{o}C and stopped by adding 5 µL of FA.

Cytochrome C was dissolved in water to a concentration of 1 mg/mL. To 100 µL of this solution, 5 µL of 1M triethylammonium bicarbonate buffer (pH 8.5) and 5 µL of 1 mg/mL trypsin solution were added. Digestion was performed over night at 37^{o}C and stopped by adding 5 µL of FA. Both cytochrome C and transferrin samples were stored at 4^{o}C until use.

For the preparation of rat liver extracts, SDS-PAGE and in gel-digestion were performed according to a previously described procedure [60]. In total 10 g rat liver from six different rats were sliced into small pieces, crushed and mixed in a solution of 50 mM Tris buffer (pH 7.4), complete ultra protease inhibitor tablet and phosphatase inhibitor cocktail tablet, using a Ultra Turax mixer (IKA Works, Inc., Wilmington, NC, USA). The sample was kept on ice during the preparation and subsequently sonicated on ice for four times one minute, and centrifuged at 16000 g at 4^{o}C for 20 minutes. From the supernatant, a 15 µL rat liver extract with a protein concentration of 40 mg/mL was diluted with 15 µL SDS-PAGE loading buffer (BioRad, Hercules, CA, USA) before performing SDS-PAGE (BioRad). One gel slice in the 50 kDa range was trypsinated over night using 50 µL 16 ng/uL trypsin (dissolved in 50 mM ammonium bicarbonate, pH = 8). Thereafter, peptides were extracted twice with 60 µL of 5% FA (*aq*)/ACN (1+1, v+v) and then once with 60 µL ACN, followed by evaporation to dryness using a Speedvac from Thermo Fisher and stored at 4^{o}C. Before injection, the sample was re-dissolved in 40 µL of 0.1% FA (v/v) in water. Further dilution was done by using 3 µL of sample and 97 µL of water. The final concentration was 45 ng/µL.

For LC-UV analyses, a test solution was prepared by dissolving ~1 µL of toluene in water (0.7 mg/mL) with 0.5 µg/mL uracil. Furthermore, a standard peptide solution was prepared by dissolving LHRH in water (with 5% ACN) to a final concentration of 0.2 mg/mL. Solutions of 0.2 mg/mL glycyl-L-tryptophan, 0.2 mg/mL L-alanyl-L-tryptophan and 0.6 mg/mL L-leucyl-L-tryptophan were prepared by dissolving each dipeptide in water.

2.4 Column preparation

A laboratory-made pressure bomb was used to force the different solutions through the fused silica capillaries. Figure 7 is a schematic description of the pressure bomb.

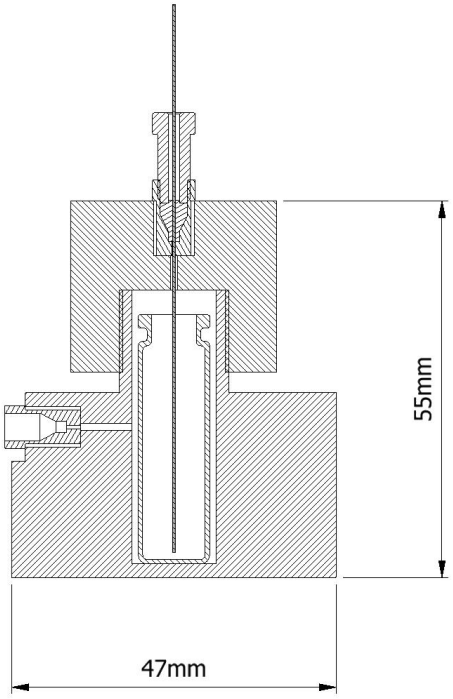

Figure 7. A schematic description of the laboratory-made pressure bomb used during column preparation. A glass vial filled with the appropriate liquid is placed inside the bomb. One end of a 10 µm or 50 µm i.d. fused silica capillary is merged inside the glass vial with liquid via an opening of the bomb lid. Nitrogen gas (≥110 bar, <200 bar) is applied through the left side of the bomb and forces the liquid through the entire capillary. Figure by Inge Mikalsen.

The 10 µm i.d. PS-DVB PLOT columns were prepared as described by Yue et al. [56] with one difference being that the volume ratio of ethanol to monomer concentration in the polymerization mixture was ~70% ethanol/30% monomer versus 60% ethanol/40% monomer by Yue et al. [61]. A detailed description of each preparation step is given in Appendix 6.1.

The pretreatment and silanization steps for the 50 µm i.d. monolithic columns were the same as that used for the 10 µm i.d. PLOT columns. The polymerization solution for BMA-EDMA monolithic columns was made as described by Geiser et al. [62] with one small

difference being that 0.41% (w/w) AIBN was used instead of 0.40% (w/w) [61]. Polymerization was carried out at 74°C for 24 hours versus 50°C for 72 hours by Geiser et al. [61, 62].

50 µm i.d. PS-DVB monolithic columns were prepared using either toluene/1-dodecanol or THF/1-decanol as the binary porogenic mixture. Tables 1 and 2 give an overview of the amount of each chemical used in the polymerization solution of each type of PS-DVB column. The binary porogenic mixture of 13% toluene and 47% 1-dodecanol (wt.%) was based on a preparation description by Svec et al. [63]. The polymerization temperature was 70°C with a duration of 20 hours. The polymerization solution of 200 µL styrene, 200 µL DVB, 70 µL THF and 530 µL 1-decanol was equal to that used by Zhang et al. [43], with the difference that 0.5% (w/v) AIBN was used instead of 0.1% (w/v). For THF/1-decanol, the polymerization temperature was 70°C and 74°C with a duration of 16 hours.

Table 1. An overview of the amount of each chemical used in the polymerization solution of PS-DVB monolithic columns with toluene/1-dodecanol as the binary solvent mixture

Chemical	**% by weight (wt.%)**	**Weighed amount in grams**
AIBN	1 (with respect to monomers)	0.0040
Styrene	21	0.2100
DVB	19	0.1900
Toluene	13	0.1300
1-Dodecanol	47	0.4700

Table 2. An overview of the amount of each chemical used in the polymerization solution of PS-DVB monolithic columns with THF/1-decanol as the binary solvent mixture

Chemical	**Volume in µL**	**Weighed amount in grams**
AIBN	–	0.0050 (0.5% (w/v))
Styrene	200	0.1818
DVB	200	0.1828
THF	60, 65, 70, 75, 80	0.0533, 0.0578, 0.0622, 0.0667, 0.0711
1-Decanol	540, 535, 530, 525, 520	0.4477, 0.4435, 0.4394, 0.4352, 0.4311

2.5 Monolith-PLOT LC-MS column switching system

The monolith-PLOT LC-MS column switching system is shown in Figure 8. Gradient separations were performed using an Agilent 1200 Series analytical pump from Agilent Technologies (Santa Clara, CA, USA). Mobile phase A consisted of 0.1% (v/v) FA in water. Mobile phase B consisted of 0.1% FA (*aq*)/ACN (10/90, v/v). A four-port VICI injector with a 500 nL internal loop from Valco Instruments (Houston, TX, USA) was used for manual injections of samples.

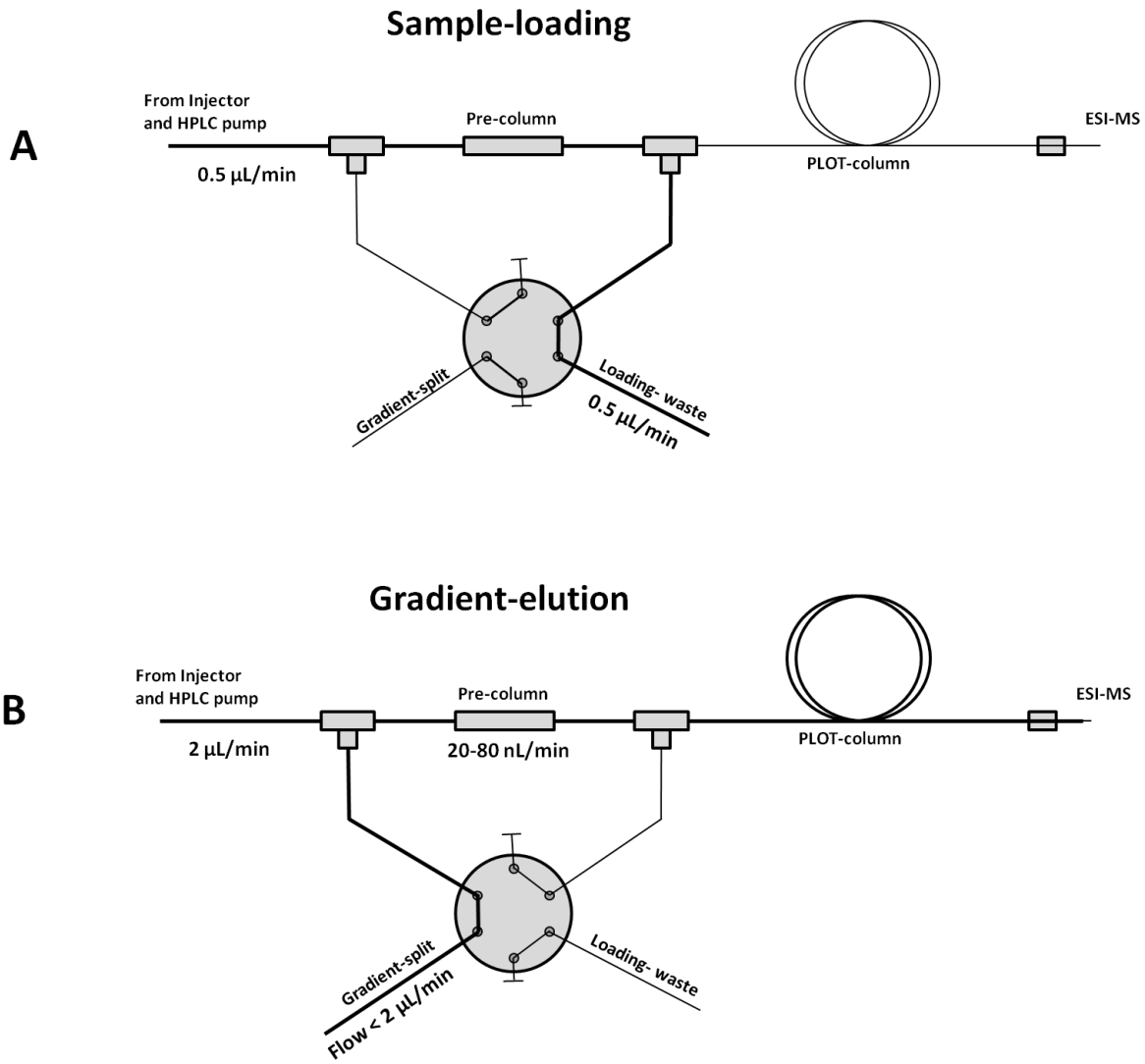

Figure 8. A schematic description of the monolith-PLOT LC-MS column switching system. The flow path is indicated by thick lines in both (A) sample-loading and (B) gradient-elution. Figure by Magnus Røgeberg.

Samples were first loaded onto a 50 µm i.d. × ~4.5 cm BMA-EDMA monolithic precolumn for analyte enrichment using 100% mobile phase A, a flow rate of 0.5 µL/min (pressure ~30 bar) and a loading time of 2.5 min. After loading, the pump was always set to 2 µL/min. A T-piece with 29 nL sweep volume from Upchurch Scientific (Oak Harbor, WA, USA), placed before the precolumn, served as a splitter. Flow rates of 20, 40, 60 or 80 nL/min were obtained by varying the length of 15 µm and 20 µm i.d. fused silica capillaries from the splitter to waste, see Table 3. Trapped analytes were fore-flushed from the precolumn onto a 10 µm i.d. PLOT column, using a six-port VICI valve from Valco Instruments (Houston, TX, USA) as the column-switching valve. A second T-piece with 29 nL sweep volume from Upchurch Scientific was used to connect the precolumn to the PLOT column. Table 4 gives an overview of flow rate, separation gradient, PLOT column length and sample used in the different experiments.

Table 3. An overview of the approximate i.d. and length of the fused silica capillaries which served as a splitter to obtain the different flow rates in the LC-MS column switching system using a 50 µm i.d. × ~4.5 cm BMA-EDMA monolithic precolumn and a 10 µm i.d. × ~2.4 m PLOT analytical column. The approximate pressure at each flow rate during gradient separations is also given.

Flow rate (nL/min)	**Capillary i.d. (µm)**	**Capillary length (cm)**	**Pressure (bar)**
20	20	54	54
40	15	38	92
60	15	57	129
80	15	80	165

Table 4. An overview of sample, PLOT column length, flow rate, and separation gradient used in the different BMA-EDMA monolith-PLOT LC-MS column switching experiments

Type of experiment	**Sample**	**PLOT column length**	**Flow rate and Separation gradient**
Repeatability	25 µg/mL trypsinated transferrin	2.4 m	60 nL/min 0–60%B over 40 min
Loadability	5 ng/mL–100 µg/mL trypsinated cytochrome C	2.4 m	40 nL/min 5–65%B over 20 min
Effect of flow rate and gradient time on peak capacity	3 µg/mL trypsinated cytochrome C	2.4 m	20–80 nL/min 5–71%B over 30–180 min
Effect of PLOT column length on peak capacity	3 µg/mL trypsinated cytochrome C	2.4, 5.4, 8.0 m	40 nL/min 5–45%B over 45–550 min
Separation of digested rat liver sample	Tryptic digest of a gel fraction (~50 kDa) of a rat liver extract	8.0 m	40 nL/min 5–45%B over 450 min

The PLOT column was connected to a silica PicoTip emitter (FS360-20-5-D-20-C7, 5 ± 1 µm tip) with a PicoClear Union (PCU-360), both from New Objective (Woburn, MA, USA). For mass spectrometric detection, a Q-Exactive Orbitrap (Thermo Fischer Scientific, Waltham, MA, USA) equipped with a nanospray ESI source was used and operated in positive ionization mode. Q Exactive 2.1 (Thermo Fischer Scientific) was used to control the Orbitrap. The ESI voltage was set at 2.1 kV. The MS resolution was set to 35000. The scan speed with the setting used was ~7.2 scans per second. Mass spectra were aquired in the *m/z* range 400-1500. Extracted ion chromatograms (EIC) were obtained using Δ*m/z* of 20 ppm.

2.6 LC-UV system

For the simple testing of the monolithic columns, a nanoACQUITY UPLC binary solvent manager from Waters (Milford, MA, USA) served as the mobile phase delivery system. Mobile phase A consisted of 0.1% (v/v) FA in water, and mobile phase B consisted of 0.1% FA (*aq*)/ACN (10/90, v/v). The monolithic columns prepared were tested with a mobile phase flow rate of 0.5 µL/min. A four-port VICI injection valve with a 50 nL internal loop from Valco Instruments (Houston, TX, USA) was used for manual injection of samples. A 50 µm × 700 mm (G1375-87313) PEEK coated fused silica (PFS) capillary with a volume of 1.4 µL [64] from Agilent Technologies (Baden-Wurttemberg, Germany) was connected from the outlet of the binary solvent manager to the four-port injection valve. The total system gradient delay volume was >1.45 µL (>2.9 min).

A WellChrom K-2600 UV-detector from Knauer (Berlin, Germany) with a flow cell of 40 nL (8 mm light path, 25 µm i.d.) was used and operated at wavelengths of 254 or 280 nm. A PE Nelson 900 Series Interface (model 941, AD-31) from Perkin Elmer (Waltham, MA, USA) was used as the analog-to-digital (A/D) converter. Chromatograms were recorded and evaluated using TotalChrom software version 6.2.1 supplied by Perkin Elmer.

Retention times (t_M and t_R, where the retention time of uracil is t_M) and peak widths at half height ($w_{0.5}$) were manually measured using the TotalChrom software. Due to unknown problems, automatic calculations of column efficiencies (*N*) could not be carried out using the TotalChrom software. Column efficiencies ($N = 5.54 \times t_R^2/w_{0.5}^2$) for the isocratic analyses were therefore calculated with Microsoft Excel using t_R and $w_{0.5}$.

Table 5 gives an overview of the columns used in the UV-experiment. Nine PS-DVB columns (1–9) and a BMA-EDMA column, each column cut to a length of 10 cm, were used in this experiment. The 10 cm BMA-EDMA column originates from the same polymerized capillary as that of the BMA-EDMA precolumn used in the monolith-PLOT LC-MS column switching system.

Table 5. An overview of the origin of the monolithic columns used in the LC-UV system.

Column	**Column origin**
BMA-EDMA	The 10 cm column piece originates from the same polymerized capillary as that of the BMA-EDMA precolumn used in the LC-MS column switching system
PS-DVB 1	*Batch 1*. The 10 cm column pieces originate from the same pretreated and silanized capillary and polymerization mixture but separate capillaries
PS-DVB 2	
PS-DVB 3	*Batch 2*. The 10 cm column pieces originate from the same pretreated and silanized capillary and polymerization mixture but separate capillaries
PS-DVB 4	
PS-DVB 5	
PS-DVB 6	
PS-DVB 7	*Batch 3*. The 10 cm column pieces originate from the same pretreated and silanized capillary and polymerization mixture but separate capillaries
PS-DVB 8	
PS-DVB 9	

2.7 LC-MS testing of precolumns

For the LC-MS testing of a 50 µm i.d. × ~4 cm BMA-EDMA and PS-DVB precolumn, 50 pg/µL angiotensin II (with 0.1% TFA) and 3 µg/mL trypsinated cytochrome C were used as samples. Separation was performed by loading 1 µL of the sample onto the precolumn using an EASY-nLC 1000 pump and an autosampler from Thermo Fisher Scientific (Waltham, MA, USA). Mobile phase A consisted of 0.1% (v/v) FA in water. Mobile phase B consisted of 0.1% (*aq*) (v/v) FA in ACN.

For injection of angiotensin II, a 10 min gradient was used. The gradient started at 0%B and increased linearly to 95%B in 10 min. The mobile phase was kept at 0%B for 10 min prior to

the gradient for sample loading and also to make sure that there was nothing wrong with the precolumn. Separation was carried out at a flow rate of 500 nL/min. For injection of trypsinated cytochrome C, a 15 min gradient was used. The gradient started at 0%B and increased linearly to 40%B in 15 min. Separation was carried out at a flow rate of 200 nL/min.

The precolumn was connected to a 20 µm i.d. × 40 mm (1/32 in. o.d.) nano-bore stainless steel emitter with a ZDV union (SC600), both from Thermo Fisher Scientific. The other end of the precolumn was connected to a T-piece with 29 nL sweep volume from Upchurch Scientific. For mass spectrometric detection, the Q-Exactive Orbitrap equipped with nanospray ESI source was used and operated in positive ionization mode. The ESI voltage was set at 2.3 kV. Mass spectra were aquired in the *m/z* range 200-2000. Extracted ion chromatograms (EIC) were obtained using Δ*m/z* of 20 ppm.

2.8 Precolumns in monolith-PLOT LC-MS column switching system

For the testing of the two 50 µm i.d. × ~4 cm BMA-EDMA and PS-DVB precolumns (from Experimental 2.7) in a monolith-PLOT LC-MS column switching system, first the BMA-EDMA and then the PS-DVB precolumn, was coupled to a 10 µm i.d. × 2.4 m PS-DVB PLOT analytical column. Separation was carried out using a flow rate of ~40 nL/min, a gradient of 5–55%B over 30 min, and a sample of 3 µg/mL trypsinated cytochrome C. The PLOT column was connected to a 20 µm i.d. × 40 mm (1/32 in. o.d.) nano-bore stainless steel emitter with a ZDV union (SC600), both from Thermo Fisher Scientific. The ESI voltage was set at 1.8 kV. Mass spectra were aquired in the *m/z* range 350-2000. Other parameters were as described in Experimental 2.5.

The 50 µm i.d. × ~4 cm monolithic precolumns were further used in a monolith-PLOT LC-MS column switching system to study the effects of increased temperature on retention, peak width, signal intensity and peak area. First the BMA-EDMA and then the PS-DVB precolumn was coupled to the 10 µm i.d. × 2.4 m PS-DVB PLOT analytical column. Separation was performed by placing first just the precolumn and then both the precolumn and the analytical column, in a type 880 Mistral oven from Spark Holland (Emmen, Netherlands). The temperature range 20–90^{o}C was investigated. 0.5 µL of 3 µg/mL trypsinated cytochrome C was loaded onto the precolumn using an EASY-nLC 1000 pump

and an autosampler from Thermo Fisher Scientific. Mobile phase A consisted of 0.1% (v/v) FA in water. Mobile phase B consisted of 0.1% (v/v) FA in ACN. Loading conditions were as described in Experimental 2.5. Trapped analytes were fore-flushed from the precolumn onto the PLOT column at a flow rate of ~40 nL/min. The pump was set to 300 nL/min. Two T-pieces from Upchurch Scientific were used as described in Experimental 2.5. The gradient elution started at 5%B and increased linearly to 40%B in 50 min, prior to an increase to 95%B in 10 min for column washing. The PLOT column was connected to a silica PicoTip emitter as described in Experimental 2.5. For mass spectrometric detection, an LTQ Orbitrap Discovery equipped with a nanospray ionization (NSI) source from Thermo Fischer Scientific was used and operated in positive ionization mode. Xcalibur 2.0.7 (Thermo Fisher Scientific) was used to control the LTQ Orbitrap. The capillary temperature was set at 250^{o}C. The ESI voltage was set at 2.5 kV. The MS resolution was set to 15000. Mass spectra were aquired in the *m/z* range 300-2000. Extracted ion chromatograms (EIC) were obtained using $\Delta m/z$ of 20 ppm.

3. Results and discussion

In this study, 10 µm i.d. PS-DVB PLOT columns with ~0.75 µm porous layer was prepared and used together with a 50 µm i.d. BMA-EDMA monolithic precolumn in a monolith-PLOT LC-MS column switching system. PS-DVB monolithic precolumns were prepared using a binary porogenic mixture of toluene/1-dodecanol and characterized by LC-UV and LC-MS testing. Furthermore, temperature effects in a monolith-PLOT LC-MS column switching system were investigated.

3.1 PS-DVB PLOT columns

Because of the low diffusion rates of solutes in liquid mobile phases, thin-film OT-LC columns must have an i.d. of 10 µm or less to obtain efficiencies comparable to that of good packed columns [65-67]**.** The preparation of 10 µm i.d. PS-DVB PLOT columns, according to the procedure described in Experimental 2.4, in general has been uncomplicated in the sense that successful preparation has not been "operator dependent". Also, first attempts have always led to usable columns.

All the PLOT-columns were inspected with an optical microscope after completed polymerization. Each time, ±10 cm of the end parts were cut off due to partial or complete absence of a polymer layer. The absence of a polymer layer always observed at the end parts of the column probably has to do with the preparation system using the laboratory-made pressure bomb. The "normal" procedure after letting the solution flow for some time, has been to first shut the nitrogen gas valve and then plug each end of the column. It seems that this procedure leads to a loss of solution at the end parts of the column. Pictures of the end part of a freshly prepared 10 µm i.d. PLOT column were taken with a smartphone, see Figure 9. From left to right, the end part is uncut, cut by 3-4 cm, and cut by a further 4-5 cm. No polymer layer can be observed in the left picture. A thin polymer layer can be observed in the middle picture, while a fuller and more even polymer layer can be seen in the picture to the right.

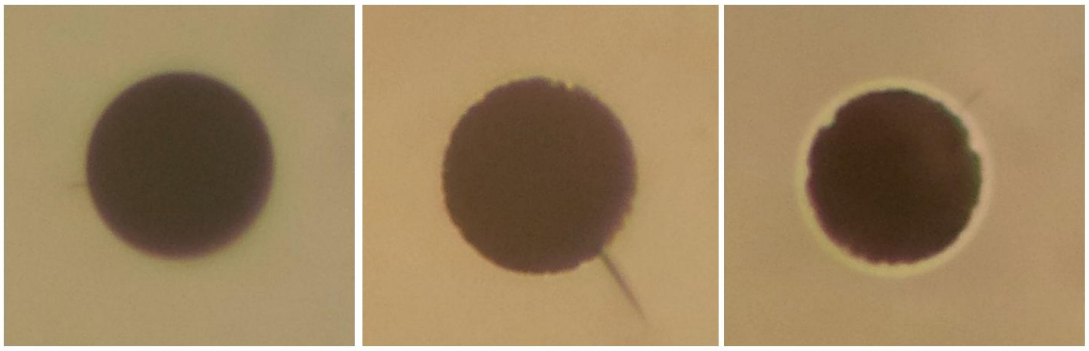

Figure 9. Pictures of the end part of a freshly prepared 10 µm i.d. PLOT column taken with a smartphone. From left to right, the end part is uncut, cut by 3-4 cm, and cut by a further 4-5 cm. Pictures taken by Magnus Røgeberg.

Figure 10 shows SEM-images of two 10 µm i.d. PS-DVB PLOT columns. The PLOT column in the image to the left, used successfully for separation of intact standard proteins and skimmed milk proteins in earlier experiments, was prepared according to the description by Yue et al. [56] with only a few practical deviations and had a film thickness of ~0.5–1 µm [58]. The volume ratio of ethanol to monomer concentration in the polymerization mixture was 60% ethanol/40% monomer. The PLOT column in the image to the right, used successfully in the PLOT-monolith LC-MS column switching system described in this thesis, was prepared with ~942 µL ethanol in the polymerization solution, corresponding to a volume ratio of approximately 70% ethanol/30% monomer in the polymerization mixture. From the SEM-picture, the film thickness was estimated to be ~0.4–0.8 µm, on average ~0.75 µm. Higher concentrations of ethanol and thus a lower percentage of monomer in the polymerization mixture likely results in thinner polymer film on the inside of the capillary wall. An advantage of having a thicker film is increased loading capacity [68], while an advantage of having a thinner film is increased permeability, allowing the use of longer columns.

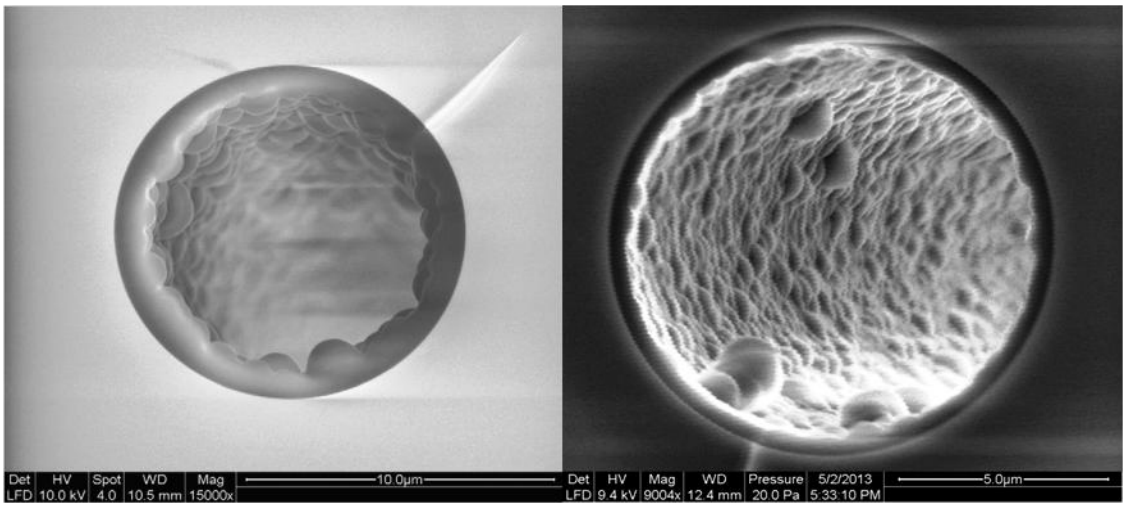

Figure 10. SEM-images of two 10 µm i.d. PS-DVB PLOT columns. Image to the left: Reprinted from [58]. The volume ratio of ethanol to monomer concentration in the polymerization mixture was 60% ethanol/40% monomer. Image to the right: The volume ratio of ethanol to monomer concentration in the polymerization mixture was ~70% ethanol/30% monomer.

PS-DVB PLOT column lengths of 2.4, 5.4 and 8.0 m were prepared to be able to use them in a monolith-PLOT LC-MS column switching system described in this study. These PLOT columns, used in combination with a monolithic precolumn, exhibited lower back pressures than the PLOT column (with higher percentage of monomer) shown to the left in Figure 10 [58]. A typical back pressure for a 2.4 m PLOT column was ~92 bar at a flow rate of 40 nL/min. Even for the longest PLOT column of 8.0 m, the back pressure was low enough (typically ~300 bar at 40 nL/min) to allow the use of an ordinary HPLC pump (≤400 bar).

3.2 Monolith-PLOT LC-MS column switching system

A simple, half-automated monolith-PLOT LC-MS column switching system, using commercially available equipment, was used for separation of tryptic digests of standard proteins and a real proteomic sample. Despite the fact that a system with narrow columns was applied, there was almost no clogging during the experiments most likely because the monolithic precolumn served as a "filter". The monolith-PLOT LC-MS column switching system was examined for its repeatability and loading capacity. Furthermore, the effect of flow rate and gradient time on peak capacity and the effect of PLOT column length on peak capacity were investigated. Finally, the system was applied to the separation of a real proteomic sample.

3.2.1 Repeatability

Good retention time repeatabilty of the LC-MS monolith-PLOT column switching system was indicated by the overlaid base peak chromatograms of three consecutive injections of 25 µg/mL trypsinated transferrin shown in Figure 11. Six peptide peaks were extracted to assess the repeatability of retention times (t_R) and peak widths at 10% of the peak height ($w_{0.1}$). Stable retention times with a relative standard deviation (RSD) of 0.2% or less were observed. The variations in peak width were characterized by RSD values ranging from 3.7 to 9.5%. Tables 6 and 7 give an overview of t_R, $w_{0.1}$ and RSD%.

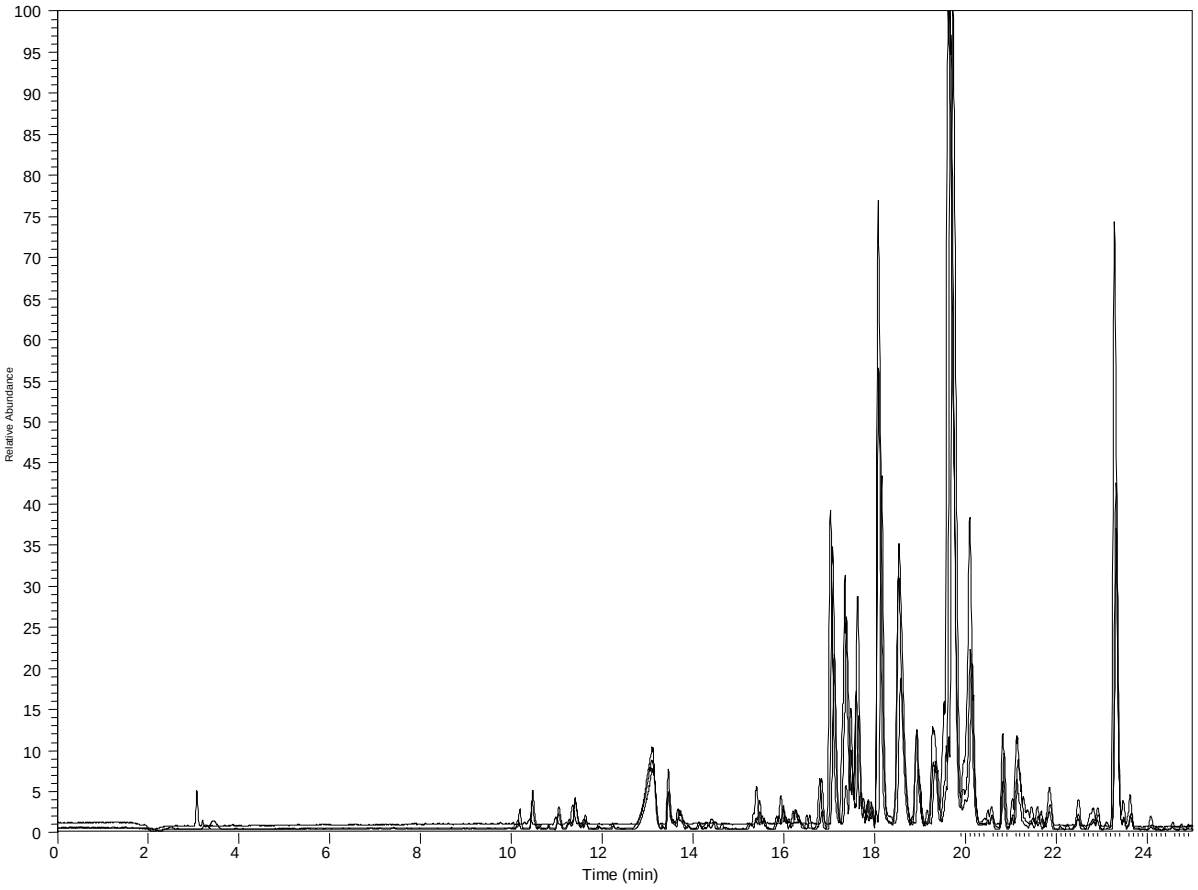

Figure 11. Overlaid base peak chromatograms of the three consecutive LC-MS separations of 25 µg/mL trypsinated transferrin. The precolumn was a 50 µm i.d. × ~4.5 cm BMA-EDMA monolith. The analytical column was a 10 µm i.d. × ~2.4 m PS-DVB PLOT column with ~0.75 µm layer thickness. Mobile phase A was 0.1% (v/v) FA in water. Mobile phase B was 0.1% FA (*aq*)/ACN (10/90, v/v). Injection volume was 500 nL. Loading conditions were 100% mobile phase A, flow rate of 0.5 µL/min and loading time of 2.5 min. Separation conditions were flow rate of 60 nL/min and gradient of 0–60% mobile phase B over 40 min. ESI was used with positive ionization mode at a voltage of 2.1 kV and a *m/z* range of 400-1500.

Table 6. An overview of the retention times (t_R) and RSD (%) of six extracted peptide peaks for three consecutive injections of trypsinated transferrin using the BMA-EDMA monolith-PLOT LC-MS column switching system. Parameters were as described in Figure 11.

***m/z* peptide**	**1. injection t_R (min)**	**2. injection t_R (min)**	**3. injection t_R (min)**	**Average t_R (min)**	**RSD (%)**
489.7492	11.60	11.64	11.64	11.63	0.2
500.7536	13.45	13.47	13.45	13.46	0.1
838.8928	17.65	17.62	17.60	17.62	0.1
657.8172	18.99	18.93	18.92	18.95	0.2
803.6308	21.16	21.13	21.14	21.14	0.1
1075.5199	23.31	23.27	23.32	23.30	0.1

Table 7. An overview of the peak widths at 10% of the peak height ($w_{0.1}$) of six extracted peptide peaks for three consecutive injections of trypsinated transferrin using the BMA-EDMA monolith-PLOT LC-MS column switching system. Parameters were as described in Figure 11.

***m/z* peptide**	**1. injection $w_{0.1}$ (sec)**	**2. injection $w_{0.1}$ (sec)**	**3. injection $w_{0.1}$ (sec)**	**Average $w_{0.1}$ (sec)**	**RSD (%)**
489.7492	13.8	12.6	11.4	12.6	9.5
500.7536	9.6	9.6	9.0	9.4	3.7
838.8928	9.6	9.6	9.0	9.4	3.7
657.8172	9.6	9.0	9.0	9.2	3.8
803.6308	13.2	13.8	12.6	13.2	4.5
1075.5199	8.4	9.6	9.0	9.0	6.7

3.2.2 Loading capacity

The loading capacity, defined as the amount of sample injected when the corresponding $w_{0.5}$ is increased by 10% over the peak width at low sample amounts [56], was determined by injecting various concentrations of trypsinated cytochrome C and measuring the corresponding $w_{0.5}$ for five extracted peptide peaks. An overview of the average $w_{0.5}$ corresponding to each concentration is given in Table 8, while a graphical illustration is shown in Figure 12.

The loading capacity of the LC-MS column switching system, applying a 10 µm i.d. × 2.4 m PS-DVB PLOT column with ~0.75 µm layer thickness together with a 50 µm i.d. × 4.5 cm BMA-EDMA precolumn, was found to be ~120 fmol for a tryptic digest of cytochrome C. Yue et al. [56] examined the loading capacities of 10 µm i.d. × 4.2 m PS-DVB PLOT columns prepared with a volume ratio of 60% ethanol/40% monomer and 70% ethanol/30% monomer. The loading capacities were ~100 fmol for angiotensin I and ~50 fmol for insulin for PLOT columns prepared with 60% ethanol/40% monomer, and ~50 fmol for angiotensin I and ~20 fmol for insulin for PLOT columns with 70% ethanol/30% monomer. This was explained by less polymer coating on the capillary wall and thus a lower loading capacity, when using higher percentage of ethanol which resulted in earlier phase separation [56]. When considering the fact that the PLOT column used in the present study was prepared using 70% ethanol/30% monomer, the value of ~120 fmol seems to indicate that analyte enrichment on the BMA-EDMA precolumn and the subsequent focusing on the PLOT column have been successful.

Table 8. An overview of the different concent[rations of trypsinated cytochrome C and the average peak width at half height ($w_{0.5}$) for five extracted peptide peaks (*m/z* = 478.2558, 478.9400, 545.2110, 713.3581, 728.8424) using the BMA-EDMA monolith-PLOT LC-MS column switching system. Parameters were as described in Figure 11, except that a flow rate of 40 nL/min and a gradient of 5–65%B over 20 min were used.

Concentration	**Loaded amount**	**Average $w_{0.5}$ (sec)**
100 µg/mL	50 ng	18.47
50 µg/mL	25 ng	13.82
20 µg/mL	10 ng	8.21
10 µg/mL	5 ng	5.60
3 µg/mL	1.5 ng	4.48
1 µg/mL	0.5 ng	3.77
100 ng/mL	50 pg	3.41
10 ng/mL	5 pg	3.47
5 ng/mL	2.5 pg	3.48

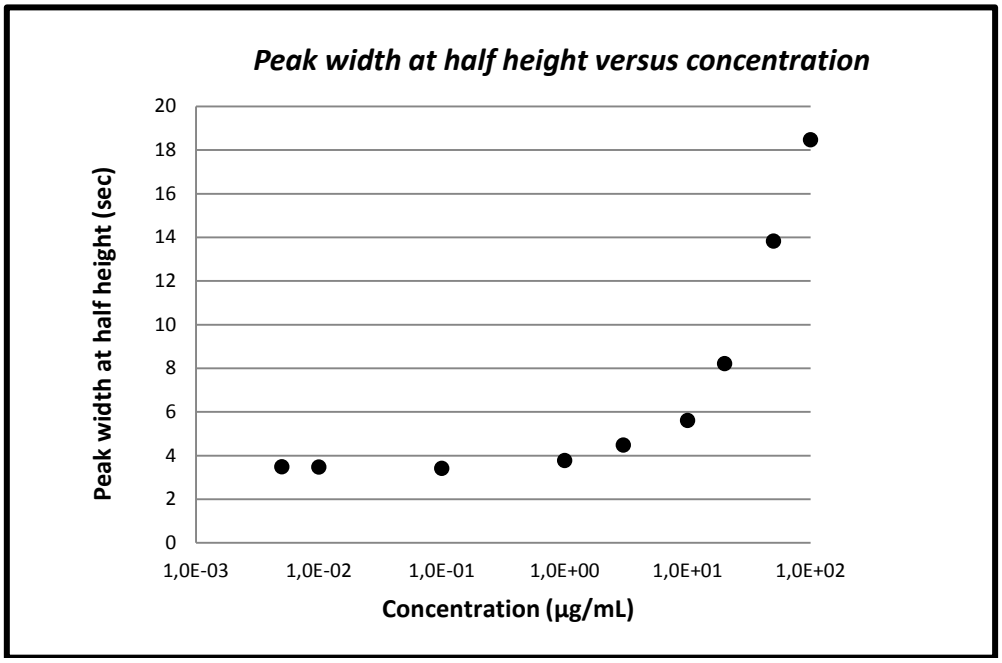

Figure 12. Peak width at half height versus concentration obtained on the BMA-EDMA monolith-PLOT LC-MS column switching system using various concentrations of trypsinated cytochrome C. Parameters and data were as described in Table 8.

3.2.3 Effect of flow rate and gradient time on peak capacity

The term peak capacity is often used as a tool for describing the resolving power of a chromatographic system in gradient separations. The peak capacity definition used throughout this study was $n_c^{**} = \frac{t_{R,n} - t_{R,1}}{W}$ where $t_{R,1}$ and $t_{R,n}$ are the first and the last eluting peptide in the tryptic digest [59]. *W* represents the peak width measured at 10% of the peak height, and was calculated from extracted ion chromatograms of five randomly selected peptides. When separation conditions (e.g. gradient steepness, flow rate) for gradient elution are varied, both the retention window and peak width will change [69, 70]. In this study, a definition of peak capacity including the retention window (rather than gradient time) has therefore been used.

The effect of flow rate and gradient time on peak capacity was investigated by using a tryptic digest of cytochrome C with flow rates of 20–80 nL/min and gradient times of 30–180 min. Peak capacity increased with increasing gradient time. Highest peak capacity was obtained with a flow rate of 40 nL/min followed by 20 nL/min at all gradient times. Overall decrease in peak capacity was seen from 40 to 60 nL/min and from 60 to 80 nL/min at all gradient times. An overview of the peak capacity values at flow rates of 20–80 nL/min and gradient times of 30–180 min is given in Table 9, while a graphical illustration is shown in Figure 13.

Since a flow rate of 40 nL/min led to highest peak capacity, 40 nL/min was applied in further experiments concerning the effect of PLOT column length on peak capacity (section 3.2.4) and the separation of a digested rat liver sample (section 3.2.5).

Table 9. An overview of peak capacity at different flow rates and gradient times using the BMA-EDMA monolith-PLOT LC-MS column switching system. A sample of 3 µg/mL trypsinated cytochrome C, flow rates of 20–80 nL/min and a gradient of 5–71%B over 30–180 min were used. Extracted peptide peaks were: *m/z* = 478.2558, 478.9400, 528.9295, 670.6595, 728.8424. Other parameters were as described in Figure 11.

$\frac{flow\ rate\ (nL/min) \rightarrow}{gradient\ time\ (\text{min}) \downarrow}$	**20**	**40**	**60**	**80**
30	65	67	56	54
60	81	83	69	68
90	89	93	81	83
120	98	101	88	87
150	101	114	100	94
180	107	117	107	94

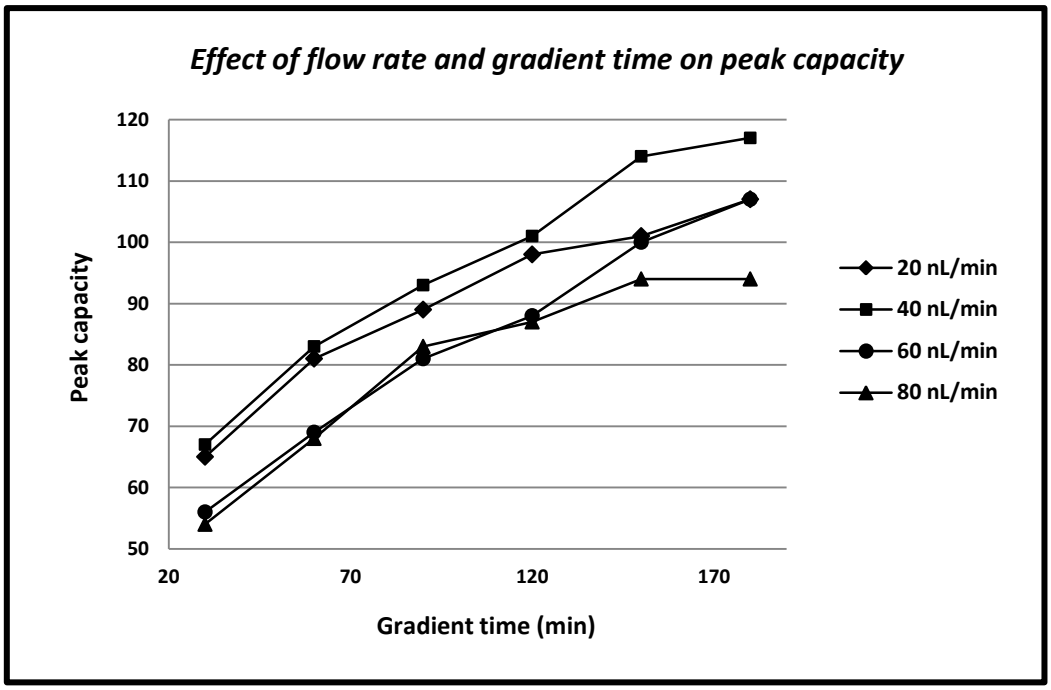

Figure 13. A graphical illustration that shows the effect of flow rate and gradient time on peak capacity using the BMA-EDMA monolith-PLOT LC-MS column switching system. Parameters and data were as described in Table 9.

3.2.4 Effect of PLOT column length on peak capacity

For the investigation of the effect of PLOT column length on peak capacity, PLOT column lengths of 2.4, 5.4 and 8.0 m at seven different gradient times in the range 45–550 min were used. Peak capacity increased with increasing gradient time for all PLOT column lengths, but seemed to flatten out after 350 min for all PLOT column lengths. Highest peak capacity was obtained using the 8.0 m PLOT column. The increase in peak capacity from PLOT column length of 2.4 m to 5.4 m was greater than from 5.4 m to 8.0 m at all gradient times.

An overview of the peak capacity values for the different PLOT column lengths are given in Table 10, while a graphical illustration is given in Figure 14. Peak capacity for the 2.4 m PLOT column at gradient time of 550 min is not included because of too low signal and broad peaks. At the shortest gradient time of 45 min, the last peak appeared at the very end of the gradient when using the 5.4 m PLOT column. In order not to "lose" any peaks, the shortest gradient was not applied with the longer PLOT column of 8.0 m.

The PLOT column of 8.0 m was made by connecting a 5.4 m and a 2.6 m PLOT column with a PicoClear Union. The successful performance of this combination column showed that it is possible to use a analytical column consisting of two connected PLOT columns in the monolith-PLOT LC-MS column switching system.

Table 10. An overview of peak capacity at seven different gradient times with three PLOT column lengths using the BMA-EDMA monolith-PLOT LC-MS column switching system. A sample of 3 µg/mL trypsinated cytochrome C, a flow rate of 40 nL/min, a gradient of 5–45%B over 45–550 min and PLOT column lengths of 2.4, 5.4 and 8.0 m were used. Extracted peptide peaks were *m/z* = 478.2558, 478.9400, 670.6595, 713.3581, 728.8424. Other parameters were as described in Figure 11.

Gradient time (min)	**PLOT length 2.4 m**	**PLOT length 5.4 m**	**PLOT length 8.0 m**
45	88	116	–
90	113	144	156
150	121	174	195
250	130	192	224
350	139	216	237
450	142	223	255
550	–	223	258

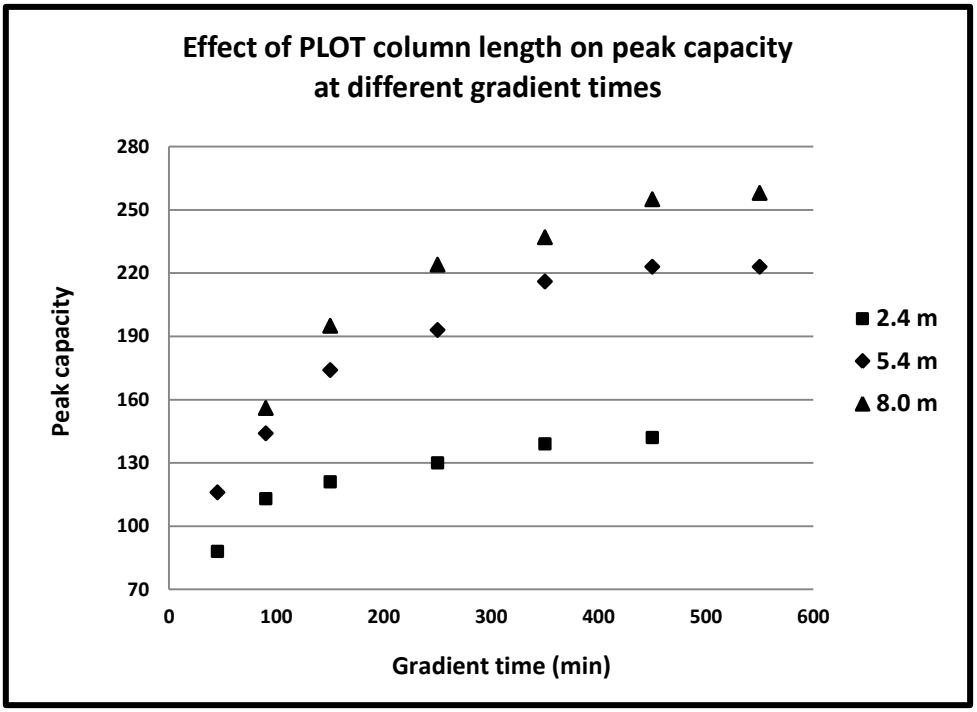

Figure 14. An overview of peak capacity at seven different gradient times with three PLOT column lengths using the BMA-EDMA monolith-PLOT LC-MS column switching system. Parameters and data are given in Table 10.

3.2.5 Separation of a digested rat liver sample

The 8.0 m PLOT column was further applied to the separation of an in-gel digested rat liver sample using a flow rate of 40 nL/min and a gradient of 5–45%B over 450 min, see Figure 15. A peak capacity of ~900 was obtained with peak width (4σ) measured at 13% of the peak height. Yue et al. [56] obtained a peak capacity of ~400 using peak width (2σ) measured at 61% of the peak height for the separation of an in-gel tryptic digest of a proteomic sample with a 10 µm i.d. × 4.2 m PS-DVB PLOT column when the off-line sample loading included a 50 µm i.d. × 4 cm PS-DVB monolithic precolumn. Although an almost as twice as long PLOT column was used in this study, the more than twice as high peak capacity value seems to demonstrate the good resolving power of the present monolith-PLOT LC-MS column switching system.

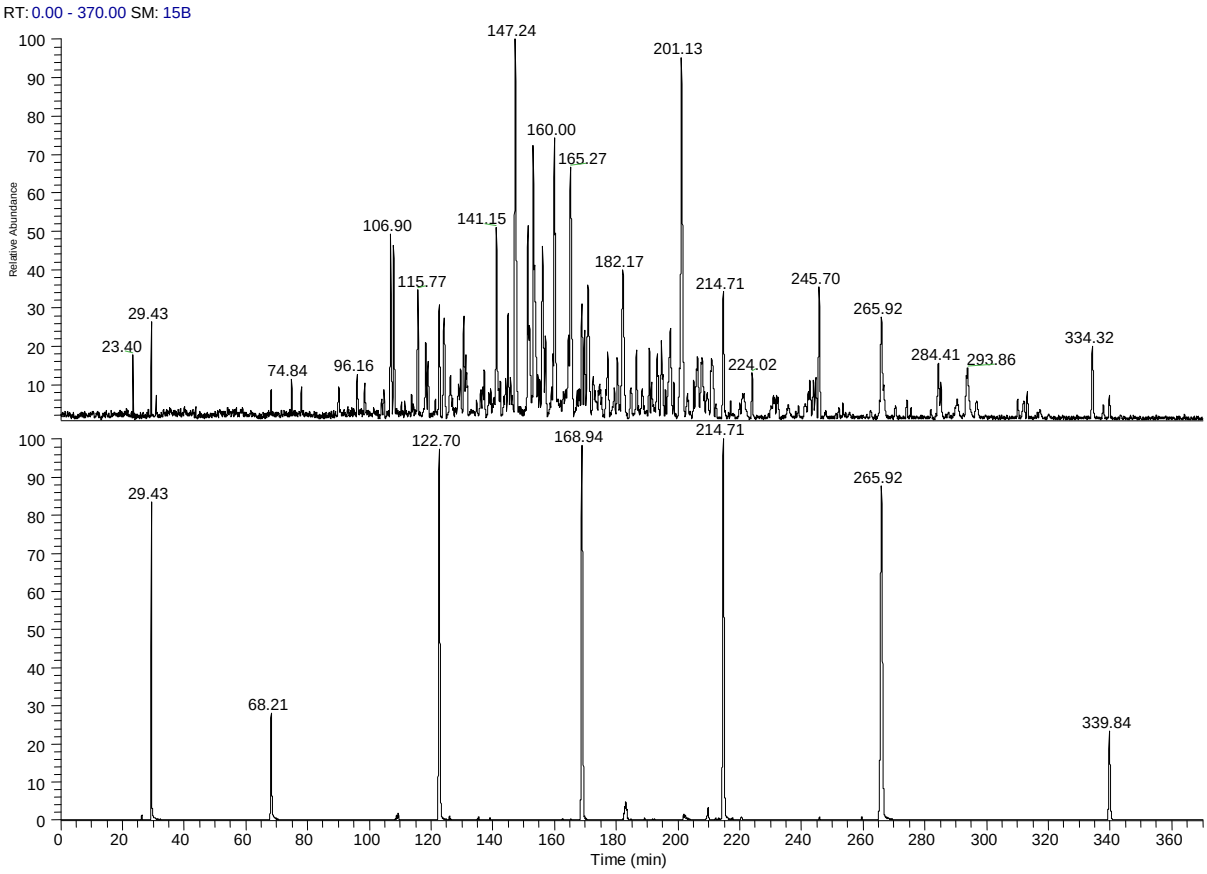

Figure 15. Top: Base peak chromatogram. Bottom: Extracted ion chromatogram. A flow rate of 40 nL/min, a 10 µm i.d. × ~8.0 m PS-DVB PLOT analytical column, a gradient of 5–45%B over 450 min and a 45 ng/µL in-gel digested rat liver sample were used. Extracted peptide peaks were *m/z* = 747.3537, 788.3969, 805.9422, 815.9759, 961.7538, 996.1733, 1045.5761. Other conditions were as described in Figure 11.

In assessing peak capacity, peak width was measured at 10%, 13%, 50% and 61% of the peak height and calculated by extracting seven peptides covering the whole retention window, see Table 11. Peak width measured at 61% of the peak height gave the highest peak capacity followed by 50%, 13% and 10%. This is not surprising since peak widths get smaller when measured at higher % of peak height, see Figure 16.

Table 11. An overview of peak capacity at 10%, 13%, 50% and 61% of the peak height. Parameters were as described in Figure 15.

	10% (at $w_{0.1}$)	**13%** (at 2σ)	**50%** (at $w_{0.5}$)	**61%** (at 4σ)
Retention window (min)	340.78	340.78	340.78	340.78
Average peak width (min)	0.8214	0.7743	0.4300	0.3586
Peak capacity	415	440	793	950

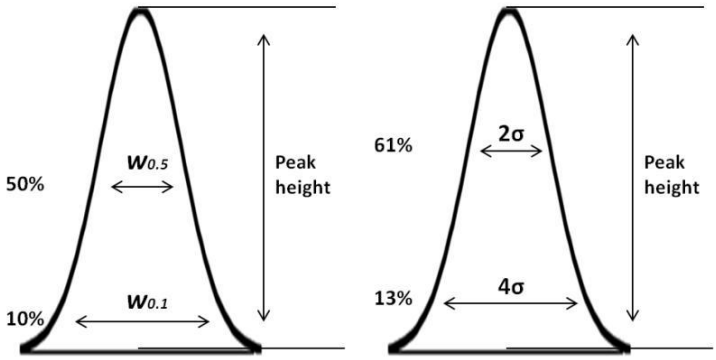

Figure 16. Widths ($w_{0.1}$, 2σ, $w_{0.5}$, 4σ) of a gaussian peak at various heights (10%, 13%, 50% and 61%).

3.3 PS-DVB monolithic columns using a binary porogenic mixture of toluene and 1-dodecanol

Considering the fact that a 50 µm i.d. BMA-EDMA monolithic column, prepared according to the procedure described in Experimental 2.4, was successfully used as a precolumn together with a 10 µm i.d. PS-DVB PLOT analytical column in a monolith-PLOT LC-MS column switching system as described earlier, the main interest of this study was to prepare and characterize 50 µm i.d. PS-DVB monolithic precolumns which could be used as an alternative to 50 µm i.d. BMA-EDMA precolumns. The choice of precolumns with an i.d. of 50 µm was first and foremost based on the successful use of the 50 µm i.d. BMA-EDMA monolithic precolumns. The approximate column volume was calculated when considering the use of larger and smaller i.d. precolumns, see Table 12. While the volume of a 75 µm i.d. column is too large (being almost the same as that of the PLOT column), the volume of a 30 µm i.d. column is too small, which may lead to lower loading capacities compared with a 50 µm i.d. column. Furthermore, preparation of 50 µm i.d. monolithic columns is from a practical point of view easier and less time-consuming than narrower (30 µm i.d. or less) columns.

Table 12. The approximate volume of a PLOT column and monolithic precolumns with different i.d.. The precolumn length of 4 cm is the shortest length that can be used in a monolith-PLOT LC-MS column switching system described in 3.2.

Column	**Approximate volume (nL)**
10 µm i.d. × 2.4 m PLOT	188
75 µm i.d. × 4 cm monolith	177
50 µm i.d. × 4 cm monolith	79
30 µm i.d. × 4 cm monolith	28

3.3.1 Column preparation

Choice of appropriate porogens for the preparation of monoliths still must mainly depend on experimentation and experience. But it is desirable to include both good and poor porogens

in the polymerization mixture so that the permeability can be adjusted by varying the ratio between the two types of porogens [71]. This is in contrast to the preparation of PLOT columns where a single solvent is used in the polymerization mixture. For the preparation of monoliths from styrene and DVB, the use of toluene or THF and long-chain alcohols (such as 1-dodecanol) as porogenic mixtures has been described during the early years of monolith development. Such mixtures still remain popular and have been routinely used [27, 29, 50, 71]. This is why a porogenic mixture of toluene (good porogen) and 1-dodecanol (poor porogen) was chosen for this study.

Figure 17 is a SEM-image of a 50 µm i.d. PS-DVB monolithic column prepared according to the procedure described in Experimental 2.4 using a binary porogenic mixture of toluene and 1-dodecanol. For the PS-DVB monolithic column shown in Figure 17, the total monomer to porogen ratio was 40/60 (wt%). The higher the percentage of monomers in the polymerization mixture, the lower is the permeability of the resulting monolith due to formation of smaller macropores. In most cases, the monomer to porogen ratio should be lower than 50% to be able to get a reasonable solvent flow within the operating pressure limits of LC instrumentation. A too low percentage of monomers, on the other hand, would lead to decreased density and rigidity of the resulting monolith [71].

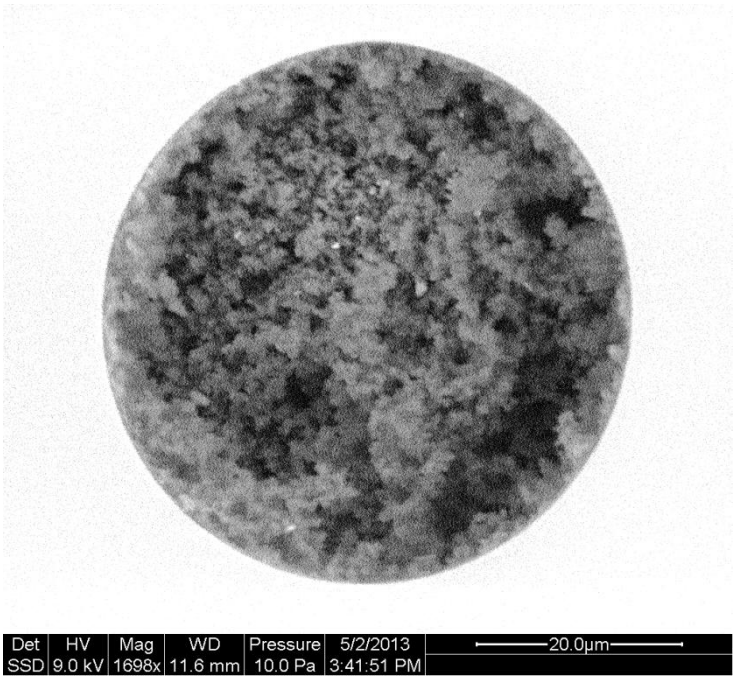

Figure 17. A SEM-image of a 50 µm i.d. PS-DVB monolithic column using a binary porogenic mixture of 13% toluene and 47% 1-dodecanol (wt.%).

When preparing 50 µm i.d. PS-DVB monolithic columns, the same pretreatment and silanization steps as for the 10 µm i.d. PS-DVB PLOT columns were applied (see Appendix 6.1 for detailed description). Pretreatment by alkaline etching (using NaOH) and a silanization process involving a solution of silanizing reagent γ-MAPS, solvent DMF and inhibitor DPPH with no water present during the whole process, resulted in good attachment of the formed monolith to the inner wall of the capillary, see Figure 18. During synthesis of organic polymers, which are known to suffer from solvent-induced swelling or contraction, modification of the capillary inner wall prior to the polymerization step is of great importance for proper chemical attachment of the monolith formed. But a high degree of γ-MAPS coverage on the inner capillary surface does not always guarantee high mechanical strength and a good homogeneity of the monolithic columns [29, 72].

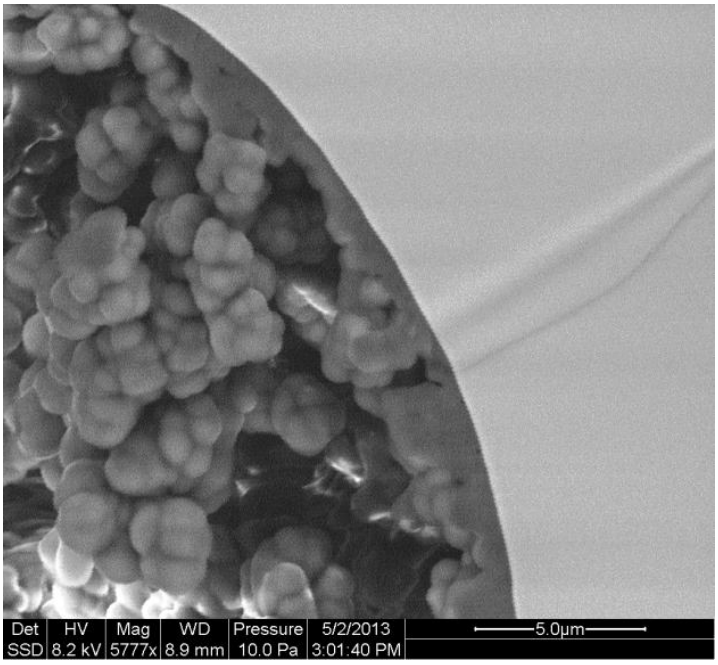

Figure 18. A SEM-image of a 50 µm i.d. PS-DVB monolithic column using a binary porogenic mixture of 13% toluene and 47% 1-dodecanol (wt.%) showing the good attachment of the monolith to the inner wall of the capillary.

The most time-consuming and practically challenging part during monolithic column synthesis was the preparation of the polymerization mixture. Pore size and pore morphology of organic monoliths are strongly dependent on the composition of the polymerization mixture [50, 51]. The polymerization mixture was therefore prepared by accurate weighing

of all chemicals to four decimal places on an analytical balance. The same glass vial was used throughout the weighing process. The weighing always started with AIBN, then the monomers, followed by the porogens. Each solution was transferred using an appropriate micropipette, dropwise for adjustment of the last two decimals, into the glass vial containing the already accurately weighed AIBN. The balance with the glass vial with a lid on was zeroed after each weighing before continuing with the next solution. One disadvantage with this weighing process is that transfer of too much solution cannot be corrected. This disadvantage is avoided if syringes are used for the weighing, which is why first weighing attempts were done using syringes. The balance with the empty syringe was zeroed and thereafter, the syringe containing the appropriate solution was weighed. The amount of solution in the syringe was adjusted until the desired weight was shown on the balance. However, some practical difficulties were also experienced with use of syringes. First, the size of the available syringes had to be considered. The syringe containing the appropriate solution had to fit inside the space of the analytical balance. Secondly, placing the syringe on the balance the same way each time (while making small adjustments) was not always easy. Thirdly, depending on the chemical solution, the process of drawing up the solution into the syringe and making small adjustments to achieve the accurate weight was difficult. All these factors considered, preparation of polymerization mixtures was therefore carried out using micropipettes and not syringes.

One practical difficulty in connection with the preparation of PS-DVB columns was related to the melting point of 1-dodecanol (24^{o}C). In total, three batches of PS-DVB monolithic columns were prepared. During preparation of batch 1 and 2 columns, 1-dodecanol was in liquid form, and no extra care (compared to other chemicals) had to be taken when preparing and homogenizing the polymerization mixture. However, when batch 3 columns were being prepared at a later time, the laboratory temperature was lower (below 24^{o}C) so that 1-dodecanol was in solid form. Before the actual weighing process, the bottle of 1-dodecanol had to be placed in luke warm water for melting. Furthermore, when homogenizing the polymerization mixture in an ultrasonic bath, warm water had to be used. When prepared polymerization mixture was solidified and became turbid after ultrasonication because the temperature of the ultrasonic bath water was too low, this mixture was not used for polymerization.

After completed pretreatment and silanization, the capillary was each time cut into lengths of ~25 cm. Using the laboratory-made pressure bomb described in Experimental 2.4, the polymerization mixture was forced through the ~25 cm long capillaries, one by one. All the filled capillaries were thereafter put into the same oven for polymerization at the same conditions.

3.3.2 Testing of columns using a LC-UV system

To characterize the prepared columns and their potential as precolumns in a monolith-PLOT LC-MS column switching system, simple tests were carried out by repeated injections of two sample solutions consisting of 0.7 mg/mL toluene (with 0.5 µg/mL uracil) and 0.2 mg/mL LHRH (with 5% ACN), using the LC-UV system described in Experimental 2.6.

Three batches of PS-DVB columns (nine columns in total) were tested. A piece of a BMA-EDMA column from the same batch as that of the BMA-EDMA precolumn used successfully in the LC-MS column switching system, was also included in the testing to be able to make comparisons with the PS-DVB columns. All the tested columns were cut to a length of ~10 cm.

Table 13 gives an overview of average retention factor (k) and column efficiency (N) for three repeated injections of 0.7 mg/mL toluene (with 0.5 µg/mL uracil). Isocratic analyses were carried out using 45%B with the BMA-EDMA column and 55%B with all the PS-DVB columns. Otherwise, the experimental conditions were the same.

Table 13. An overview of average retention factor (*k*) and column efficiency (*N*) for three repeated injections of 0.7 mg/mL toluene (with 0.5 µg/mL uracil) applying the LC-UV system described in Experimental 2.6, with detection at 254 nm.

Batch	**Column**	**k** $\left(\frac{t_R - t_M}{t_M}\right)$	**N** $\left(5.54 \frac{t_R^2}{w_{0.5}^2}\right)$
	BMA-EDMA	1.56	5931
1	PS-DVB 1	1.70	596
	PS-DVB 2	1.74	767
2	PS-DVB 3	1.87	1648
	PS-DVB 4	1.77	815
	PS-DVB 5	1.76	910
	PS-DVB 6	1.81	675
3	PS-DVB 7	1.86	278
	PS-DVB 8	1.89	286
	PS-DVB 9	1.79	259

Although the average values for retention factors (RSD ranging from 0 to 4.4%) are only approximate, it could still be seen that the retention factors for the PS-DVB columns at 55%B overall were higher compared with that of the BMA-EDMA column at 45%B. Hence, there seems to be significantly more retention of toluene on the PS-DVB columns.

The fact that toluene had larger retention on the PS-DVB columns compared to the BMA-EDMA column, may be due to greater hydrophobicity of the PS-DVB columns. This would be in line with the investigation by Peroni et al. [53], where contact angle measurements showed that the hydrophobicity was higher for PS-DVB monoliths than BMA-EDMA monoliths, both monoliths having been prepared using the same binary porogenic mixtures as the columns used in this experiment.

Another possible reason for the enhanced retention of toluene in the PS-DVB columns could be related to the difference in chemical structure between the BMA-EDMA and the PS-DVB columns, see Figure 19. Although PS-DVB monoliths basically interact with analytes through Van der Waals forces due to their hydrophobic structure, PS-DVB monoliths can also interact with analytes (in this case toluene, which is an aromatic hydrocarbon) through π-π interactions of the aromatic rings that make up the sorbent structure [73]. This

assumption is also supported by the fact that LHRH had a somewhat higher retention on the BMA-EDMA compared to PS-DVB.

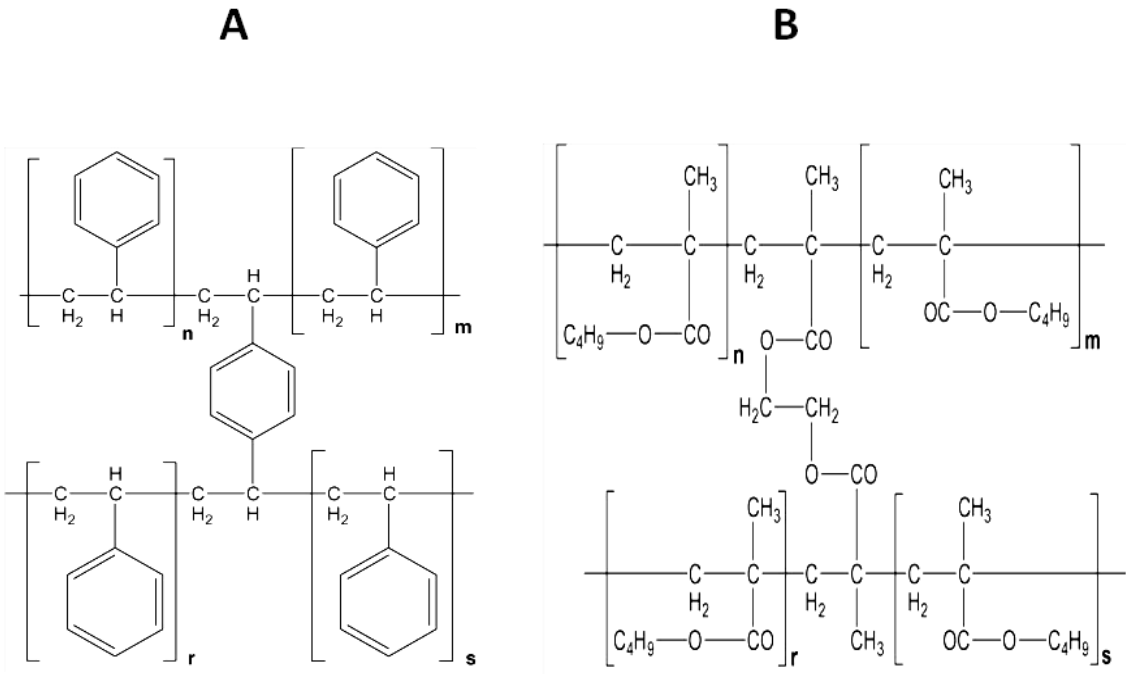

Figure 19. Chemical structure of a polystyrene monolith (A) and a poly(butyl methacrylate) monolith (B). Reprinted from [41].

The actual column efficiency values are most likely lower than the values shown in Table 13 since the manual calculations using $N = 5.54 \times t_R^2/w_{0.5}^2$ do not take into account peak tailing and peak shape. Despite the fact that the column efficiency values are only approximate, it is still possible to see some characteristics.

The efficiency of the BMA-EDMA column was higher than that of all the PS-DVB columns. The calculated efficiency for the BMA-EDMA column was ~6000, while that of PS-DVB column 3, showing the highest column efficiency amongst all the PS-DVB columns, was ~1600. This shows that these PS-DVB columns may be less suited for separation of small compounds such as toluene compared to the BMA-EDMA column. Column efficiency of batch 3 PS-DVB columns (no. 7–9), centering around 270, was two to three times lower than that of the rest of the PS-DVB columns which, aside from column no. 3, exhibited a column efficiency of ~750. The approximate back pressure, shown in the chromatographic system, was ~90 bar for batch 3 PS-DVB columns while that of batch 1 and 2 PS-DVB columns was

centered around 35 bar, see Table 14. Although this may not bear any direct relation to the lower column efficiency of batch 3 PS-DVB columns, it is something to take note of as a possible connection. The lower efficiency may be due to a greater degree of structural inhomogeneity of batch 3 PS-DVB columns, which in turn may be due to difficult batch-to-batch reproducibility of these columns.

Table 14. An overview of the approximate back pressure data shown in the chromatographic system during the isocratic analyses applying the LC-UV-system. The mobile phase composition was 45%B for BMA-EDMA column and 55%B for all the PS-DVB columns.

Batch	**Column**	**Approximate back pressure (bar)**
	BMA-EDMA	159
1	PS-DVB 1	58
	PS-DVB 2	27
2	PS-DVB 3	27
	PS-DVB 4	34
	PS-DVB 5	34
	PS-DVB 6	27
3	PS-DVB 7	83
	PS-DVB 8	83
	PS-DVB 9	103

Table 15 gives an overview of average retention time (t_R) and peak width at half height ($w_{0.5}$) for three repeated injections of 0.2 mg/mL LHRH (with 5% ACN). Gradient separations were carried out using 0–100%B over 10 min. The experimental conditions were the same for all columns during gradient analyses.

Table 15. An overview of average retention time (t_R) and peak width at half height ($w_{0.5}$) for three repeated injections of LHRH solution applying the LC-UV-system. A UV-wavelength of 280 nm was used with gradient elution from 0 to 100%B in 10 min.

Batch nr.	**Column**	**Average t_R**	**Average $w_{0.5}$**
	BMA-EDMA	8.29	0.40
1	PS-DVB 1	8.08	0.29
	PS-DVB 2	8.08	0.41
2	PS-DVB 3	7.83	0.23
	PS-DVB 4	7.86	0.25
	PS-DVB 5	7.85	0.28
	PS-DVB 6	7.71	0.24
3	PS-DVB 7	7.69	Peak Splitting
	PS-DVB 8	7.73	
	PS-DVB 9	7.83	

The measured t_R was centered around 8 min for all columns with RSD ranging from 0.1 to 2.3%. The retention of LHRH was somewhat higher on the BMA-EDMA column. The overall repeatability for retention times seemed to be quite good. As can be seen from Table 15, the retention time was approximately the same for both the BMA-EDMA and the PS-DVB columns. This is not surprising considering the fact that a very steep gradient was used.

For the batch 1 and 2 PS-DVB columns, the measured values of $w_{0.5}$ was ~0.30, with RSD ranging from 0.0 to 6.5%. Peak splitting was observed for all the batch 3 PS-DVB columns. This can indicate poorer capacity of these columns compared to the batch 1 and 2 PS-DVB columns. Three overlaid chromatograms, using the same scale, are shown in Figure 20. Peak splitting can be seen in the chromatogram to the right which represents a batch 3 PS-DVB column, as opposed to the left chromatogram representing the BMA-EDMA column and the middle chromatogram representing a batch 2 PS-DVB column.

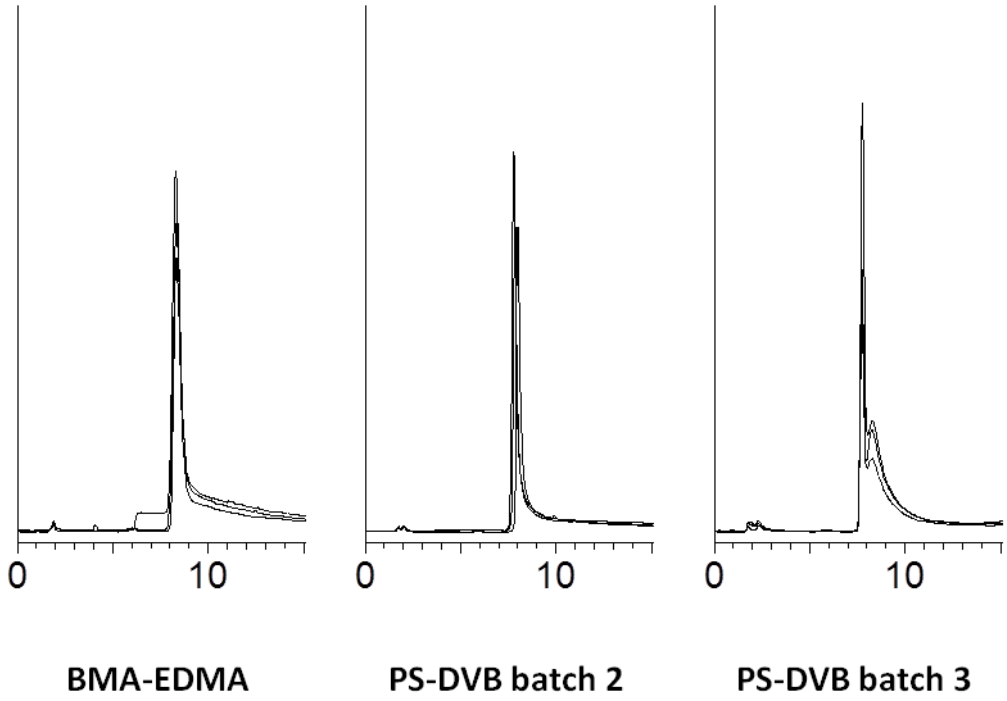

Figure 20. Overlaid chromatograms of three injections of 0.2 mg/mL LHRH (dissolved in water with 5% ACN). The same scale is used. Mobile phase A was 0.1% (v/v) FA in water. Mobile phase B was 0.1% FA (*aq*)/ACN (10/90, v/v). Separation conditions were flow rate of 0.5 µL/min and gradient of 0–100%B over 10 min. Injection volume was 50 nL. Injected amount of LHRH was 10 ng. UV-wavelength was 280 nm. Column (50 µm i.d. × 10 cm) used from left was BMA-EDMA, PS-DVB from batch 2 and PS-DVB from batch 3.

Since both the BMA-EDMA and PS-DVB columns exhibited sufficient retention of toluene with molecular mass of ~100 and LHRH with molecular mass of ~900, it was of interest to investigate the retention of dipeptides with hydrophobic side chains having a molecular mass of ~300, lying between the mass of toluene and LHRH. Three dipeptide samples, consisting of 0.2 mg/mL glycyl-L-tryptophan, 0.2 mg/mL L-alanyl-L-tryptophan and 0.6 mg/mL L-leucyl-L-tryptophan, were used. The same gradient (0–100%B over 10 min) and detection wavelength (280 nm) as for LHRH were used. All dipeptide peaks appeared at around 2 min in the chromatogram for all columns.

The fact that there was sufficient retention of LHRH, but not of dipeptides on both the BMA-EDMA and PS-DVB columns seems to indicate that analyte size and hydrophobicity play a role, see Table 16. There was, however, also sufficient retention of toluene on both the BMA-EDMA and PS-DVB columns, although toluene is, as can be seen from Table 16, smaller in size than the dipeptides. Reasons for insufficient retention of dipeptides may be

related to size and insufficient hydrophobicity, while a reason for sufficient retention of toluene may be related to hydrophobicity and π-π interactions.

Table 16. Structure and molecular mass (MW) of compounds used for testing the BMA-EDMA and PS-DVB monolithic columns applying the LC-UV system.

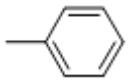	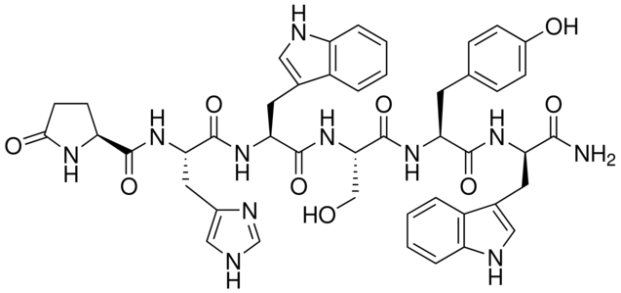	
Toluene MW 92.14	**[D-Trp^{6}]-LHRH Fragment 1-6** MW 887.94	
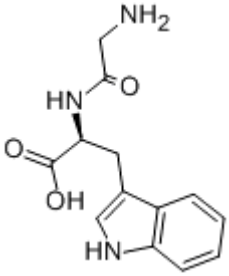	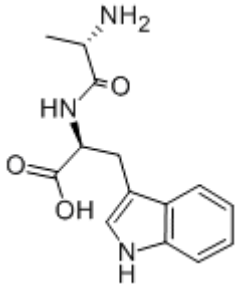	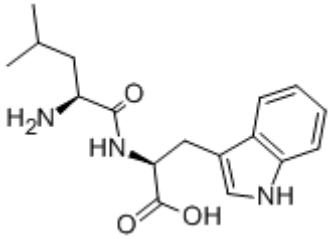
Glycyl-L-Tryptophan MW 261.28	**L-Alanyl-L-Tryptophan** MW 275.30	**L-Leucyl-L-Tryptophan** MW 317.38

Although only a few compounds were used for testing the columns, it was still of interest to make a comparison between the prepared PS-DVB columns and the BMA-EDMA column and between the three batches of PS-DVB columns. The tests showed that there was sufficient retention of both toluene and LHRH on the PS-DVB columns, as on the BMA-EDMA column. All the PS-DVB columns were quite similar with regard to retention factor of the tested compounds. The fact that batch 3 PS-DVB columns, with lower column efficiency values and peak splitting, did not perform as well as batch 1 and 2 PS-DVB columns, may simply be an indication of difficult batch-to-batch reproducibility of these columns. The difficulty could be related to the inherent structural inhomogeneity of porous polymeric monoliths. In the creation of matter, a free radical polymerization is principally

robust and easily accomplishable. But on a molecular and nanoscale level, it is a process that cannot be controlled [74]. The uncontrolled phase separation between growing cross-linked polymer material and porogenic solvent may result in coarsening of the monolithic structure which inherently leads to heterogeneous macroporous monoliths. Both axial and radial heterogeneities significantly contribute to band broadening [74].

The LC-UV tests gave no definite answer as to whether PS-DVB columns are suitable as precolumns for PS-DVB PLOT analytical columns. However, the tests give an indication that some of the "successful" (batch 1 and 2) PS-DVB columns may be candidates for such use. These alternative precolumns were prepared to be able to use them for trapping of tryptic peptides. LHRH, with a molecular mass of ~900, can be seen as a "typical" peptide from a tryptic digest. The fact that there was somewhat less retention of LHRH on the PS-DVB columns compared to the BMA-EDMA column, may indicate the suitability of these PS-DVB columns for separating large analytes within a reasonable time. To get better knowledge, a PS-DVB column, together with a BMA-EDMA column, were studied further in LC-MS experiments.

3.4 Comparison of BMA-EDMA and PS-DVB precolumns

The BMA-EDMA precolumn and one PS-DVB precolumn from batch 2 (nr. 4) were further tested in an LC-MS system. Both the precolumns were cut to a length of ~4 cm. These two precolumns were used throughout all experiments described in section 3.4. The same five peptide peaks were extracted in all experiments of section 3.4 after injections of trypsinated cytochrome C. In all the extracted chromatograms, the five peptide peaks are shown in the same order.

3.4.1 LC-MS testing of precolumns

The retention time for angiotensin II was approximately the same ((1)4.60 and (1)4.49 min) on both the BMA-EDMA and the PS-DVB precolumn, see Figure 21. This is not surprising considering the fact that a very steep gradient was used (0-95%B over 10 min with a loading time of 10 min at 0%B prior to gradient). A higher signal intensity (*NL*) was obtained with the PS-DVB precolumn, 5.89E7 versus 9.40E6 for the BMA-EDMA precolumn, while the peak area was approximately the same for both columns, ~4.05E8. To make sure that the broader peak observed with the BMA-EDMA column was not related to poor/improper connections, tests were also carried out with the BMA-EDMA precolumn (cut to 4 cm) used successfully in the monolith-PLOT LC-MS column switching system described earlier. Similar results (broad peaks) were observed. This observation is consistent with the findings from the earlier LC-UV testing where the peak width of LHRH was found to be larger for the BMA-EDMA column compared to most of the PS-DVB columns (Table 15). Injections of angiotensin II also indicated that the PS-DVB precolumn can produce a much narrower peak than the BMA-EDMA precolumn. Although peak tailing could be observed for the PS-DVB precolumn, this problem would most likely be "solved" through refocusing on a PLOT analytical column.

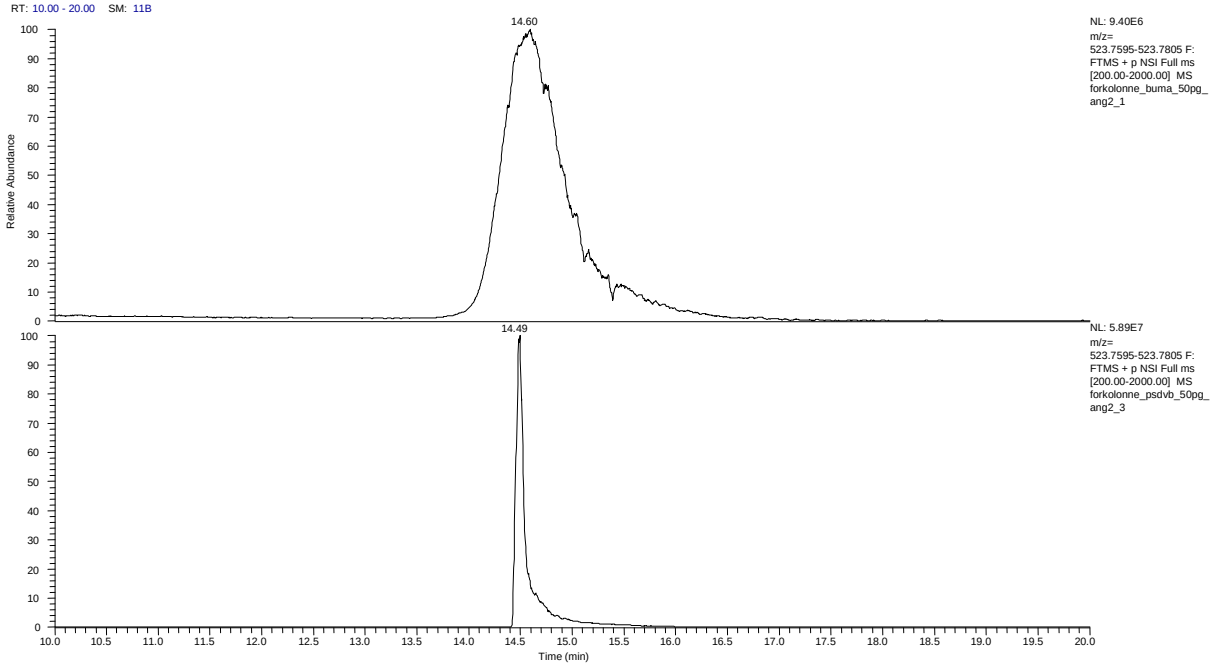

Figure 21. Extracted ion chromatograms of 50 pg/µL angiotensin II. The columns used were 50 µm i.d. × ~4 cm **BMA-EDMA monolith (top)** and 50 µm i.d. × ~4 cm **PS-DVB monolith (bottom)**. Mobile phase A was 0.1% (v/v) FA in water. Mobile phase B was 0.1% (v/v) FA in ACN. Flow rate was 500 nL/min. Gradient was 0–95%B over 10 min including loading time of 10 min at 0%B prior to gradient. Sample amount loaded was 50 pg. Extracted peptide peak was *m/z* = 523.77.

Injections of trypsinated cytochrome C showed that better separation could be obtained with the PS-DVB precolumn, see Figures 22 and 23. The PS-DVB precolumn produced narrower peaks and gave higher signals. The peaks obtained with the BMA-EDMA precolumn seem to be "smeared out". Table 17 gives an overview of retention times and signal intensities of five extracted peptide peaks. As can be seen from Table 17, the peptides appear in the same order. The retention times were shorter when the BMA-EDMA precolumn was used.

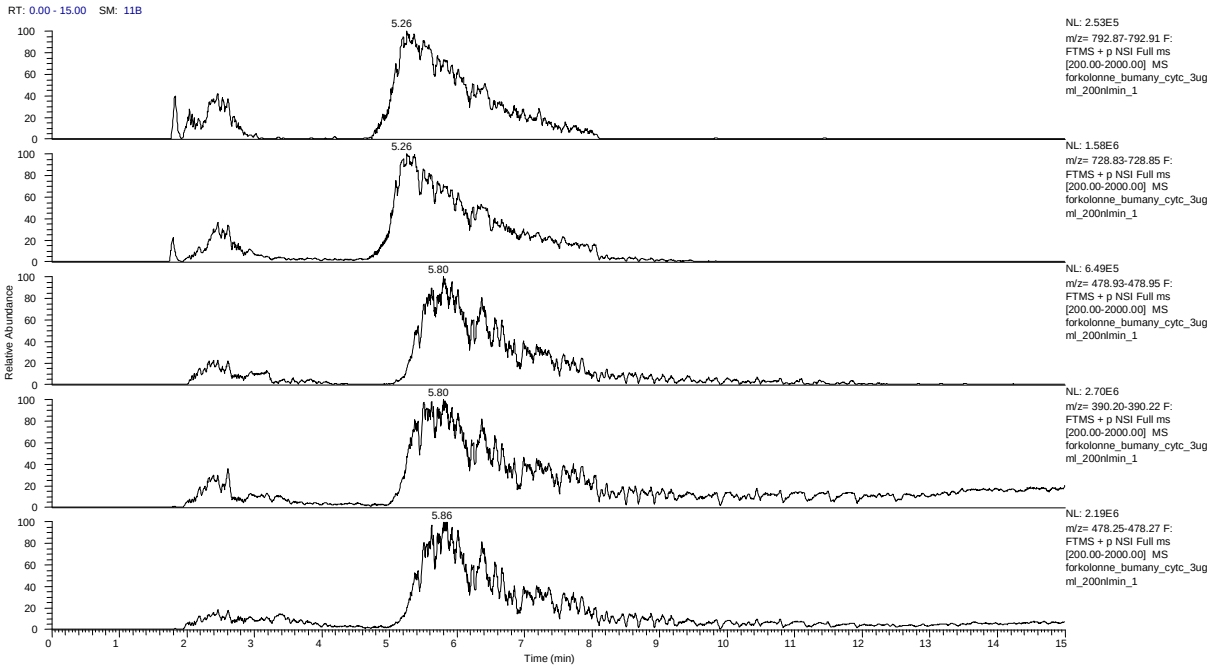

Figure 22. Extracted ion chromatograms of of 3 µg/mL trypsinated cytochrome C. The column used was a 50 µm i.d. × ~4 cm **BMA-EDMA monolith**. Mobile phase A was 0.1% (v/v) FA in water. Mobile phase B was 0.1% (v/v) FA in ACN. Flow rate was 200 nL/min. Gradient was 0–40%B over 15 min. Sample amount loaded was 3 ng. Extracted peptide peaks were *m/z* = 792.89, 728.84, 478.94, 390.21, 478.26. (Loading time is not included in the chromatogram.)

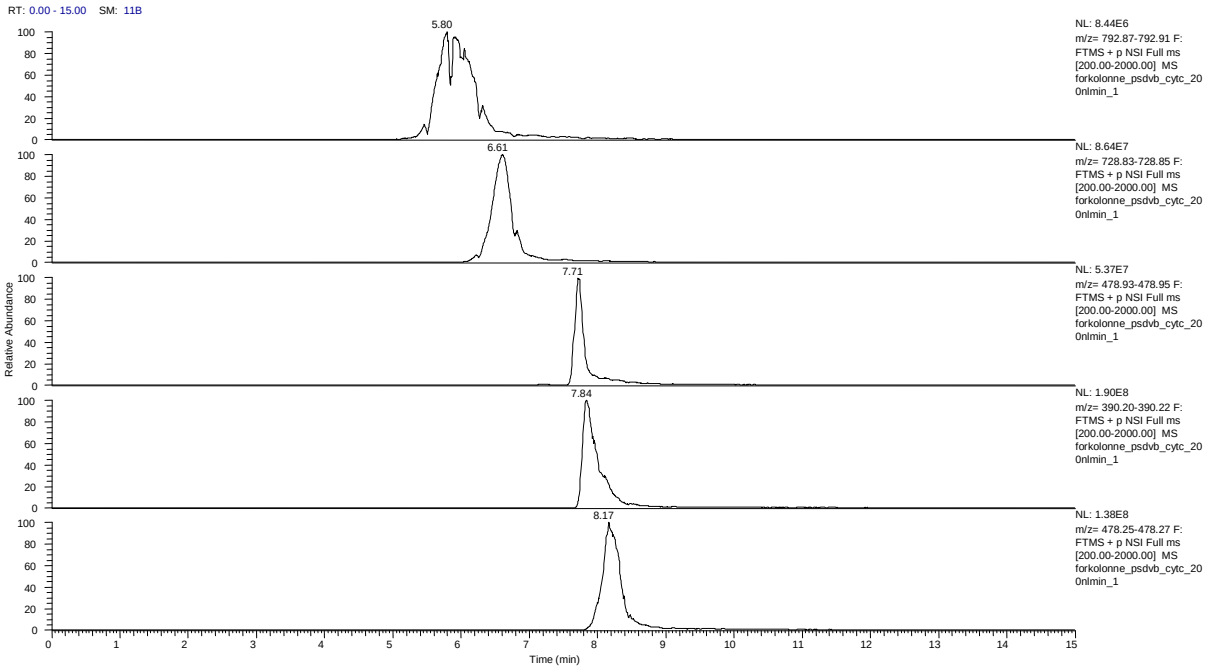

Figure 23. Extracted ion chromatograms of 3 µg/mL trypsinated cytochrome C. The column used was a 50 µm i.d. × ~4 cm **PS-DVB monolith**. Other parameters were as described in Figure 22.

Table 17. An overview of retention times (t_R) and signal intensities (*NL*) of five extracted peptide peaks from LC-MS testing of 50 µm i.d. × ~4 cm BMA-EDMA and PS-DVB monolithic precolumns using a sample of 3 µg/mL trypsinated cytochrome C. Parameters were as described in Figures 22 and 23.

Extracted peptide	BMA-EDMA	PS-DVB	BMA-EDMA	PS-DVB
m/z	**t_R (min)**	**t_R (min)**	**NL**	**NL**
792.89	5.26	5.80	2.53E5	8.44E6
728.84	5.26	6.61	1.58E6	8.64E7
478.94	5.80	7.71	6.49E5	5.37E7
390.21	5.80	7.84	2.70E6	1.90E8
478.26	5.86	8.17	2.19E6	1.38E8

3.4.2 Precolumns in monolith-PLOT LC-MS column switching system

Retention times, peak widths ($w_{0.5}$ and $w_{0.1}$), signal intensities (*NL*) and peak areas (*MA*) for five extracted peptide peaks were compared using each of the two ~4 cm monolithic precolumns in the monolith-PLOT LC-MS column switching system described earlier (Experimental 2.6), see Figures 24, 25 and Table 18. The peptides seem to appear in similar order as when only the precolumn was used (section 3.4.1). The retention times were generally shorter when the PS-DVB precolumn was used (contrary to what was observed when only the precolumns were used). Although the differences were very small, we do not at present have an explanation for this behavior. Since a fore-flush system was used, we would have expected the same retention relation as when only the precolumns were used.

The peak widths were smaller when the BMA-EDMA precolumn was used. This may indicate that better refocusing was obtained when the BMA-EDMA precolumn is used together with the PLOT analytical column. When used alone (section 3.4.1), higher column efficiency was achieved with the PS-DVB precolumn. However, this does not necessarily mean that better refocusing is obtained when the PS-DVB precolumn is used in combination with a PLOT analytical column. Although the peaks were broader when using PS-DVB precolumn-PLOT system, higher signals and larger peak areas were obtained compared with the BMA-EDMA precolumn-PLOT system. The high signals may be an indication of good trapping.

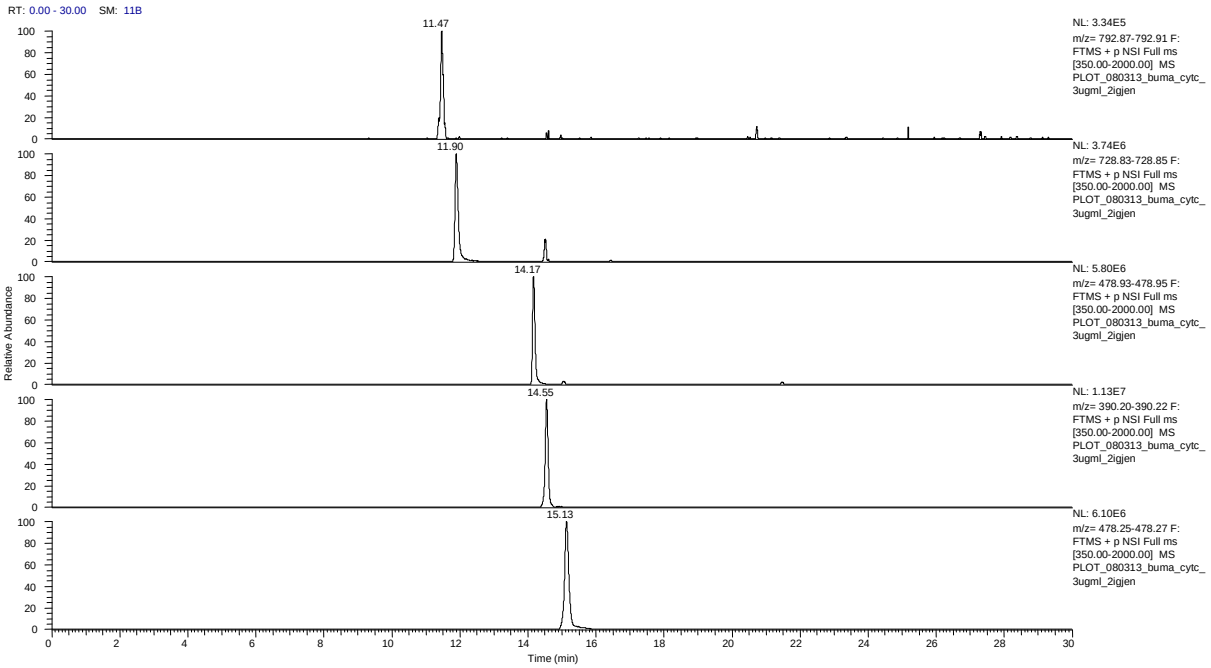

Figure 24. Extracted ion chromatograms of 3 µg/mL trypsinated cytochrome C. The 50 µm i.d. × ~4 cm **BMA-EDMA monolithic precolumn** was coupled to the 10 µm i.d. × 2.4 m PS-DVB PLOT analytical column. Mobile phase A was 0.1% (v/v) FA in water. Mobile phase B was 0.1% (*aq*) FA/ACN (10/90, v/v). Loading conditions were 100% mobile phase A, flow rate of 0.5 µL/min and loading time of 2.5 min. Separation conditions were flow rate of ~40 nL/min and gradient of 5–55%B over 30 min. Sample amount loaded was 1.5 ng. Extracted peptide peaks were *m/z* = 792.89, 728.84, 478.94, 390.21, 478.26

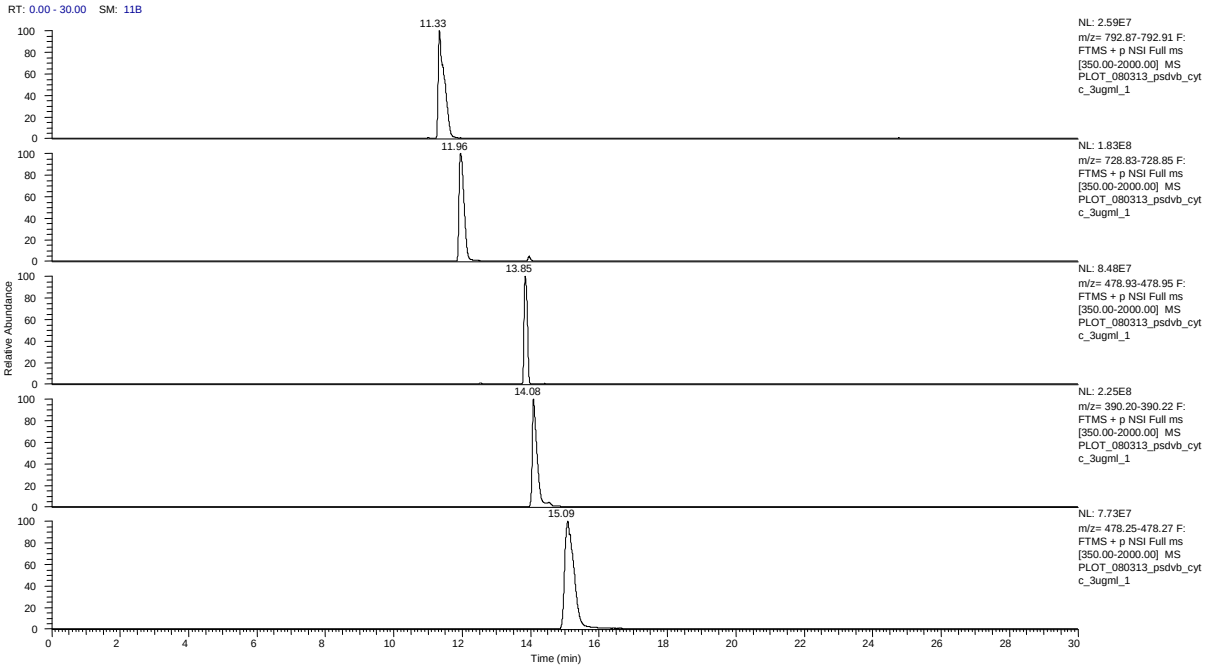

Figure 25. Extracted ion chromatograms of 3 µg/mL trypsinated cytochrome C. The 50 µm i.d. × ~4 cm **PS-DVB monolithic precolumn** was coupled to the 10 µm i.d. × 2.4 m PS-DVB PLOT analytical column. Other parameters were as described in Figure 24.

Table 18. Testing of the two 50 µm i.d. × ~4 cm monolithic precolumns coupled to the 10 µm i.d. × 2.4 m PS-DVB PLOT analytical column in the monolith-PLOT LC-MS column switching system. An overview of retention times (t_R), peak widths ($w_{0.5}$ and $w_{0.1}$), signal intensities (*NL*) and peak areas (*MA*) for five extracted peptide peaks. Parameters were as described in Figures 24 and 25.

peptide	BMA-EDMA					PS-DVB				
m/z	t_R **(min)**	$w_{0.5}$ **(sec)**	$w_{0.1}$ **(sec)**	***NL***	***MA***	t_R **(min)**	$w_{0.5}$ **(sec)**	$w_{0.1}$ **(sec)**	***NL***	***MA***
792.89	11.47	5.4	13.2	3.34E5	1.99E6	11.33	13.2	22.2	2.59E7	3.19E8
728.84	11.90	5.4	12.0	3.74E6	2.50E7	11.96	9.6	16.4	1.83E8	1.85E9
478.94	14.17	4.8	9.0	5.80E6	2.93E7	13.85	7.2	10.2	8.48E7	5.70E8
390.21	14.55	5.4	10.8	1.13E7	6.85E7	14.08	8.4	17.4	2.25E8	2.21E9
478.26	15.13	7.2	16.2	6.10E6	5.42E7	15.09	18.0	31.2	7.73E7	1.41E9

3.4.3 Study of temperature effects in monolith-PLOT LC-MS column switching system

Precolumn and analytical column temperatures of 20, 40, 60, 80 and 90^{o}C were investigated to study the effect of increased temperature on retention, peak width, signal intensity and peak area.

The general trend which was observed with the use of increased temperatures was (sometimes to a great extent) lower signal intensities and peak areas and modest reduction in retention times. At 60^{o}C and above, often no clear peaks could be observed in the extracted ion chromatograms (see Appendix 6.4). Retention times, peak widths, signal intensities and peak areas were therefore measured and compared using temperatures of 20^{o}C and 40^{o}C.

3.4.3.1 Precolumn temperatures of 20°C and 40°C

Retention time, peak width, signal intensity and peak area for five extracted peptide peaks at BMA-EDMA precolumn temperatures of 20°C and 40°C were investigated, see Figures 26, 27 and Table 19. All the retention times were shortened by ~6 min at 40°C. The two early eluting peaks were much broader at 40°C. Although peak widths at half height ($w_{0.5}$) for the three late eluting peaks were smaller at 40°C, the values for peak widths at 10% of the peak height ($w_{0.1}$) were larger. Furthermore, all the signal intensities at 40°C were reduced, by ~55%−93%. All the peak areas were also reduced by ~28%−84%.

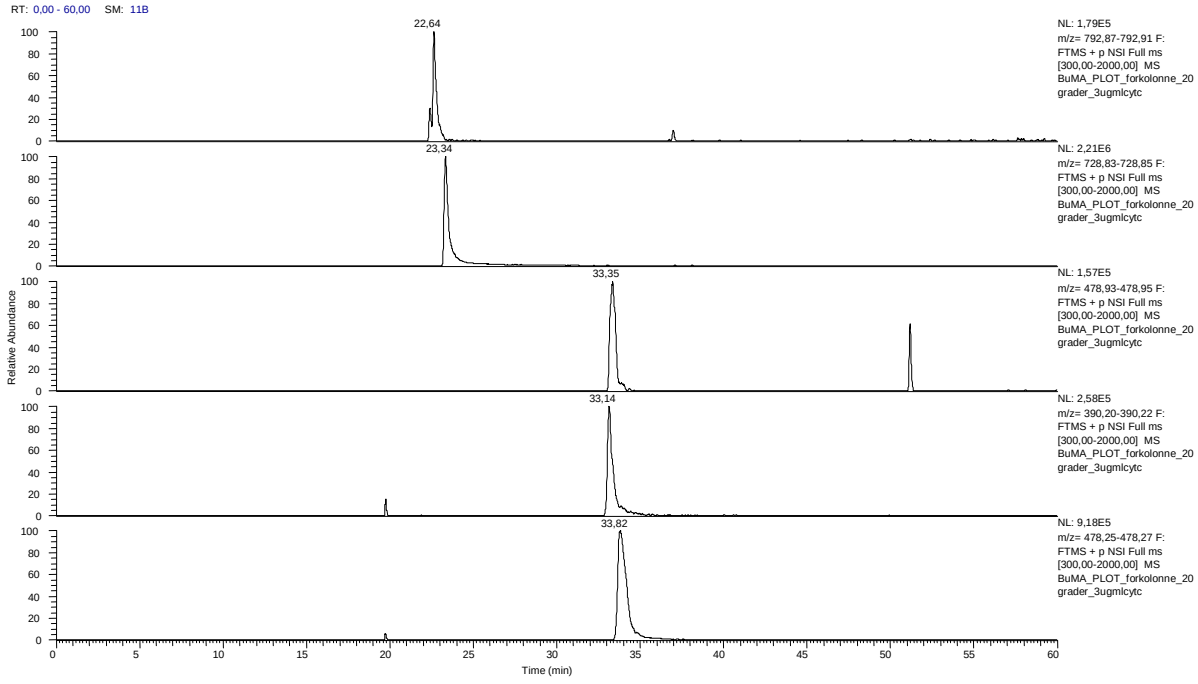

Figure 26. Extracted ion chromatograms of 3 µg/mL trypsinated cytochrome C. The 50 µm i.d. × ~4 cm BMA-EDMA monolithic precolumn was coupled to the 10 µm i.d. × 2.4 m PS-DVB PLOT analytical column in a LC-MS system. Only the precolumn was thermostated. **Temperature of BMA-EDMA precolumn was 20°C.** Mobile phase A was 0.1% (v/v) FA in water. Mobile phase B was 0.1% (v/v) FA in ACN. Loading conditions were 100% mobile phase A, flow rate of 0.5 µL/min and loading time of 2.5 min. Separation conditions were flow rate of ~40 nL/min and gradient of 5–40%B over 50 min. Sample amount loaded was 1.5 ng. Extracted peptide peaks were *m/z* = 792.89, 728.84, 478.94, 390.21, 478.26

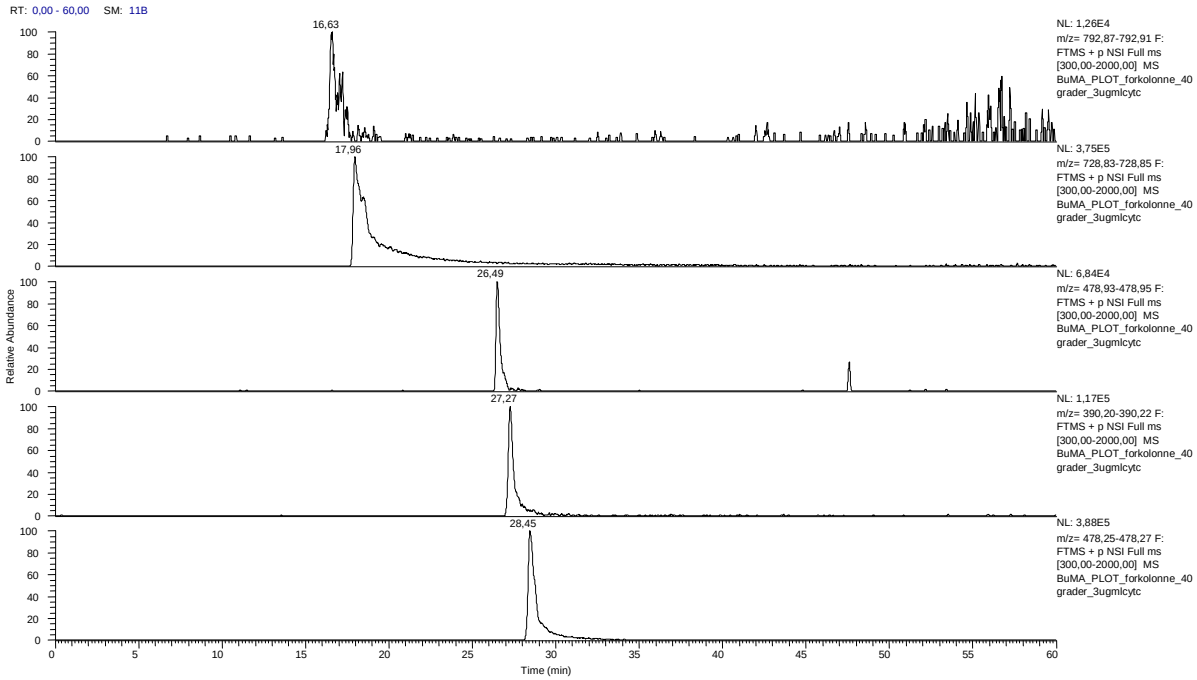

Figure 27. Extracted ion chromatograms of 3 μg/mL trypsinated cytochrome C. The 50 μm i.d. × ~4 cm BMA-EDMA monolithic precolumn was coupled to the 10 μm i.d. × 2.4 m PS-DVB PLOT analytical column in a LC-MS system. Only the precolumn was thermostated. **Temperature of BMA-EDMA precolumn was 40°C.** Other conditions were as described in Figure 26.

Table 19. BMA-EDMA monolithic precolumn coupled to PS-DVB PLOT analytical column in a LC-MS system. An overview of retention times (t_R), peak widths at half height ($w_{0.5}$) and 10% of the peak height ($w_{0.1}$), signal intensities (*NL*) and peak areas (*MA*) for five extracted peptide peaks at **BMA-EDMA precolumn temperatures of 20°C and 40°C**. Conditions were as described in Figures 26 and 27.

peptide	Temperature **20°C**					Temperature **40°C**				
m/z	t_R **(min)**	$w_{0.5}$ **(sec)**	$w_{0.1}$ **(sec)**	***NL***	***MA***	t_R **(min)**	$w_{0.5}$ **(sec)**	$w_{0.1}$ **(sec)**	***NL***	***MA***
792.89	22.64	12.0	43.8	1.79E5	3.12E6	16.63	20.4	78.0	1.26E4	5.00E5
728.84	23.34	14.4	43.8	2.21E6	3.84E7	17.96	47.4	217.2	3.75E5	2.76E7
478.94	33.35	24.0	36.0	1.57E5	3.83E6	26.49	15.0	40.8	6.84E4	1.26E6
390.21	33.14	19.2	45.0	2.58E5	6.04E6	27.27	17.4	50.4	1.17E5	2.96E6
478.26	33.82	33.6	64.8	9.18E5	3.34E7	28.45	26.4	75.6	3.88E5	1.24E7

With regard to the PS-DVB precolumn, narrower peaks were obtained at 40°C, see Figures 28, 29 and Table 20. All the values for $w_{0.5}$ and $w_{0.1}$ were reduced at 40°C. The retention times, however, were only shortened by ~1 min at 40°C. Both the signal intensities and peak areas at 40°C were generally much lower than at 20°C, three of the peaks being reduced by almost 100%.

It is difficult to know the exact reason for the loss of analytes shown by the overall reduction in signal intensity and peak area. Applying high temperature on the short monolithic precolumn and a lower temperature on the PLOT column in combination with a low flow rate may have a negative effect on proper refocusing. The same trend of loss in signal intensity and peak area was also observed by Tore Vehus when only the PLOT analytical column temperature was increased (see Appendix 6.4).

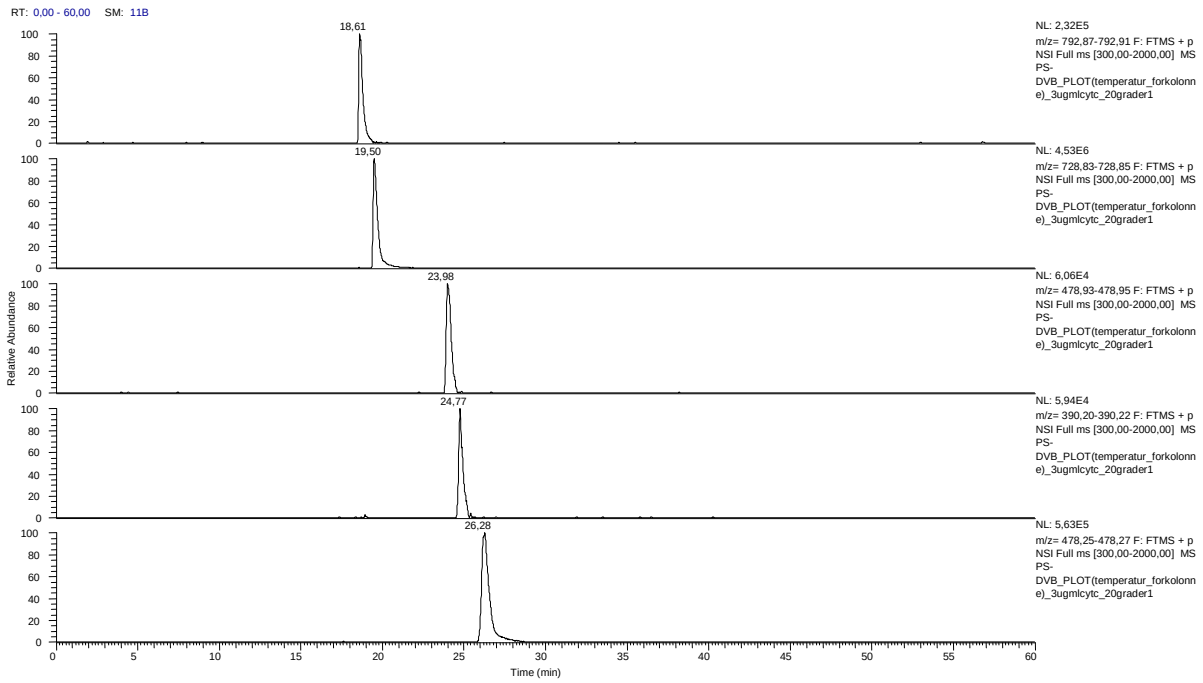

Figure 28. Extracted ion chromatograms of 3 µg/mL trypsinated cytochrome C. The 50 µm i.d. × ~4 cm PS-DVB monolithic precolumn was coupled to the 10 µm i.d. × 2.4 m PS-DVB PLOT analytical column in a LC-MS system. Only the precolumn was thermostated. **Temperature of PS-DVB precolumn was 20°C**. Other conditions were as described in Figure 26.

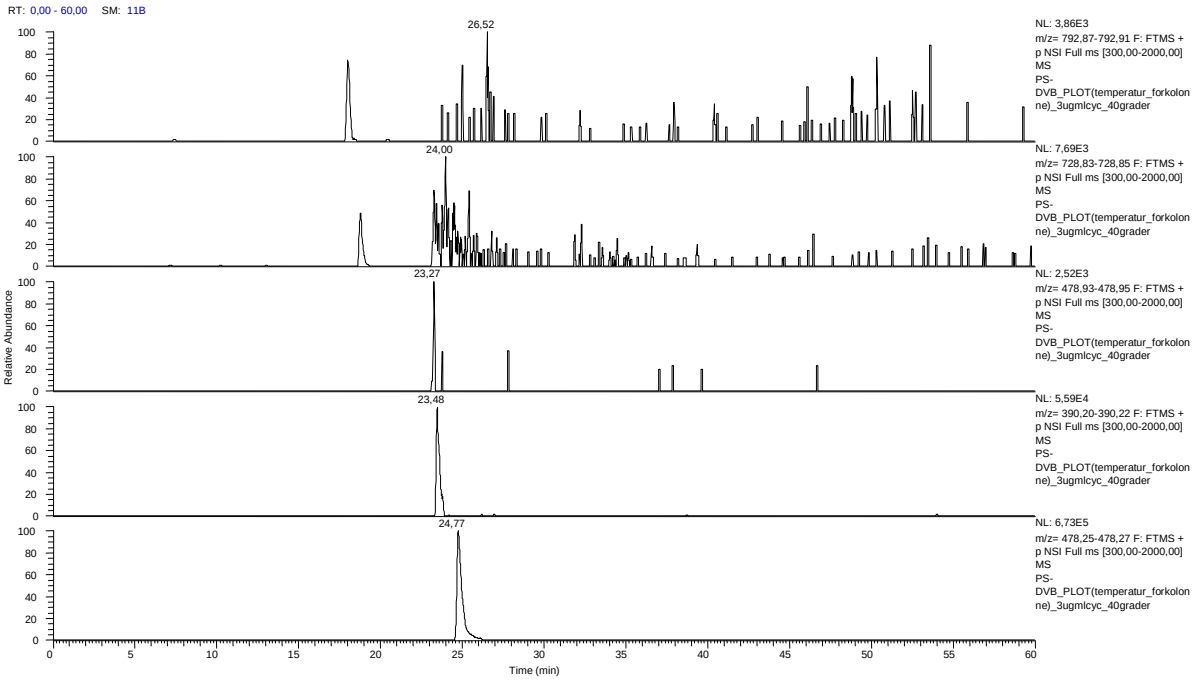

Figure 29. Extracted ion chromatograms of 3 μg/mL trypsinated cytochrome C. The 50 μm i.d. × ~4 cm PS-DVB monolithic precolumn was coupled to the 10 μm i.d. × 2.4 m PS-DVB PLOT analytical column in a LC-MS system. Only the precolumn was thermostated. **Temperature of PS-DVB precolumn was 40°C**. Other conditions were as described in Figure 26.

Table 20. PS-DVB monolithic precolumn coupled to PS-DVB PLOT analytical column in a LC-MS system. An overview of retention times (t_R), peak widths at half height ($w_{0.5}$) and 10% of the peak height ($w_{0.1}$), signal intensities (*NL*) and peak areas (*MA*) for five extracted peptide peaks at **PS-DVB precolumn temperatures of 20°C and 40°C**. Conditions were as described in Figures 28 and 29.

peptide	Temperature **20°C**					Temperature **40°C**				
m/z	t_R **(min)**	$w_{0.5}$ **(sec)**	$w_{0.1}$ **(sec)**	***NL***	***MA***	t_R **(min)**	$w_{0.5}$ **(sec)**	$w_{0.1}$ **(sec)**	***NL***	***MA***
792.89	18.61	14.4	33.6	2.32E5	4.23E6	18.00	13.2	24.6	3.86E3	4.12E4
728.84	19.50	15.6	34.8	4.53E6	8.91E7	18.80	12.0	26.4	7.69E3	5.45E4
478.94	23.98	19.2	38.4	6.06E4	1.30E6	23.27	4.8	9.6	2.52E3	1.50E4
390.21	24.77	16.2	36.0	5.94E4	1.08E6	23.48	13.8	30.6	5.59E4	8.08E5
478.26	26.28	27.0	56.4	5.63E5	1.88E7	24.77	17.4	40.8	6.73E5	1.49E7

At precolumn temperature of 20°C, the retention times were shorter and the peak widths overall smaller when the PS-DVB precolumn was used. The signal intensities were lower for the two early eluting peaks (~1.3 to 2 times) but higher for the three late eluting peaks (~1.6 to 4.3 times) when the BMA-EDMA precolumn was used.

The gain of shorter retention times and narrower peaks in general do not seem to outweigh the overall loss of signal intensities and reduced peak areas. Increasing precolumn temperature from 20°C to 40°C does not seem to be beneficial for obtaining better separation.

3.4.3.2 Precolumn and analytical column temperatures of 20°C and 40°C

The trend of shorter retention times, overall smaller values for $w_{0.5}$, and reduced signal intensities and peak areas was also observed when both precolumn and analytical column temperature were increased from 20°C to 40°C.

At precolumn and analytical column temperature of 20°C, the signal intensities were higher and the peak areas larger when the PS-DVB precolumn was used, see Tables 21 and 22. With the PS-DVB precolumn, retention times of the two early eluting peaks were somewhat larger, while that of the three late eluting peaks were smaller compared with the BMA-EDMA precolumn. The values of $w_{0.5}$ were smaller or greater depending on the compound when using the PS-DVB precolumn. More peak tailing was observed when the BMA-EDMA precolumn was used.

Retention times of the two early eluting peaks were shortened by ~6 min at BMA-EDMA precolumn and PLOT column temperature of 40°C, see Figures 30, 31 and Table 21. Peak widths of the two early eluting peaks, both $w_{0.5}$ and $w_{0.1}$, were reduced at 40°C. However, for the three late eluting peaks, either the peaks were broader or no obvious peaks could be found. At 40°C, all the signal intensities were reduced by ~45%−98% while all the peak areas were reduced by ~39%−87%.

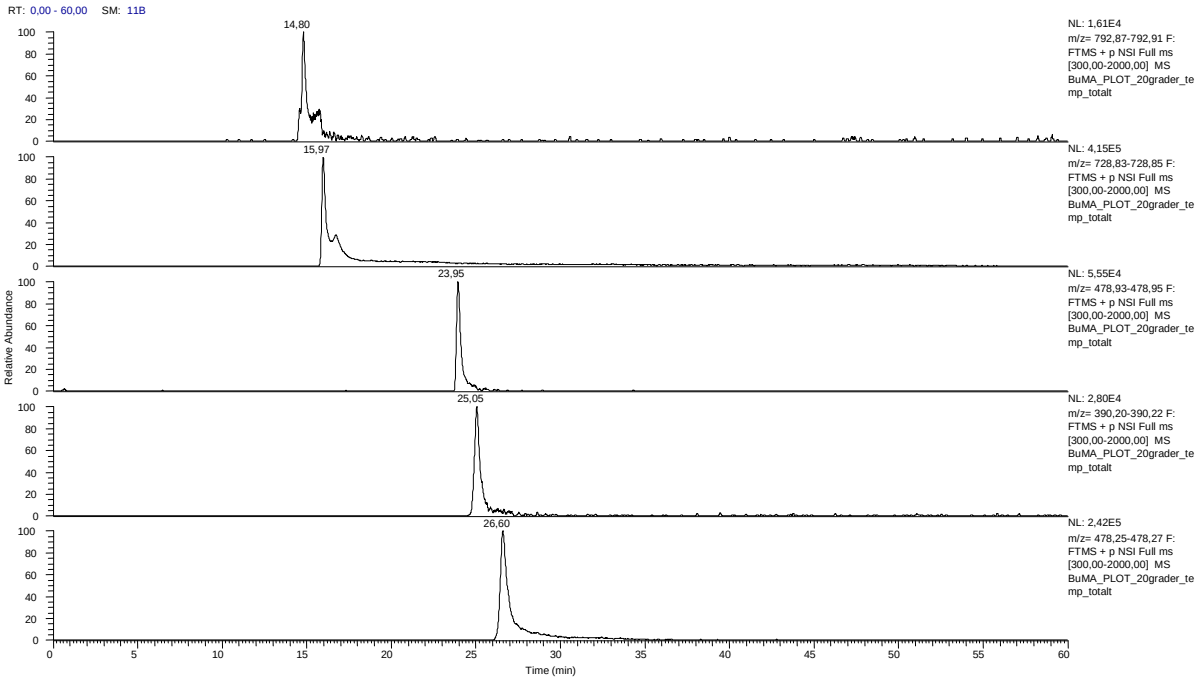

Figure 30. Extracted ion chromatograms of 3 µg/mL trypsinated cytochrome C. Both the 50 µm i.d. × ~4 cm BMA-EDMA monolithic precolumn and the 10 µm i.d. × 2.4 m PS-DVB PLOT analytical column were thermostated in a LC-MS system. **BMA-EDMA precolumn and PLOT column temperature was 20°C**. Other conditions were as described in Figure 26.

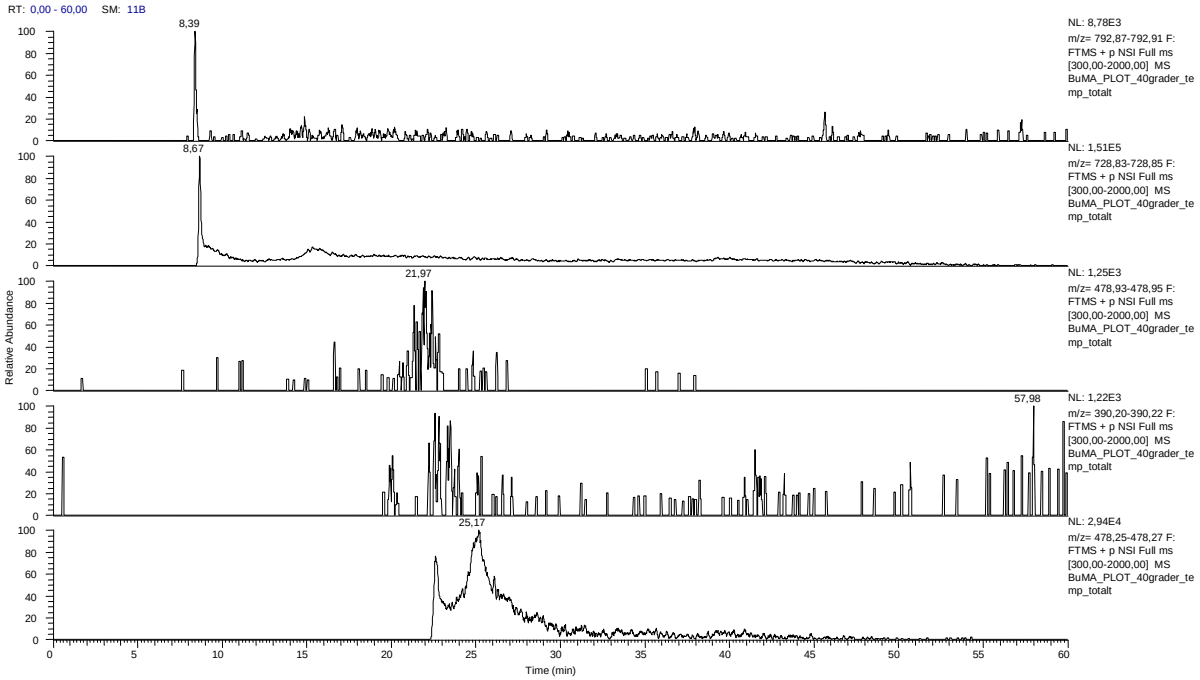

Figure 31. Extracted ion chromatograms of 3 µg/mL trypsinated cytochrome C. Both the 50 µm i.d. × ~4 cm BMA-EDMA monolithic precolumn and the 10 µm i.d. × 2.4 m PS-DVB PLOT analytical column were thermostated in a LC-MS system. **BMA-EDMA precolumn and PLOT column temperature was 40°C**. Other conditions were as described in Figure 26.

Table 21. BMA-EDMA monolithic precolumn coupled to PS-DVB PLOT analytical column in a LC-MS system. An overview of retention times (t_R), peak widths at half height ($w_{0.5}$) and 10% of the peak height ($w_{0.1}$), signal intensities (*NL*) and peak areas (*MA*) for five extracted peptide peaks at column temperatures of 20°C and 40°C. **Both the BMA-EDMA precolumn and the PLOT column were thermostated**. Conditions were as described in Figures 30 and 31.

peptide	Temperature **20°C**					Temperature **40°C**				
m/z	t_R **(min)**	$w_{0.5}$ **(sec)**	$w_{0.1}$ **(sec)**	***NL***	***MA***	t_R **(min)**	$w_{0.5}$ **(sec)**	$w_{0.1}$ **(sec)**	***NL***	***MA***
792.89	14.80	13.8	84.0	1.61E4	5.28E5	8.39	6.0	15.0	8.78E3	6.86E4
728.84	15.97	14.4	93.0	4.15E5	1.52E7	8.67	8.4	86.4	1.51E5	3.81E6
478.94	23.95	15.6	40.8	5.55E4	1.13E6	–	–	–	1.25E3	–
390.21	25.05	19.8	55.2	2.80E4	7.90E5	–	–	–	1.22E3	–
478.26	26.60	25.2	91.8	2.42E5	9.67E6	25.17	85.2	433.2	2.94E4	5.90E6

At PS-DVB precolumn and PLOT column temperature of 40°C, all the retention times and peak widths (both $w_{0.5}$ and $w_{0.1}$) were reduced, see Figures 32, 33 and Table 22. The retention times were only reduced by ~1 min. As was the case with the BMA-EDMA precolumn, all the signal intensities and peak areas were reduced at 40°C. Although the extent of signal loss was not as large as when the BMA-EDMA precolumn was used, a clear reduction could be observed, ranging from ~13% to ~68%.

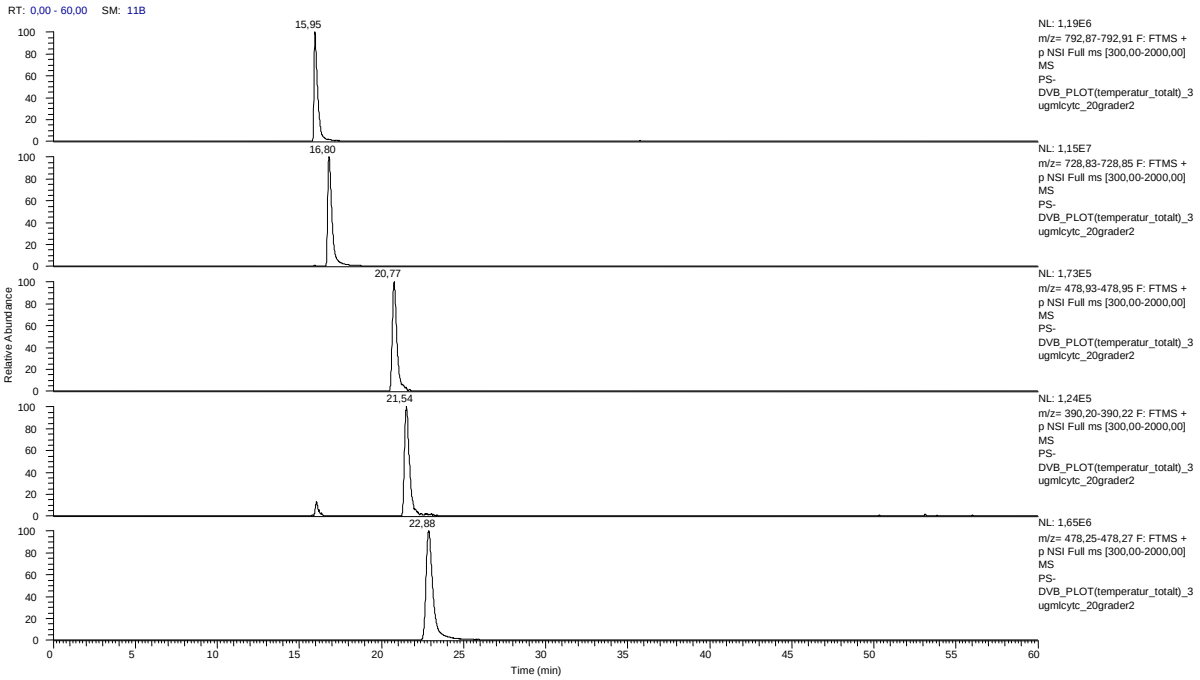

Figure 32. Extracted ion chromatograms of 3 µg/mL trypsinated cytochrome C. Both the 50 µm i.d. × ~4 cm PS-DVB monolithic precolumn and the 10 µm i.d. × 2.4 m PS-DVB PLOT analytical column were thermostated in a LC-MS system. **PS-DVB precolumn and PLOT column temperature was 20°C**. Other conditions were as described in Figure 26.

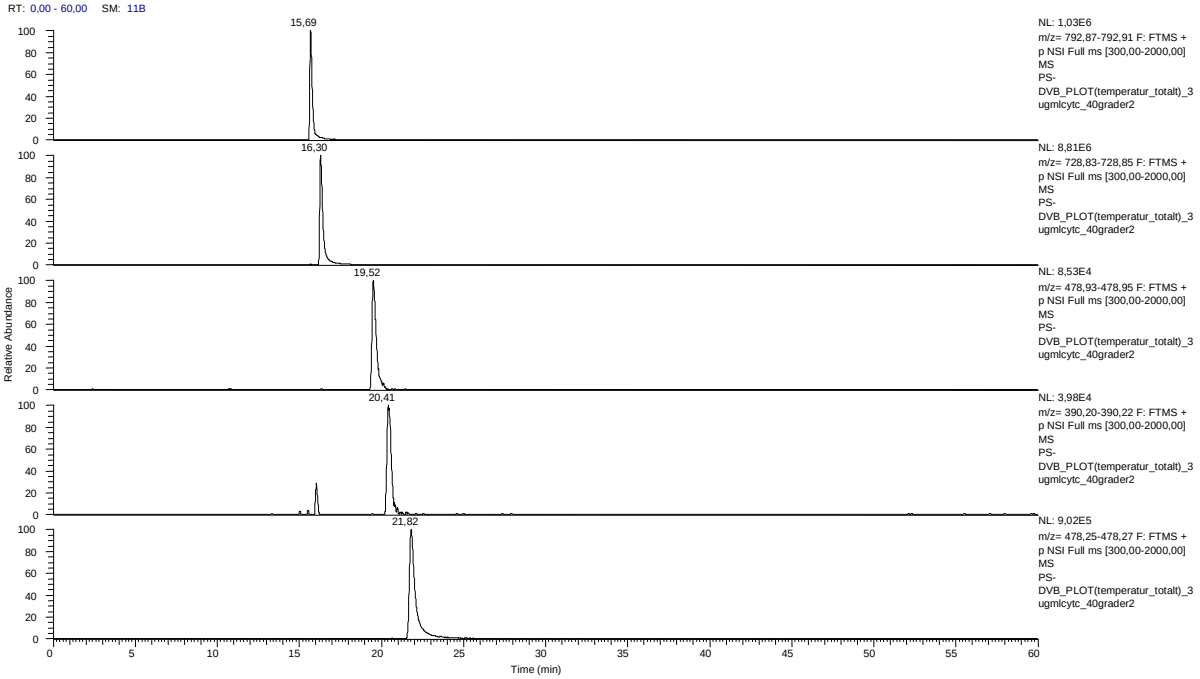

Figure 33. Extracted ion chromatograms of 3 µg/mL trypsinated cytochrome C. Both the 50 µm i.d. × ~4 cm PS-DVB monolithic precolumn and the 10 µm i.d. × 2.4 m PS-DVB PLOT analytical column were thermostated in a LC-MS system. **PS-DVB precolumn and PLOT column temperature was 40°C**. Other conditions were as described in Figure 26.

Table 22. PS-DVB monolithic precolumn coupled to PS-DVB PLOT analytical column in a LC-MS system. An overview of retention times (t_R), peak widths at half height ($w_{0.5}$) and 10% of the peak height ($w_{0.1}$), signal intensities (*NL*) and peak areas (*MA*) for five extracted peptide peaks at column temperatures of 20°C and 40°C. **Both the PS-DVB precolumn and the PLOT column were thermostated**. Conditions were as described in Figures 32 and 33.

peptide	Temperature **20°C**					Temperature **40°C**				
m/z	t_R **(min)**	$w_{0.5}$ **(sec)**	$w_{0.1}$ **(sec)**	***NL***	***MA***	t_R **(min)**	$w_{0.5}$ **(sec)**	$w_{0.1}$ **(sec)**	***NL***	***MA***
792.89	15.95	12.6	28.8	1.19E6	1.81E7	15.69	9.0	19.2	1.03E6	1.13E7
728.84	16.80	15.6	32.4	1.15E7	2.12E8	16.30	10.8	25.2	8.81E6	1.20E8
478.94	20.77	16.8	34.8	1.73E5	3.42E6	19.52	16.2	33.6	8.53E4	1.58E6
390.21	21.54	19.2	38.4	1.24E5	2.69E6	20.41	17.4	31.2	3.98E4	7.49E5
478.26	22.88	25.2	52.8	1.65E6	4.90E7	21.82	19.8	50.4	9.02E5	2.25E7

Taking into account the sometimes very large loss in signal intensities and peak areas, increasing precolumn and analytical column temperature from 20°C to 40°C does not seem to be very promising. Again, the reason for the overall loss is difficult to know, but it could be related to a combination of low flow rate and high temperature which negatively affects proper refocusing. Loss of signal with high temperature at low flow rate was also observed with other MS-instruments (Magnus Røgeberg unpublished results). Such loss of signal was not observed when elevated temperatures with larger flow rates were applied with silica-based monolithic columns [59]. What seems to be the most important finding from the study of temperature effects in monolith-PLOT LC-MS column switching system, is that increased temperature does not seem to be beneficial regardless of thermostating of just the precolumn, just the PLOT column or both the precolumn and PLOT column. In future studies, heating of columns probably should be avoided.

4. Conclusion

A 50 µm i.d. × 4.5 cm BMA-EDMA precolumn, coupled to a 10 µm i.d. PS-DVB PLOT analytical column with 0.75 µm layer thickness, has been sucessfully used in a monolith-PLOT LC-MS column switching system for proteomic samples. Loading capacity of ~120 fmol showed that analyte enrichment on the BMA-EDMA precolumn and the subsequent focusing on the PLOT column prepared by 70% ethanol/30% monomer have been successful. A 10 µm i.d. × 2.4 m PLOT column was used to investigate the effect of flow rate and gradient time on peak capacity. Highest peak capacity was obtained with a flow rate of 40 nL/min at all gradient times, and using the longest investigated column (8.0 m). LC-UV testing of the 50 µm i.d. PS-DVB precolumns, prepared using a binary porogenic mixture of toluene and 1-dodecanol, showed that reproducible monolithic PS-DVB precolumn preparation is difficult. LC-MS experiments using one of the "successful" PS-DVB precolumns (giving comparable peaks as that of the BMA-EDMA precolumn in the LC-UV tests), showed that a PS-DVB precolumn could perform as well as the BMA-EDMA precolumn in a column switching system with a PLOT analytical column. The often higher signal intensities obtained with the PS-DVB precolumn indicated good trapping of peptides. Although batch-to-batch reproducibility may seem difficult, the findings from the LC-MS experiments are very promising, and it seems worth while to further study the"recipe" of PS-DVB polymerization mixture. The study of temperature effects in monolith-PLOT LC-MS column switching system showed that increasing precolumn and analytical column temperature (from 20^{o}C to 90^{o}C) is not beneficial due to overall large loss in signal intensity and peak area. In future studies, higher temperature separation (when using LC-MS column switching system with monolithic precolumn and PLOT analytical column) probably should be avoided.

5. References

[1] N. C. Mishra (**2010**). *Introduction to Proteomics: Principles and Applications* (*Methods of Biochemical Analysis*). New Jersey: John Wiley & Sons, Inc. ISBN: 978-0-471-75402-2

[2] G. Mitulovic, K. Mechtler (**2006**). HPLC techniques for proteomics analysis – a short overview of latest developments. *Briefings in Functional Genomics and Proteomics, 5,* 249-260.

[3] M. H. M. van de Meent, G. J. de Jong (**2011**). Novel liquid-chromatography columns for proteomics research. *Trends in Analytical Chemistry, 30,* 1809-1818.

[4] A. L. Capriotti, C. Cavaliere, P. Foglia, R. Samperi, A. Lagana (**2011**). Intact protein separation by chromatographic and/or electrophoretic techniques for top-down proteomics. *Journal of Chromatography A, 1218,* 8760-8776.

[5] A. Staub, D. Guillarme, J. Schappler, J-L. Veuthey, S. Rudaz (**2011**). Intact protein analysis in the biopharmaceutical field. *Journal of Pharmaceutical and Biomedical Analysis, 55,* 810-822.

[6] N. Siuti, N. L. Kelleher (**2007**). Decoding protein modifications using top-down mass spectrometry. *Nature Methods, 4,* 817-821.

[7] H. J. Issaq, K. C. Chan, J. Blonder, X. Ye, T. D. Veenstra (**2009**). Separation, detection and quantitation of peptides by liquid chromatography and capillary electrochromatography. *Journal of Chromatography A, 1216,* 1825-1837.

[8] W. M. A. Niessen (**2006**). LC-MS analysis of proteins. *Chromatographic Science Series, 97* (Liquid Chromatography – Mass Spectrometry), 441-461. Boca Raton: Taylor & Francis Group. ISBN: 978-0-8247-4082-5

[9] F. Detobel, K. Broeckhoven, J. Wellens, B. Wouters, R. Swart, M. Ursem, G. Desmet, S. Eeltink (**2010**). Parameters affecting the separation of intact proteins in gradient-elution reversed-phase chromatography using poly(styrene-co-divinylbenzene) monolithic capillary columns. *Journal of Chromatography A, 1217,* 3085-3090.

[10] K. Shinoda, M. Sugimoto, M. Tomita, Y. Ishihama (**2008**). Informatics for peptide retention properties in proteomic LC-MS. *Proteomics, 8,* 787-798.

[11] Y. Saito, K. Jinno, T. Greibrokk (**2004**). Capillary columns in liquid chromatography: between conventional columns and microchips. *Journal of Separation Science, 27,* 1379-1390.

[12] J. P. C. Vissers, H. A. Claessens, C. A. Cramers (**1997**). Microcolumn liquid chromatography: instrumentation, detection and applications. *Journal of Chromatography A, 779,* 1-28.

[13] H. Kalish, T. M. Phillips (**2011**). Micro-HPLC. *Chromatographic Science Series, 101* (Handbook of HPLC), 77-100.

[14] H. D. Meiring, E. van der Heeft, G. J. ten Hove, A. P. J. M. de Jong (**2002**). Nanoscale LC-MS: technical design and applications to peptide and protein analysis. *Journal of Separation Science, 25*, 557-568.

[15] J. P. Chervet, M. Ursem (**1996**). Instrumental requirements for nanoscale liquid chromatography. *Analytical Chemistry, 68*, 1507-1512.

[16] K. K. Unger, R. Skudas, M. M. Schulte (**2008**). Particle packed columns and monolithic columns in high-performance liquid chromatography – comparison and critical appraisal. *Journal of Chromatography A, 1184*, 393-415.

[17] R. Bakry, C. W. Huck, G. K. Bonn (**2009**). Recent applications of organic monoliths in capillary liquid chromatographic separation of biomolecules. *Journal of Chromatographic Science, 47*, 418-431.

[18] E. Pitarch, F. Hernandez, J. ten Hove, H. Meiring, W. Niesing, E. Dijkman, L. Stolker, E. Hogendoorn (**2004**). Potential of capillary-column-switching liquid chromatography-tandem mass spectrometry for the quantitative trace analysis of small molecules – Application to the on-line screening of drugs in water. *Journal of Chromatography A, 1031*, 1-9.

[19] J. P. C. Vissers (**1999**). Recent developments in microcolumn liquid chromatography. *Journal of Chromatography A, 856*, 117-143.

[20] T. A. Van de Goor (**2007**). HPLC-chip/MS: a new approach to nano-LC/MS. *Journal of Chromatography Library, 72* (advances in LC-MS instrumentation), 165-192.

[21] Harris, D.C. (**2010**). *Quantitative chemical analysis*. New York: W. H. Freeman and Company. ISBN: 978-1-4292-1815-3

[22] N. Tanaka, H. Kobayashi, N. Ishizuka, H. Minakuchi, K. Nakanishi, K. Hosoya, T. Ikegami (**2002**). Monolithic silica columns for high-efficiency chromatographic separations. *Journal of Chromatography A, 965*, 35-49.

[23] F. M. Lancas, J. C. Rodrigues, S. de S. Freitas (**2004**). Preparation and use of packed capillary columns in chromatographic and related techniques. *Journal of Separation Science, 27*, 1475-1482.

[24] N. Tanaka, M. Motokawa, H. Kobayashi, K. Hosoya, T. Ikegami (**2003**). Monolithic silica columns for capillary liquid chromatography. *Journal of Chromatography Library, 67* (Monolithic Materials), 173-196.

[25] P. Aggarwal, H. D. Tolley, M. L. Lee (**2012**). Monolithic bed structure for capillary liquid chromatography. *Journal of Chromatography A, 1219*, 1-14.

[26] F. Svec, C. G. Huber (**2006**). Monolithic Materials: Promises, Challenges, Achievements. *Analytical Chemistry, 78*, 2100-2107.

[27] P. Jandera, J. Urban (**2010**). Characterization of Pore Structure and Its Impact on the Chromatographic Properties of Organic Polymer Monolithic Capillary Columns. *Monolithic Chromatography and its Modern Applications*, edited by P. Wang, 27-58.

[28] J. Urban, P. Jandera, P. Schoenmakers (**2006**). Preparation of monolithic columns with target mesopore-size distribution for potential use in size-exclusion chromatography. *Journal of Chromatography A, 1150*, 279-289.

[29] A. Greiderer, S. C. Ligon Jr., C. W. Huck, G. K. Bonn (**2010**). Organic Monoliths as Stationary Phases in Chromatography. *Monolithic Chromatography and its Modern Applications*, edited by P. Wang, 139-174.

[30] F. Svec (**2004**). Preparation and HPLC applications of rigid macroporous organic polymer monoliths. *Journal of Separation Science, 27*, 747-766.

[31] H. Oberacher, C. G. Huber (**2002**). Capillary monoliths for the analysis of nucleic acids by high-performance liquid chromatography-electrospray ionization mass spectrometry. *Trends in Analytical Chemistry, 21*, 166-174.

[32] J. Rozenbrand, W. P. van Bennekom (**2011**). Silica-based and organic monolithic capillary columns for LC: Recent trends in proteomics. *Journal of Separation Science, 34*, 1934-1944.

[33] S. Eeltink, W. M. C. Decrop, G. P. Rozing, P. J. Schoenmakers, W. T. Kok (**2004**). Comparison of the efficiency of microparticulate and monolithic capillary columns. *Journal of Separation Science, 27*, 1431-1440.

[34] A.-M. Siouffi (**2006**). About the *C* term in the van Deemter's equation of plate height in monoliths. *Journal of Chromatography A, 1126*, 86-94.

[35] Y. Moliner-Martinez, C. Molins-Legua, J. Verdu-Andres, R. Herraez-Hernandez, P. Campins-Falco (**2011**). Advantages of monolithic over particulate columns for multiresidue analysis of organic pollutants by in-tube solid-phase microextraction coupled to capillary liquid chromatography. *Journal of Chromatography A, 1218*, 6256-6262.

[36] K. Cabrera (**2004**). Applications of silica-based monolithic HPLC columns. *Journal of Separation Science, 27*, 843-852.

[37] F. C. Leinweber, U. Tallarek (**2003**). Chromatographic performance of monolithic and particulate stationary phases: Hydrodynamics and adsorption capacity. *Journal of Chromatography A, 1006*, 207-228.

[38] T. Nakaze, A. Kobayashi, T. Hirano, S. Kitagawa, H. Ohtani (**2012**). Determination of monomer conversion in methacrylate-based polymer monoliths fixed in a capillary column by pyrolysis-gas chromatography. *The Japan Society for Analytical Chemistry, 28*, 917-920.

[39] R. Wu, H. Zou (**2010**). Monolithic Columns in Microscale Separations. *Monolithic Chromatography and its Modern Applications*, edited by P. Wang, 215-264.

[40] R. D. Arrua, M. Talebi, T. J. Causon, E. F. Hilder (**2012**). Review of recent advances in the preparation of organic polymer monoliths for liquid chromatography of large molecules. *Analytica Chimica Acta*, *738*, 1-12.

[41] K. Stulik, V. Pacakova, J. Suchankova, P. Coufal (**2006**). Monolithic organic polymeric columns for capillary liquid chromatography and electrochromatography. *Journal of Chromatography B*, *841*, 79-87.

[42] G. Hasegawa, K. Kanamori, N. Ishizuka, K. Nakanishi (**2012**). New monolithic capillary columns with well-defined macropores based on poly(styrene-co-divinylbenzene). *ACS Applied Materials and Interfaces*, *4*, 2343-2347.

[43] J. Zhang, S-L. Wu, J. Kim, B. L. Karger (**2007**). Ultratrace liquid chromatography/mass spectrometry analysis of large peptides with post-translational modifications using narrow-bore poly(styrene-divinylbenzene) monolithic columns and extended range proteomic analysis. *Journal of Chromatography A*, *1154*, 295-307.

[44] I. Nischang, O. Brueggemann, F. Svec (**2010**). Advances in the preparation of porous polymer monoliths in capillaries and microfluidic chips with focus on morphological aspects. *Analytical and Bioanalytical Chemistry*, *397*, 953-960.

[45] J. Wang, I. Tanret, D. Mangelings, G. Fan, Y. Wu, Y. V. Heyden (**2010**). Fingerprint development for *Ginkgo biloba* extracts by pressurized capillary electrochromatography: Comparison of column types. *Journal of Chromatographic Science*, *48*, 428-435.

[46] J. Courtois, M. Szumski, E. Byström, A. Iwasiewicz, A. Shchukarev, K. Irgum (**2006**). A study of surface modification and anchoring techniques used in the preparation of monolithic microcolumns in fused silica capillaries. *Journal of Separation Science*, *29*, 14-24.

[47] I. Gusev, X. Huang, C. Horvath (**1999**). Capillary columns with in situ formed porous monolithic packing for micro high-performance liquid chromatography and capillary electrochromatography. *Journal of Chromatography A*, *855*, 273-290.

[48] P. Coufal, Z. Bosakova, J. Sirc, V. Pacakova, K. Stulik (**2010**). Preparation and Characterization of Organic Polymer Monolithic Capillary Columns. *Monolithic Chromatography and its Modern Applications*, edited by P. Wang, 79-100.

[49] I. Nischang, I. Teasdale, O. Bruggemann (**2011**). Porous polymer monoliths for small molecule separations: advancements and limitations. *Analytical and Bioanalytical Chemistry*, *400*, 2289-2304.

[50] J. H. Mohr, R. Swart, C. G. Huber (**2011**). Morphology and efficiency of poly(styrene-co-divinylbenzene)-based monolithic capillary columns for the separation of small and large molecules. *Analytical and Bioanalytical Chemistry*, *400*, 2391-2402.

[51] F. Svec (**2010**). Porous polymer monoliths: Amazingly wide variety of techniques enabling their preparation. *Journal of Chromatography A*, *1217*, 902-924.

[52] K. Marcus, H. Schafer, S. Klaus, C. Bunse, R. Swart, H. E. Meyer (**2007**). A new fast method for nanoLC-MALDI-TOF/TOF-MS analysis using monolithic columns for peptide preconcentration and separation in proteomic studies. *Journal of Proteome Research, 6*, 636-643.

[53] D. Peroni, D. Vanhoutte, F. Vilaplana, P. Schoenmakers, S. de Koning, H. Janssen (**2012**). Hydrophobic polymer monoliths as novel phase separators: Application in continuous liquid-liquid extraction systems. *Analytica Chimica Acta, 720,* 63-70.

[54] D. A. Collins, E. P. Nesterenko, D. Brabazon, B. Paull (**2012**). Controlled ultraviolet (UV) photoinitiated fabrication of monolithic porous layer open tubular (monoPLOT) capillary columns for chromatographic applications. *Analytical Chemistry, 84*, 3465-3472.

[55] K. Sandra, M. Moshir, F. D'hondt, K. Verleysen, K. Kas, P. Sandra (**2008**). Highly efficient peptide separations in proteomics. Part 1. Unidimensional high performance liquid chromatography. *Journal of Chromatography B, 866,* 48-63.

[56] G. Yue, Q. Luo, J. Zhang, S.-L. Wu, B. L. Karger (**2007**). Ultratrace LC/MS Proteomic Analysis Using 10-μm-i.d. Porous Layer Open Tubular Poly(styrene-divinylbenzene) Capillary Columns. *Analytical Chemistry, 79,* 938-946.

[57] Q. Luo, T. Rejtar, S.-L. Wu, B. L. Karger (**2009**). Hydrophilic interaction 10 μm I.D. porous layer open tubular columns for ultratrace glycan analysis by liquid chromatography-mass spectrometry. *Journal of Chromatography A, 1216*, 1223-1231.

[58] M. Røgeberg, S. R. Wilson, T. Greibrokk, E. Lundanes (**2010**). Separation of intact proteins on porous layer open tubular (PLOT) columns. *Journal of Chromatography A, 1217*, 2782-2786.

[59] M. Røgeberg, S. R. Wilson, H. Malerod, E. Lundanes, N. Tanaka, T. Greibrokk (**2011**). High efficiency, high temperature separations on silica based monolithic columns. *Journal of Chromatography A, 1218,* 7281-7288.

[60] A. Moen, T. T. Hafte, H. Tveit, W. Egge-Jacobsen, K. Prydz (**2011**). *N*-Glycan synthesis in the apical and basolateral secretory pathway of epithelial MDCK cells and the influence of a glycosaminoglycan domain. *Glycobiology, 21*, 1416-1425.

[61] Dorna Misaghian (**2012**). Thesis for the Master's degree in chemistry. Department of Chemistry, Faculty of mathematics and natural sciences, University of Oslo.

[62] L. Geiser, S. Eeltink, F. Svec, J. M. J. Fréchet (**2007**). Stability and repeatability of capillary columns based on porous monoliths of poly(butylmethacrylate-co-ethylene dimethacrylate). *Journal of Chromatography A*, 1140, 140-146.

[63] Y. Lv, Z. Lin, F. Svec (**2012**). Hypercrosslinked porous polymer monoliths for hydrophilic interaction liquid chromatography of small molecules featuring zwitterionic functionalities attached to gold nanoparticles hold in layered structure. *Analytical Chemistry, 84*, 8457-8460.

[64] http://www.chem.agilent.com/Library/usermanuals/Public/G1388-90001_031240.pdf Agilent Technologies (**2002**), Germany.

[65] J. H. Knox, M. T. Gilbert (**1979**). Kinetic optimization of straight open-tubular liquid chromatography. *Journal of Chromatography*, *186*, 405-418.

[66] S. Eguchi, J. G. Kloosterboer, C. P. G. Zegers, P. J. Schoenmakers (**1990**). Fabrication of columns for open-tubular liquid chromatography using photopolymerization of acrylates. *Journal of Chromatography*, *516*, 301-312.

[67] G. Guiochon (**2006**). The limits of the separation power of unidimensional column liquid chromatography. *Journal of Chromatography A*, *1126*, 6-49.

[68] T. J. Causon, R. A. Shellie, E. F. Hilder, G. Desmet, S. Eeltink (**2011**). Kinetic optimisation of open-tubular liquid-chromatography capillaries coated with thick porous layers for increased loadability. *Journal of Chromatography A*, *1218*, 8388-8393.

[69] N. Marchetti, G. Guiochon (**2007**). High peak capacity separations of peptides in reversed-phase gradient liquid chromatography on columns packed with porous shell particles. *Journal of Chromatography A*, *1176*, 206-216.

[70] N. Marchetti, A. Cavazzini, F. Gritti, G. Guiochon (**2007**). Gradient elution separation and peak capacity of columns packed with porous shell particles. *Journal of Chromatography A*, *1163*, 203-211.

[71] Y. Li, P. Aggarwal, H. D. Tolley, M. L. Lee (**2012**). Organic monolith column technology for capillary liquid chromatography. *Advances in Chromatography*, *50*, edited by E. Grushka, N. Grinberg, 249-254.

[72] J. Courtois, M. Szumski, F. Georgsson, K. Irgum (**2007**). Assessing the macroporous structure of monolithic columns by transmission electron microscopy. *Analytical Chemistry*, *79*, 335-344.

[73] N. Fontanals, R. M. Marce, F. Borrull (**2007**). New materials in sorptive extraction techniques for polar compounds. *Journal of Chromatography A*, *1152*, 14-31.

[74] I. Nischang (**2013**). Porous polymer monoliths: Morphology, porous properties, polymer nanoscale gel structure and their impact on chromatographic performance. *Journal of Chromatography A*, *1287*, 39-58.

6. Appendix

6.1 Column preparation using a laboratory-made pressure bomb

PRETREATMENT	
1	The capillary is filled with 1M NaOH
2	Both ends of the capillary are plugged (with rubber septum or ferrule + union)
3	The capillary is placed in an oven at 100 °C for 2 hours or in room temperature overnight
4	The capillary is rinsed with type I water for ~30 min
5	The capillary is rinsed with ACN for ~30 min
6	The capillary is dried with N_2 for ~1 hour

SILANIZATION	
1	The silanization solution is prepared by mixing the following compounds: 0.0050 g DPPH, 0.3135 g γ-MAPS and 0.6608 g DMF
2	The capillary is filled with the silanization solution
3	Both ends of the capillary are plugged (with rubber septum or ferrule + union)
4	The capillary is placed in an oven at 110 °C for 6 hours
5	The capillary is rinsed with ACN for ~30 min
6	The capillary is dried with N_2 for ~30 min

POLYMERIZATION: 10 µm i.d. PS-DVB PLOT columns	
1	The polymerization solution is prepared by mixing the following compounds: 0.0050 g AIBN, 0.1818 g styrene, 0.1828 g DVB, 0.7434 g EtOH
2	The polymerization mixture is homogenized by ultrasonication for 5 min
3	The capillary is filled with the polymerization solution
3	Both ends of the capillary are plugged (with rubber septum or ferrule + union)
4	The capillary is placed in an oven at 74°C for 16 hours
5	The capillary is rinsed with ACN for ~30 min
6	The capillary is dried with N_2 for ~30 min

POLYMERIZATION: 50 µm i.d. PS-DVB monolithic columns	
1	The appropriate amount of each chemical of the polymerization mixture is weighed out and transferred to a glass vial
2	The polymerization mixture is homogenized by ultrasonication for 5-10 min
3	The capillary is filled with the polymerization solution
3	Both ends of the capillary are plugged (with rubber septum)
4	The capillary is placed in an oven at 70°C for 20 h or 70°C/74^{o}C for 16 h
5	The capillary is rinsed with ACN for ~15 min

6.2 PS-DVB monolithic precolumns using a binary porogenic mixture of THF and 1-decanol

50 µm i.d. PS-DVB columns using a binary porogenic mixture of THF and 1-decanol were prepared as described in Experimental 2.4 (Table 2). Regardless of the volume ratio of THF/1-decanol and polymerization temperature (70°C and 74°C) used, the measured column pressures were found to be too high for use as precolumns. The lowest column pressure was ~30 bar/cm (60/540, 65/535, 70/530 at 70°C) measured using a flow rate of 500 nL/min with 0.1% FA in ACN (v/v). Table 23 shows SEM images of columns prepared with porogenic volume ratio of 70/530 and 80/520 at both temperatures.

Table 23. SEM images of 50 µm i.d. PS-DVB monolithic columns prepared using a binary porogenic mixture of THF and 1-decanol.

Vol. ratio THF/1-decanol	**Polymerization: 16 hours at 70°C**	**Polymerization: 16 hours at 74°C**
70/530	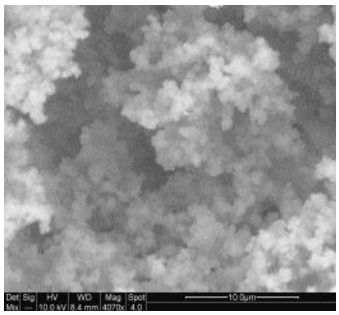	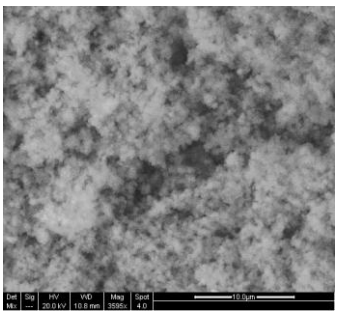
80/520	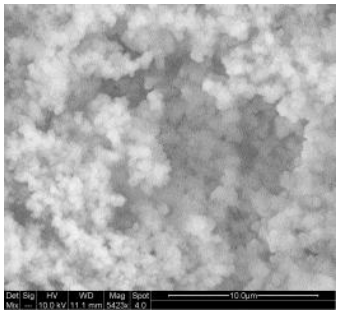	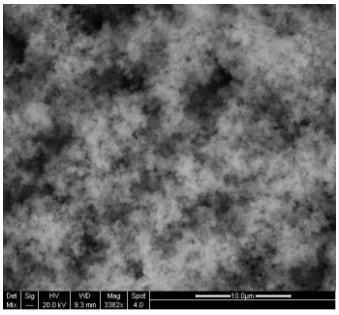

Two replicates of 50 µm i.d. PS-DVB columns, using a binary porogenic mixture of THF and 1-decanol, were prepared based on a recipe of Mohr et al. [50], see Table 24. Columns prepared from both mixtures 1 and 2 could not be considered as precolumn candidates because of too high column pressures. Table 25 shows SEM images of columns prepared with mixtures 1 and 2.

Table 24. Two polymerization mixtures used for preparation of 50 µm i.d. PS-DVB columns using a binary porogenic mixture of THF and 1-decanol.

Chemical	**Polymerization mixture 1**	**Polymerization mixture 2**
AIBN	0,0089 g	0,0088 g
Styrene	0,2042 g	0,2028 g
DVB	0,2069 g	0,2033 g
THF	0,0822 g	0,0882 g
1-Decanol	0,4978 g	0,4969 g

Table 25. SEM images of 50 µm i.d. PS-DVB monolithic columns prepared using a binary porogenic mixture of THF and 1-decanol.

Mixture	**Polymerization: 24 hours at 70°C**	
1	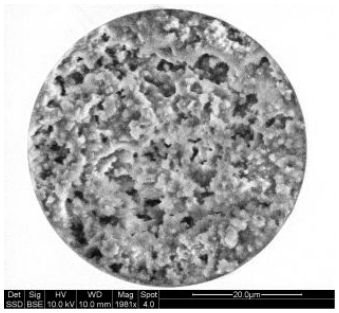	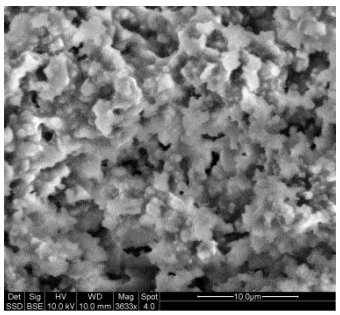
2	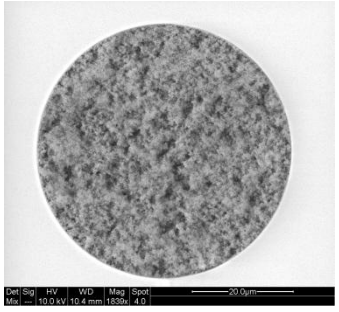	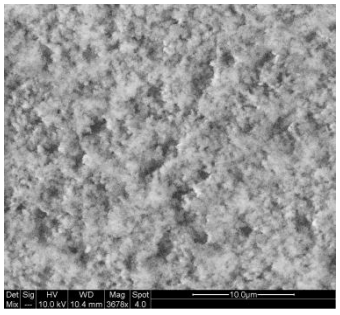

6.3 PS-DVB monolithic precolumns using a binary porogenic mixture of toluene and 1-dodecanol

Two replicates of 50 µm i.d. PS-DVB columns, using a binary porogenic mixture of toluene and 1-dodecanol, were prepared based on a recipe of Peroni et al. [53], see Table 26. With 2 wt% and 5 wt% toluene, the column pressure was too low and only short parts (<5 cm) of the column seemed to have been "properly" polymerized. With 10 wt% toluene, the column pressure was too high (~20 bar/cm). The columns could not be considered as precolumn candidates .

Table 26. Three polymerization mixtures used for preparation of 50 µm i.d. PS-DVB columns using a binary porogenic mixture of toluene and 1-dodecanol.

Chemical	**wt.%**	**weight (g)**	**wt.%**	**weight (g)**	**wt.%**	**weight (g)**
AIBN	1%	0,0040	1%	0,0040	1%	0,0040
Styrene	20%	0,2000	20%	0,2000	20%	0,2000
DVB	20%	0,2000	20%	0,2000	20%	0,2000
Toluene	2%	0,0200	5%	0,0500	10%	0,1000
1-Dodecanol	58%	0,5800	55%	0,5500	50%	0,5000

6.4 Study of temperature effects

The general trend which was observed with the use of increased temperature (up to 90^{o}C) on just the precolumn and on both the precolumn and analytical column in monolith-PLOT LC-MS column switching system was lower signal intensities and reduced peak areas, see Figures 34-37. The same trend of overall loss in signal intensity and peak area was also observed when only the PLOT analytical column temperature was increased, see Figures 38-41.

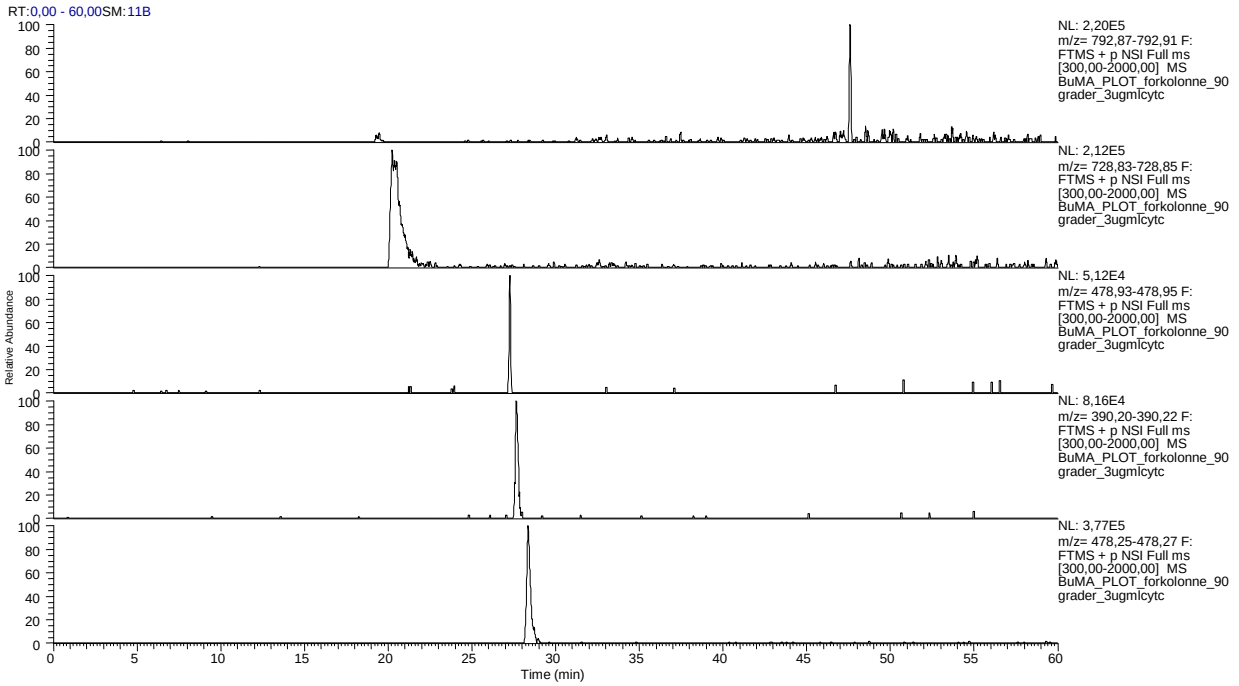

Figure 34. Extracted ion chromatograms of 3 µg/mL trypsinated cytochrome C. The 50 µm i.d. × ~4 cm BMA-EDMA monolithic precolumn was coupled to the 10 µm i.d. × 2.4 m PS-DVB PLOT analytical column in a monolith-PLOT LC-MS column switching system. Only the precolumn was thermostated. **Temperature of BMA-EDMA precolumn was 90°C.** Other conditions were as described in Figure 26.

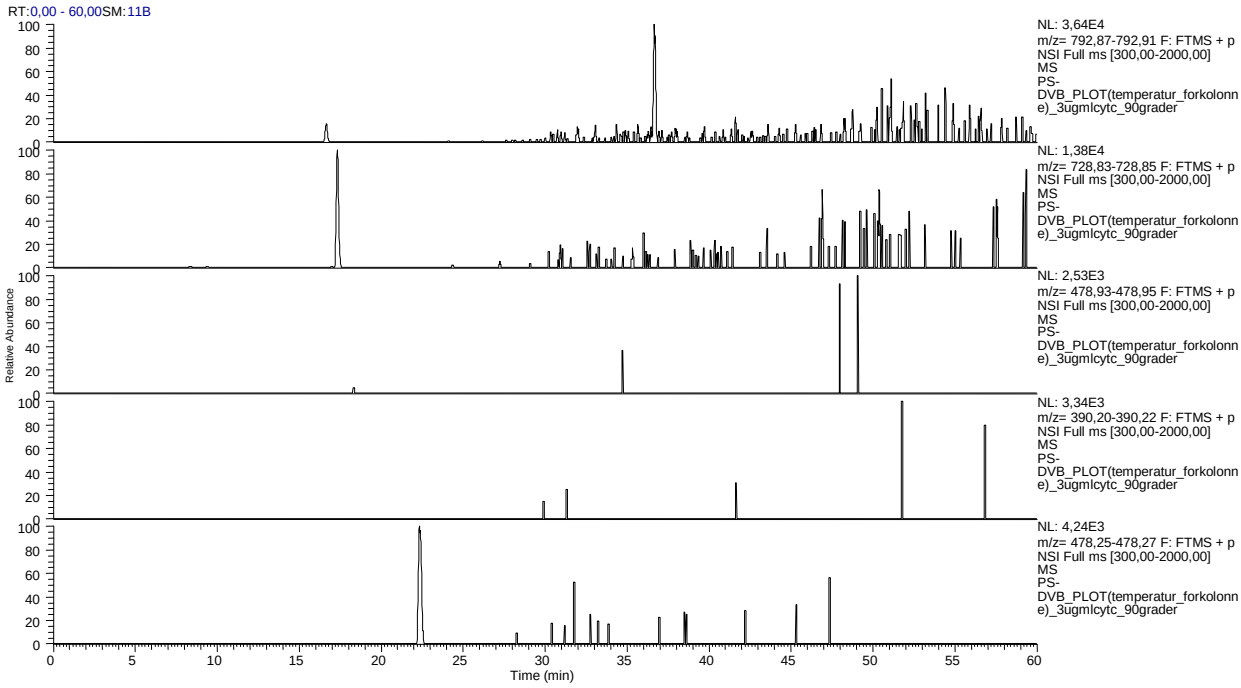

Figure 35. Extracted ion chromatograms of 3 µg/mL trypsinated cytochrome C. The 50 µm i.d. × ~4 cm PS-DVB monolithic precolumn was coupled to the 10 µm i.d. × 2.4 m PS-DVB PLOT analytical column in a monolith-PLOT LC-MS column switching system. Only the precolumn was thermostated. **Temperature of PS-DVB precolumn was 90°C.** Other conditions were as described in Figure 26.

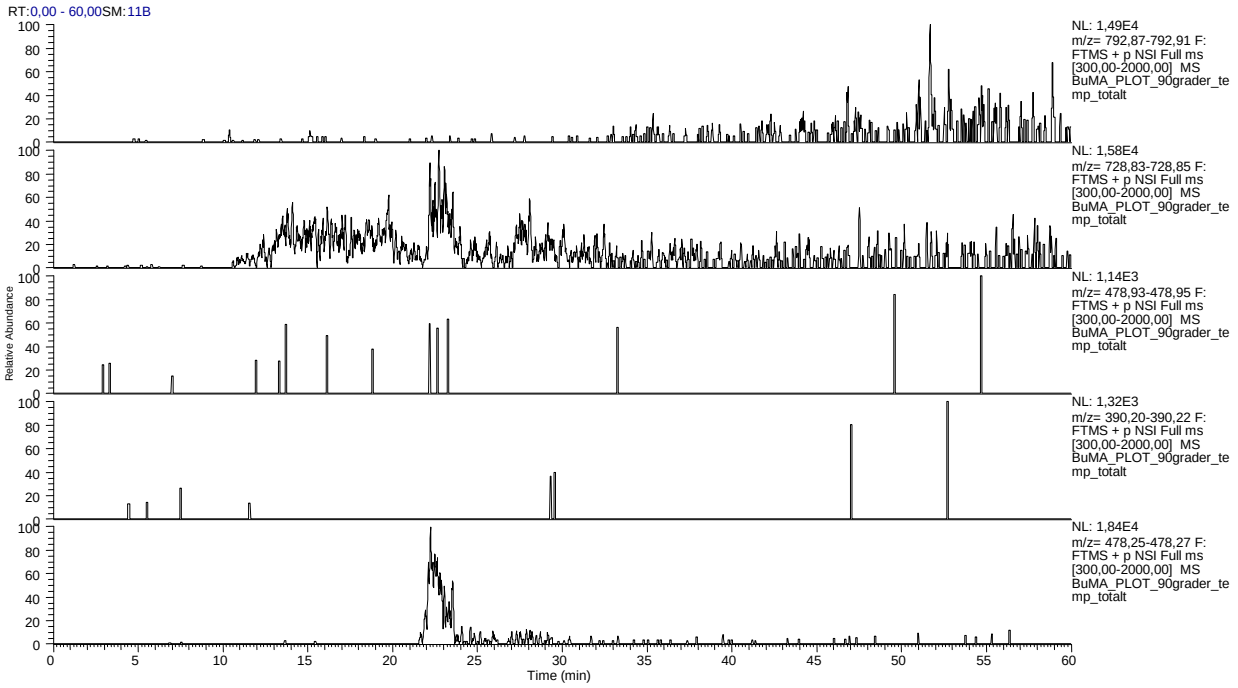

Figure 36. Extracted ion chromatograms of 3 µg/mL trypsinated cytochrome C. Both the 50 µm i.d. × ~4 cm BMA-EDMA monolithic precolumn and the 10 µm i.d. × 2.4 m PS-DVB PLOT analytical column were thermostated in a monolith-PLOT LC-MS column switching system. **BMA-EDMA precolumn and PLOT column temperature was 90°C**. Other conditions were as described in Figure 26.

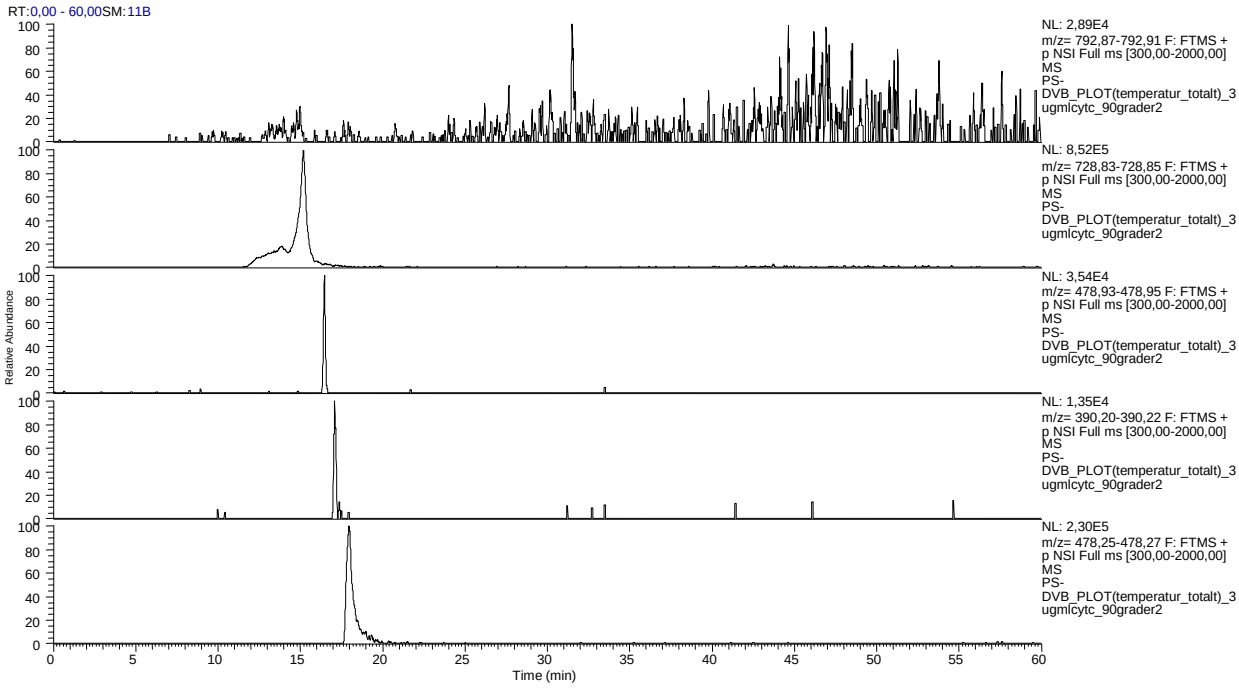

Figure 37. Extracted ion chromatograms of 3 µg/mL trypsinated cytochrome C. Both the 50 µm i.d. × ~4 cm PS-DVB monolithic precolumn and the 10 µm i.d. × 2.4 m PS-DVB PLOT analytical column were thermostated in a monolith-PLOT LC-MS column switching system. **PS-DVB precolumn and PLOT column temperature was 90°C**. Other conditions were as described in Figure 26.

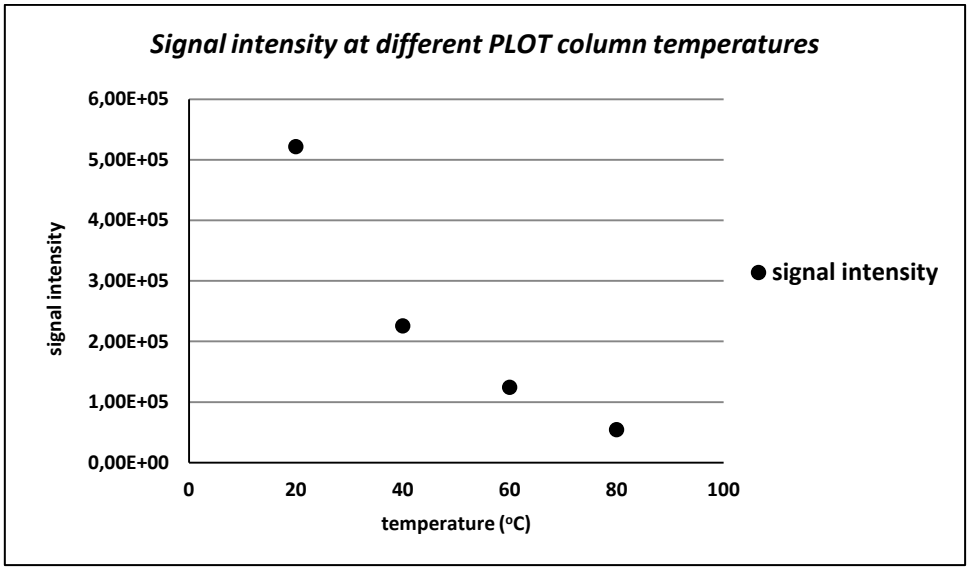

Figure 38. Signal intenstiy as a function of temperature (20–90°C). Signal intensity at 90°C was not included since no clear peaks could be observed. The 50 μm i.d. × ~4 cm **BMA-EDMA monolithic precolumn** was coupled to the 10 μm i.d. × 2.4 m PS-DVB PLOT analytical column in a monolith-PLOT LC-MS column switching system. **Only the PLOT analytical column was thermostated.** Average signal intensity was obtained from five extracted peptide peaks with *m/z* = 792.89, 728.84, 478.94, 390.21, 478.26. Other conditions were as described in Figure 26.

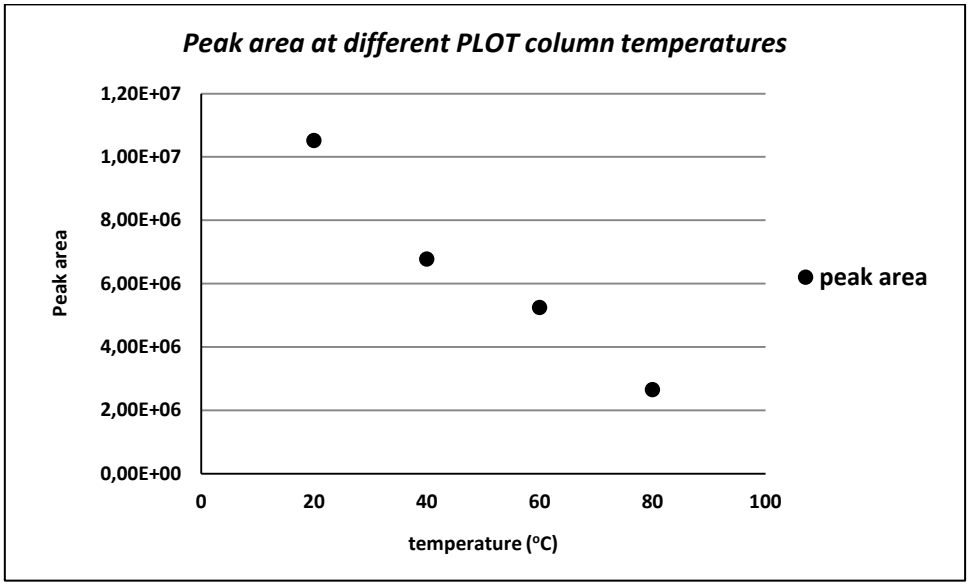

Figure 39. Peak area as a function of temperature (20–90°C). Peak area at 90°C was not included since no clear peaks could be observed. The 50 μm i.d. × ~4 cm **BMA-EDMA monolithic precolumn** was coupled to the 10 μm i.d. × 2.4 m PS-DVB PLOT analytical column in a monolith-PLOT LC-MS column switching system. **Only the PLOT analytical column was thermostated.** Average peak area was obtained from five extracted peptide peaks with *m/z* = 792.89, 728.84, 478.94, 390.21, 478.26. Other conditions were as described in Figure 38.

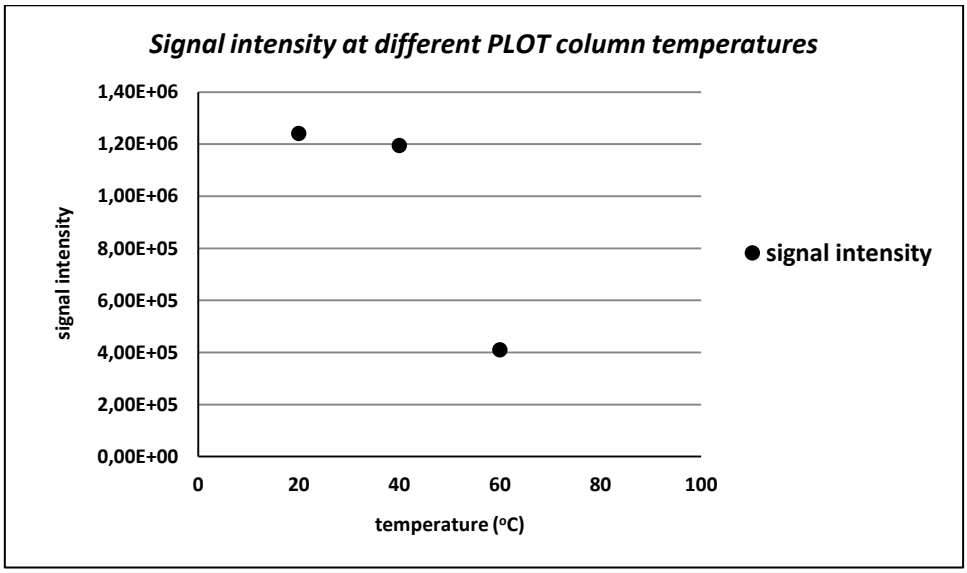

Figure 40. Signal intensity as a function of temperature (20–90°C). Signal intensities at 80 and 90°C are not included since no clear peaks could be observed. The 50 µm i.d. × ~4 cm **PS-DVB monolithic precolumn** was coupled to the 10 µm i.d. × 2.4 m PS-DVB PLOT analytical column in a monolith-PLOT LC-MS column switching system. **Only the PLOT analytical column was thermostated.** Other conditions were as described in Figure 38.

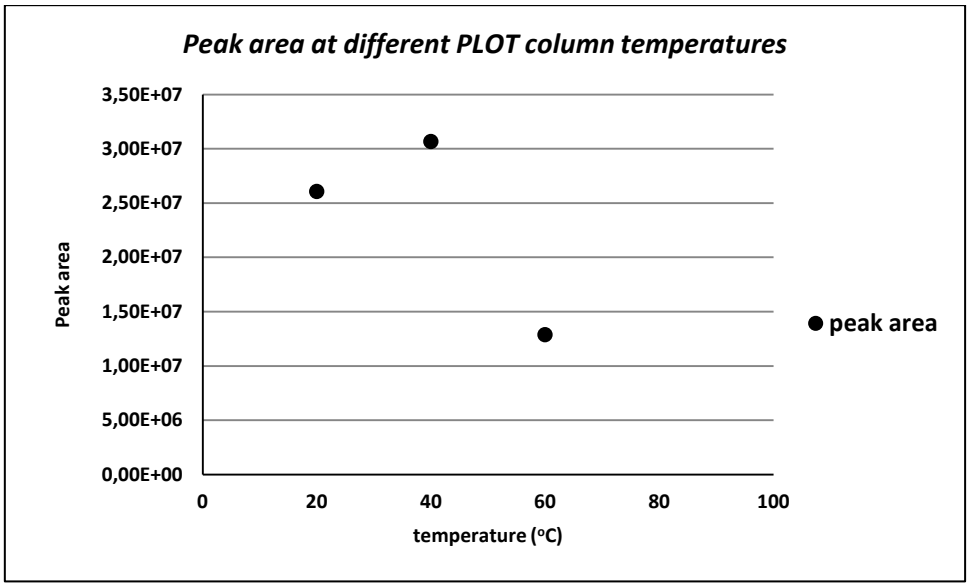

Figure 41. Peak area as a function of temperature (20–90°C). Peak areas at 80 and 90°C were not included since no clear peaks could be observed. The 50 µm i.d. × ~4 cm **PS-DVB monolithic precolumn** was coupled to the 10 µm i.d. × 2.4 m PS-DVB PLOT analytical column in a monolith-PLOT LC-MS column switching system. **Only the PLOT analytical column was thermostated.** Other conditions were as described in Figure 38.